uOttawa

L'Université canadienne
Canada's university

FACULTÉ DES ÉTUDES SUPÉRIEURES ET POSTOCTORALES

uOttawa

L'Université canadienne
Canada's university

FACULTY OF GRADUATE AND POSDOCTORAL STUDIES

Clayton Crawley
AUTEUR DE LA THÈSE / AUTHOR OF THESIS

Ph.D. (Biochemistry)
GRADE / DEGREE

Department of Biochemistry, Microbiology and Immunology
FACULTÉ, ÉCOLE, DÉPARTEMENT / FACULTY, SCHOOL, DEPARTMENT

Interplay of Ku antigen and Poly (ADP-Ribose) Polymerase-1 in the Regulation of Non Homologous DNA-End Joining

TITRE DE LA THÈSE / TITLE OF THESIS

Robert Haché
DIRECTEUR (DIRECTRICE) DE LA THÈSE / THESIS SUPERVISOR

CO-DIRECTEUR (CO-DIRECTRICE) DE LA THÈSE / THESIS CO-SUPERVISOR

EXAMINATEURS (EXAMINATRICES) DE LA THÈSE / THESIS EXAMINERS

Marc Ekker

Martin Pelchat

Douglas Gray

Louise Winn

Gary W. Slater
Le Doyen de la Faculté des études supérieures et postdoctorales / Dean of the Faculty of Graduate and Postdoctoral Studies

Interplay of Ku antigen and Poly(ADP-Ribose) Polymerase-1 in the Regulation of Non Homologous DNA-End Joining

Clayton D. Crawley

Thesis submitted to the
Faculty of Graduate and Postdoctoral Studies
In partial fulfillment of the requirements
For the PhD degree in Biochemistry

Department of Biochemistry, Microbiology, and Immunology
Faculty of Science
University of Ottawa

Your file Votre référence
ISBN: 978-0-494-51796-3
Our file Notre référence
ISBN: 978-0-494-51796-3

"*Wisdom and knowledge shall be the stability of thy times*"

– Isaiah 33:6

Abstract

The detection and repair of double-stranded DNA breaks (DSBs) is crucial to the functioning of the cell and the integrity of the genome. In higher eukaryotes, the non-homologous end joining (NHEJ) pathway is the more widely used mechanism for repairing DSBs. The NHEJ pathway is initiated by the binding of Ku to the DSB. Ku is a ring-shaped heterodimer that binds to DNA with high affinity by threading the DNA through its central pore. Current models of the NHEJ pathway suggest that as repair proceeds, Ku is pushed to the interior of the DNA, away from the ends. According to these scenarios, upon repair of the break Ku would be trapped on the ligated DNA without a means of dissociating from the DNA once repair is completed. PARP1 is member of the poly(ADP-ribose) polymerase (PARP) enzyme family, and is believed to be involved in the resolution of DSBs. When active, PARP1 transfers and polymerizes ADP-ribose polymers to target nuclear proteins, which in turn, alters their activity. The enzymatic activity of PARP1 is stimulated by the binding of PARP1 to DNA breaks and strand interruptions. Recent work has suggested a functional interaction between Ku and PARP1 in DNA repair. Given reports that PARP1 can affect the affinity of Ku for DNA and the enzymatic role of PARP1, I have developed the hypothesis that PARP1 stimulates the release of Ku from DNA. My work in this thesis has shown that the release of Ku from DNA is dramatically accelerated by the addition of PARP1 under ADP-ribosylation permissive conditions. This release is dependent upon the enzymatic activity of PARP1 rather than the presence of PAR polymers. The PARP-mediated release of Ku from DNA is not dependent upon the presence of free ends as Ku was no longer detected on closed circular DNA after incubation with PARP1. PARP1 ADP-ribosylates three glutamate residues within the C-terminal SAP domain of the Ku70 subunit

of the heterodimer, and mutation of these residues abrogates the effect of PARP1 on Ku. The ribosylation of Ku by PARP1 is necessary for an appropriate DNA damage response *in vivo*, as mutation of these residues resulted in an increased sensitivity to DNA damaging agents and a prolonged retention of Ku at repair sites. In addition to the deficiencies in responding to DNA damage the mutations resulted in dramatically reduced V(D)J recombination potential and defects in the formation of signal joints. The findings from the current study provide a novel and significant insight into the importance of ribosylation in regulating Ku function in DNA repair, and imply a further significance for ribosylation in regulating other roles of Ku.

Acknowledgements

I would first like to extend my thanks to my supervisor Dr. Robert Haché for his insight, patience, and support over the past years. I would also like to express my thanks to my thesis advisory committee members, Dr. Steffany Bennett and Dr. Martin Holcik. Their time, advice, and encouragement throughout the course of my research was greatly appreciated.

Too often the world of scientific research isn't black and white and it takes years of colorful discussions and intensely hued debates to work out the grayness in which the world of science exists. I would like to thank all of the members of the Haché lab – past and present – for shedding some light and filling the void between experiments with a little color. I would especially like to thank Dr. Sebastien Soubeyrand for all of the stimulating conversations, scientific input, constructive criticisms, and his ability to score on his own net. Without his constant cheerleading this would not have been possible.

I would like to thank my family, which seems to grow continuously, for their love and support over the years. I am in deep gratitude to my parents, Norm and Yvonne Crawley, for all of their love, patience and support.

Finally I would like to extend a most sincere and unending thanks to my beautiful wife, Dr. Jenny Ma. It is because of her that the hurdles of this project did not seem so large and the world didn't stop turning every time I hit a wall. With everything that was dealt over the past four years, I am glad that I had you by my side. You always manage to lift my spirits and remind me that I am smart – not just a smartass. Thank you for believing in me, even when I found it hard to do so myself.

Table of Contents

List of Abbreviations

3-AB 3-aminobenzamide

4-ANI 4-amino-1,8-napthalimide

APLF .....aprataxin PNK-like factor

CAT..... chloramphenicol acetyltransferase

ccDNA..... closed circular DNA

CHFR ..... checkpoint protein with FHA and RING domains

ChIP..... chromatin immunoprecipitation

CHO .....Chinese hamster ovarian

CPT .....camptothecin

DAPI .....4'-6-diamidino-2-phenylindole

DBD ..... DNA binding domain

DNA .....deoxyribonucleic acid

DNA-PK..... DNA-dependent protein kinase

DSB ..... double stranded DNA break

dsDNA.....double-stranded DNA

EMSA.....electrophoretic mobility shift assay

FISH ..... fluorescent *in situ* hybridization

GFP ..... green fluorescent protein

GPB ..... glycophorin B

γH_2AX .....phospho-histone $2A_X$

H_2O_2 ..... hydrogen peroxide

HMGB1 ..... high mobility group protein B1

HR ..... homologous recombination

HTH..... helix-turn-helix

IF .....immunofluorescence

IR..... ionizing radiation

IRIF ..... ionizing radiation induced foci

LD_{50}..... median lethal dose

LET ..... linear energy transfer

MEF..... mouse embryonic fibroblast

Mg^{2+} .....magnesium

MRE ..... meiotic recombination element

NaCl ..... sodium chloride

NAD^{+}..... Nicotinamide adenine dinucleotide

NBS ..... Nijmegen breakage syndrome

NHEJ ..... nonhomologous DNA-end joining

NLS ..... nuclear localization signal

NRE.....negative regulatory element

ors..... origin-enriched sequences

PAR..... poly(ADP-ribose)

PARG .....poly(ADP-ribose) glycohydrolase

PARP.....poly(ADP-ribose) polymerase

RAG .....recombination activating gene

RPA.....replication protein A

RSS..... Recombination Signal Sequence

ΔSAP ..... deletion of the SAP domain

ssDNA ..... single stranded DNA

TCR ..... T-cell receptor

TLC1 ..... telomerase component 1

TRF ..... telomeric repeat binding factor

Tris ..... tris(hydroxymethyl)aminomethane

vWA ..... von Willebrand factor A-like

WCE ..... whole cell extract

WT ..... wild-type

XRCC ..... x-ray cross complementing group

xrs ..... x-ray sensitive

List of Figures

1. Introduction

1.1 DNA damage and repair

Double stranded DNA breaks (DSBs) result from a number of cellular processes, including errors in replication, immunoglobulin gene diversification or meiosis; they can also arise from exogenous sources, such as ionizing radiation (IR) and exposure to some chemicals (1). Compared to other types of DNA lesions which affect only one strand of the DNA double-helix, DSBs affect both strands of the DNA duplex and therefore prevent use of the complementary strand as a template for repair, which makes them the most dangerous form of DNA lesions to the cell. If not repaired quickly and appropriately, DSBs can have hazardous effects on the integrity of the genome, the functioning of the cell, and the health of the organism; accumulation and misrepair of DSBs can lead to DNA sequence insertions or deletions, and chromosomal recombinations that can result in harmful mutations (1). As a result, cells have evolved groups of proteins that function in signaling networks that sense DSBs or other DNA damage, arrest the cell cycle, and activate DNA repair pathways. The rate of detection and the efficiency of the subsequent repair is dependent upon many factors, including the cell type, the age of the cell, the cell cycle, cellular repair factors, and the extracellular environment (1; 2; 3).

In eukaryotic cells, DSBs are predominantly repaired by one of two repair pathways, non-homologous end-joining (NHEJ) and homologous recombination (HR). These pathways are distinct and function in complementary ways to effectively repair DSBs. Homologous recombination primarily uses the undamaged sister chromatid as a DNA template allowing for accurate repair of the lesions. Alternatively, NHEJ is an error-prone joining of DNA ends that requires the use of little or no sequence homology and plays a

major role in the repair of IR-induced DSBs, especially when sister chromatids are not available (4). Which of the repair pathways is used to repair the DSB is dependent on the type of break, the stage in the cell cycle at which the break occurs, and the availability of the sister chromatid and repair proteins. Simple eukaryotes, such as yeast, rely mainly on HR to repair DSBs, while in higher eukaryotes NHEJ predominates, with HR being restricted to the late S/G2 phase of the cell cycle (4; 5). In addition to NHEJ and HR, there is evidence for addition "back-up" repair pathways, but these pathways provide lesser contributions to the repair of DSBs compared to HR and the NHEJ process (6; 7; 8; 9).

1.1.1 Regulation of the DNA damage response

Almost as important as the repair of DSBs is the regulation of the repair pathway used to repair the breaks. Although the two DSB repair pathways could act in parallel, it is suggested that the NHEJ pathway predominates the repair of DSBs in most higher eukaryotes, and it is the initial binding of repair factors to the DNA break may affect the choice of repair mechanism. Within eukaryotic cells the repair pathways are thought to compete for the repair of the DSBs, with each pathway being given preference depending on the cell cycle, type of break, or availability of repair enzymes.

Mammalian cells have been described as having a cell cycle bias towards DSB repair with NHEJ repairing the majority of DSBs during G0, G1 or early S-phase, while HR is restricted to late S/G2 phase (10; 11). The cell cycle restriction of repair pathways may be the most appropriate way of preventing unwanted NHEJ-mediated chromosomal translocations, while utilizing HR when homologous templates are locally present in the form of sister chromatids (10; 11). In addition to a cell cycle regulation, other systems must

be in place to regulate the repair of DSBs and the choice of repair pathway is suggested to be influenced by the availability and interaction of the repair proteins themselves, and this may be best illustrated through the differences in NHEJ bias between mammalian cells and other eukaryotic cells. Yeast and chicken cells repair the majority of DSBs by HR (12; 13), whereas mammalian cells predominantly utilize the NHEJ repair pathway. This NHEJ bias in mammalian cells is reflected in the sheer abundance of the NHEJ repair proteins within the nucleus in mammalian cells as compared with other higher eukaryotes cell (14; 15). Upon induction of DSB, the Ku heterodimer is recruited to DSBs more rapidly than HR factors (16), implying that NHEJ could interfere with HR but not necessarily *vice versa*. In fact, NHEJ is not always the preferred method for repairing DSBs, and under conditions where HR is the preferred method of DSB repair, the presence of Ku at the break site has been shown to have an inhibitory effect on HR (17). In such instances, there must be a mechanism to either prevent Ku from binding to the ends in the first place, or to remove Ku from the DNA ends after binding has occurred.

1.1.2 Homologous recombination

Homologous recombination is considered a more accurate mechanism for DSB repair because the repair machinery uses homologous sequences elsewhere in the genome as a template to prime repair synthesis at the broken ends and can resynthesize gaps or lost information. However repair templates are often not perfectly homologous, which can result in gene conversion (18). The fact that HR repair is predominately restricted to the late S/G2-phase in mammalian cells can be reconciled by the availability of the sister chromatids, a perfectly homologous template for HR, which are readily available during this stage of the

cell cycle. Most of the initial studies defining the HR process were performed in bacteria and yeast in which HR constitutes the main mechanism for DSB repair. The proteins identified through these studies are largely conserved evolutionarily, and homologues for each have been identified in most eukaryotes. In eukaryotes, the protein complexes involved in the HR process include the Rad51 complex (which includes RAD51, RAD52, RAD54, RAD55, RAD57, RAD59), the MRN complex (which includes MRE11 (Meiotic Recombination-11), RAD50 and NBS1 (Nijmegen Breakage Syndrome-1)) and RPA-1(Replication Protein-A) (19).

The HR repair process has four steps: resection, strand invasion, D-loop formation, repair synthesis and resolution of D-loop structure (Figure 1). The initial steps in HR DSB repair is believed to be the nucleolytic resection of the DSB in the 5' to 3' direction to produce 3' single-stranded (ss) DNA tails which acts as a substrate for the follow steps of repair. Next, in a process called strand invasion, one of the ensuing ssDNA tails are then bound by the Rad protein complex forming a presynaptic filament. The Rad51 nucleoprotein filament then searches the undamaged DNA on the sister chromatid for a homologous repair template. Once the homologous DNA has been identified, Rad51 catalyzes strand exchange events in which the damaged DNA strand invades the undamaged DNA duplex displacing one strand, forming a structure called a D-loop (with a shape resembling the letter 'D'). After strand invasion, a DNA polymerase extends the invading 3' strand using information from the undamaged partner, and the ends are ligated by DNA ligase I which results in a Holliday junction (20). Finally, after migration, the Holliday junctions are resolved by cleavage and ligation to yield two intact DNA molecules.

Figure 1. Schematic model of DSB repair by homologous recombination. Homologous recombination can conceptually be divided into four stages: resection, strand invasion, D-loop formation, repair synthesis and resolution of the D-loop structure. During the resection stage, 5' end of the DSB are recognized and processed to a 3'-OH ending single-stranded tail. In strand invasion, the ssDNA tails are bound by the Rad51 complex to generate a presynaptic filament, which invades the sister chromatid in search of a homologous template. The invasion of the homologous DNA and displacement of one strand generates a D-loop structure. After the homologous DNA template is found, a DNA polymerase extends the invading strand and the ends are ligated by DNA ligase I. This results in the formation of a Holliday junction. Finally after migration and ligation, the Holliday junction structures are resolved by a resolvase, cleaving the DNA at the junction and religating the DNA, resulting in either non-crossover or crossover products. Figure modified from (21).

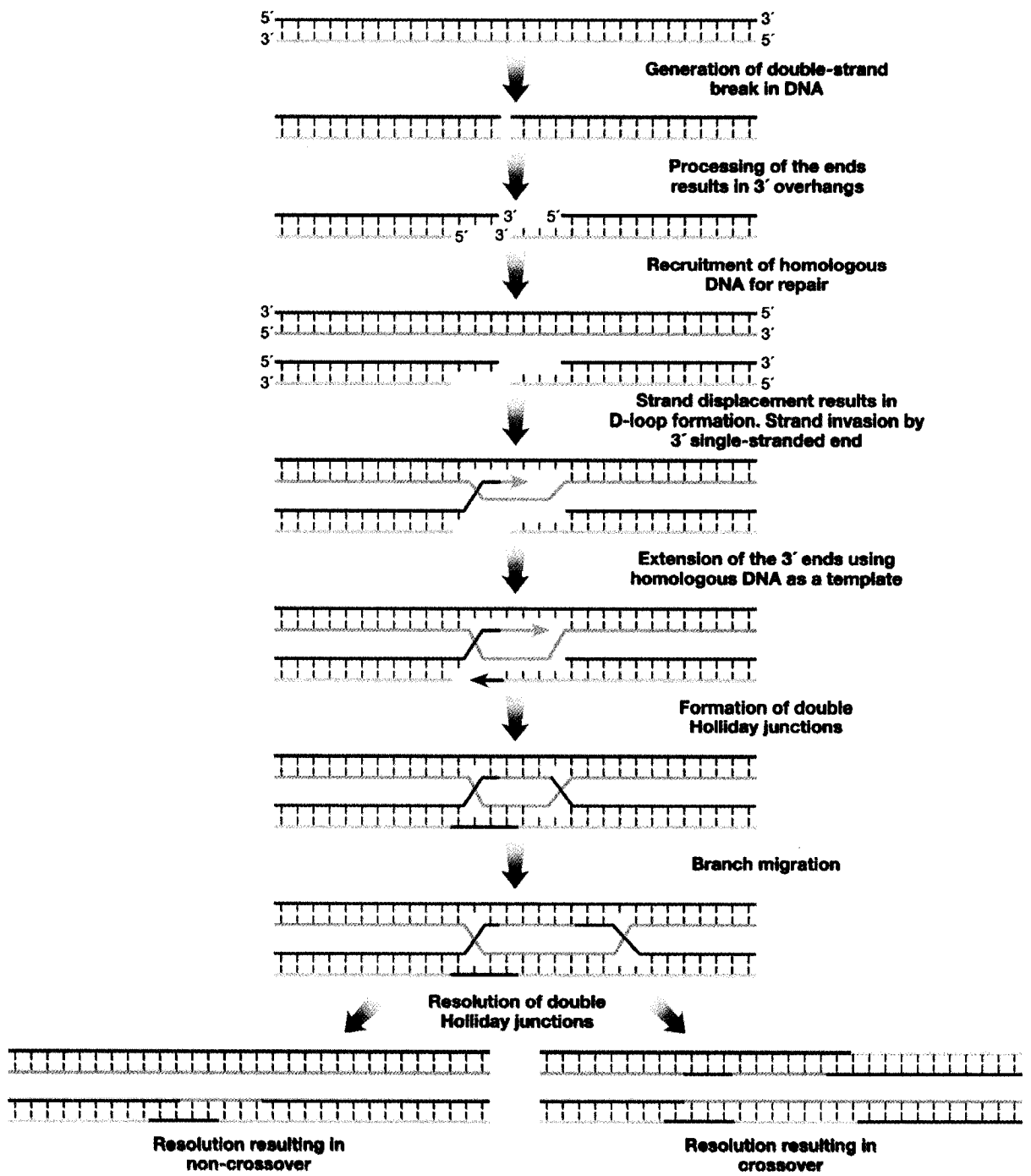
5′
3′
3′
5′
Generation of double-strand break in DNA
Processing of the ends results in 3′ overhangs
3′
5′
5′
3′
Recruitment of homologous DNA for repair
3′
5′
5′
3′
5′
3′
3′
5′
Strand displacement results in D-loop formation. Strand invasion by 3′ single-stranded end
Extension of the 3′ ends using homologous DNA as a template
Formation of double Holliday junctions
Branch migration
Resolution of double Holliday junctions
Resolution resulting in non-crossover
Resolution resulting in crossover

1.1.3 The non-homologous end joining repair pathway

Non-homologous end joining can mediate repair of DSBs whether or not homology between the broken ends is present. In instances where there is no homology between the broken ends, the NHEJ apparatus is able to process the DNA ends and repair the breaks, which leads to the introduction of mutations ranging from loss of nucleotides at the break site to the joining of non-matching termini resulting in translocations. It is for this reason that NHEJ-mediated repair is referred to as "imprecise repair" or "error-prone repair" (10). However, when the broken ends are compatible, NHEJ-mediated repair can ligate the ends without the loss of nucleotides.

The NHEJ apparatus is comprised of a group of proteins that bind and bring together the DNA termini and repair the break through a complex series of ordered events (Figure 2). The core components of the NHEJ apparatus are DNA-dependent protein kinase (DNA-PK), Artemis and DNA ligase IV/XRCC4 (22). DNA-dependent protein kinase is a trimeric nuclear serine/threonine kinase composed of a large catalytic subunit (DNA-PK_{cs}) and a heterodimeric DNA-targeting protein called the Ku heterodimer (Ku). The activity of the core NHEJ components can be supplemented by a variety of other factors, including Cernunos and others, however the extent of their involvement has yet to be fully elucidated (23).

The initiation step of NHEJ is the recognition and binding of the DSB by the Ku heterodimer which facilitates recruitment of the DNA-PK_{CS} to the DSB. Upon binding of DNA-PK_{CS}, the Ku heterodimer moves approximately 10 bp inward, but remains closely associated with the catalytic subunit (24; 25). The simultaneous and specific binding of both Ku and DNA-PK_{CS} to DNA ends activates the serine/threonine kinase activity of

Figure 2. Schematic model of DSB repair through NHEJ. NHEJ is initiated by the recognition and binding of the Ku protein to the broken DNA ends. Ku binds to the broken DNA ends and recruits DNA-PK_{cs}, which mediates synapsis of the ends. Upon recruitment and binding of DNA-PK_{cs}, Ku migrates inward on the DNA providing other proteins access to the DNA lesion. XRCC4, DNA ligase IV and Artemis are assembled at the synaptic complex. DNA-PK_{cs} phosphorylates Artemis activating its endonuclease activity. DNA-PK_{cs} undergoes autophosphorylation and moves away from the DNA ends. XRCC4 and DNA ligase IV process the ends into a compatible substrate and complete the joining reaction. Figure modified from (27).

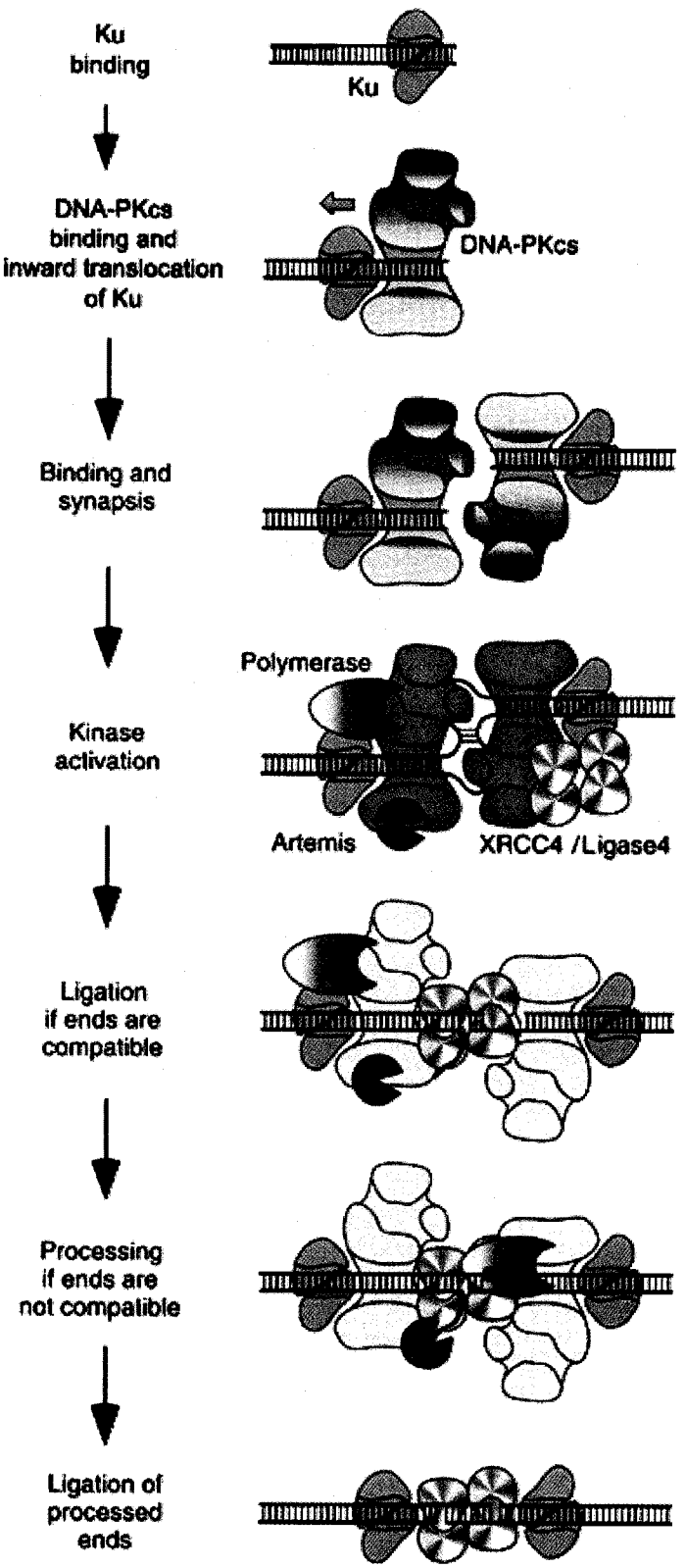
Ku
binding
Ku
DNA-PKcs
binding and
inward translocation
of Ku
DNA-PKcs
Binding and
synapsis
Polymerase
Kinase
activation
Artemis
XRCC4 /Ligase4
Ligation
if ends are
compatible
Processing
if ends are
not compatible
Ligation of
processed
ends

DNA-PK_{CS}. In cases where the DNA ends require further processing, the Artemis protein binds to form a complex with DNA-PK_{CS}, which activates the endonuclease activity of Artemis in an ATP dependent manner (26). The DNA-PK_{CS}–Artemis complex processes the complex breaks and open hairpin structures (22). Once processing of the ends is complete the DNA ligase IV/XRCC4 complex is recruited to and ligates two adjacent DNA ends during NHEJ. In addition to facilitating the binding of the ligase IV/XRCC4 complex to DNA fragments, Ku has been shown to increase the ligation efficiency of ligase IV/XRCC4 by 20-fold (28).

Although there has been a great number of studies focused on resolving how the NHEJ machinery assembles and process the DSB, very few studies have examined how the machinery is disassembled following repair. Once the DNA has been repaired a number of cellular processes need to take place to reestablish cellular functions (i.e. transcription, replication, or re-establishment of heterochromatin) and in order for these processes to occur the repair machinery needs to be cleared from the DNA. For the majority of the repair components, mechanisms for their disembarkment from the repair site have either already been established, or are insinuated through identified modifications. However there is little information suggesting a means for the release of the Ku heterodimer following repair.

1.2 The Ku heterodimer

The Ku heterodimer (Ku) is an abundant nuclear protein comprised of a 70-kiloDalton (kDa) subunit (Ku70) and an 82 kDa subunit (Ku80), with approximately 4×10^5 copies of the dimer per human cell (14; 15). The human Ku70 subunit is composed of 609 amino acids and has a molecular weight of 69,851 Da. The Ku80 subunit consists of 732

amino acids and has a molecular weight of 82,713 Da. The Ku heterodimer is highly conserved amongst eukaryotic organisms, with mice and humans sharing over 80% amino acid identity between the Ku70 subunit, and 78% amino acid identity between Ku80 subunit. Within the nucleus, the Ku heterodimer forms an intricately folded ring-shaped heterodimer. The dimerization of the Ku70 and Ku80 subunits stabilizes each monomer, and artificially decreasing protein levels of one subunit results in a concomitant decrease in the levels of the other (29). The destabilization of the subunits when expressed individually is reflected in the proteins half-life ($T_{1/2}$) in the nucleus; in the absence of Ku70, the Ku80 monomer has a $T_{1/2}$ of 1.5 hours, but when dimerized the $T_{1/2}$ of Ku is over 16 hours (30).

Ku is a versatile DNA binding protein, binding in a specific orientation to double-standed (ds) DNA ends, DNA nicks, gaps, and single-to-double-strand transitions in DNA (15; 24; 31). Given its high affinity for DNA ends, Ku has been implicated in multiple nuclear processes, including the detection and repair of DSBs by NHEJ (32; 33), V(D)J recombination during lymphocyte development (34; 35; 36; 37; 38), DNA replication (39; 40; 41), transcriptional regulation (42; 43), telomere maintenance (44; 45), and stabilization of the genome (46; 47; 48).

Given the numerous roles and pathways that Ku is proposed to be involved in, it is not surprising that there are no reported cases of Ku-deletions in humans and the loss of Ku80 was lethal in human somatic cells (48). However the loss of Ku is not lethal in all organisms, as Ku-deficiencies have been characterized in mice, hamsters and a number of isolated cell lines (29; 46; 49; 50). While each of the deficiencies associated with the loss of Ku can be attributed to the individual roles of Ku in the cell, the majority of the deficiencies can be directly attributed to defects in DSB repair. Ku80-deficient x-ray sensitive mutant 6

(xrs-6) cells, Ku80-deficient Chinese hamster ovarian (CHO) fibroblasts XR-V15B from the XRCC5 (X-ray cross complementing group 5), and Ku70-deficient mouse embryonic cells all exhibited increased radiosensitivity (35; 49; 51; 52; 53; 54). Both mice and cells deficient for either Ku70 or Ku80 were also compromised for V(D)J recombination (49; 55). Double stranded DNA break repair by NHEJ maintains chromosomal stability throughout the cell cycle, and $Ku70^{-/-}$ mouse embryonic fibroblasts (MEFs) exhibited spontaneous fragmentation of chromosomes and nonreciprocal translocations involving two or more chromosomes (47). Similarly, $Ku80^{-/-}$ mouse cells displayed chromosomal breakage, translocations and aneuploidy (46).

Interestingly, the loss of Ku also results in growth defects and premature entry into cellular senescence as Ku70- or Ku80-deficient mice were significantly smaller than their wild-type littermates (49; 56) and isolated fibroblasts from these mice underwent premature senescence (49). Additionally human somatic cells containing a targeted disruption in Ku80 only survived 8 to 10 cell doublings and, compared with its wild-type counterparts, $Ku80^{+/-}$ cells demonstrated slowed cell proliferation (48). Although these studies suggest that the growth defects observed in the mutant cells are probably due to a deregulation of the roles of Ku beyond DSB repair, these studies did not investigate further the mechanism by which the senescence was stimulated (49).

1.2.1 Domain structure of Ku

The Ku70 and Ku80 subunits share the same basic three domain topology: an N-terminal von Willebrand factor A-like (vWA) domain, a central β–barrel Ku core domain, and a helical C-terminal arm (Figure 3) (57). Both the central β–barrel Ku core domains and

Figure 3. The modular structure of the Ku70 and the Ku80 subunits of the Ku autoantigen. (a) The Ku70 subunit consists of 609 amino acids and has a three domain topology comprised of a central β–barrel Ku core domain, an N-terminal von Willebrand factor A-like (vWA) domain, and a helical C-terminal arm. The domain from amino acid residues 257 to 482 is involved in heterodimerization with Ku80 (59; 63; 64; 65; 66). Amino acid residues from 572 to 609 form the so-called SAP (SAF-A/B, Acinus and PIAS) domain, which corresponds to the carboxy- (C-) terminal Ku-80 independent DNA binding domain and contains a helix-loop-helix (HLH) structure (67). The nuclear localization signal (NLS) is localized in amino acid residues from 539 to 556 (60; 61). The von Willebrand factor A-like (vWA) domain covers amino acid residues from 37 to 260 (57; 68). (b) The larger Ku80 subunit consists of 732 amino acids and shares the same basic three domain topology as the Ku70 subunit. The DNA end binding domain covers amino acid residues from 210 to 531 (63; 66). Ku80 also contains a vWA-like domain from amino acid residues 9 to 235 (57). The NLS spans from amino acid residues 561 to 569 (60; 61). Amino acid residues from 261 to 492 are involved in heterodimerization with Ku70 (59; 63; 64; 65; 66). The C-terminal 28 amino acid residues are involved in interaction with the catalytic subunit of DNA-PK (DNA-PKcs) (58; 64). The numbers indicate the positions of amino acid residues in each subunit of the Ku autoantigen. Figure was modified from (69).

a.

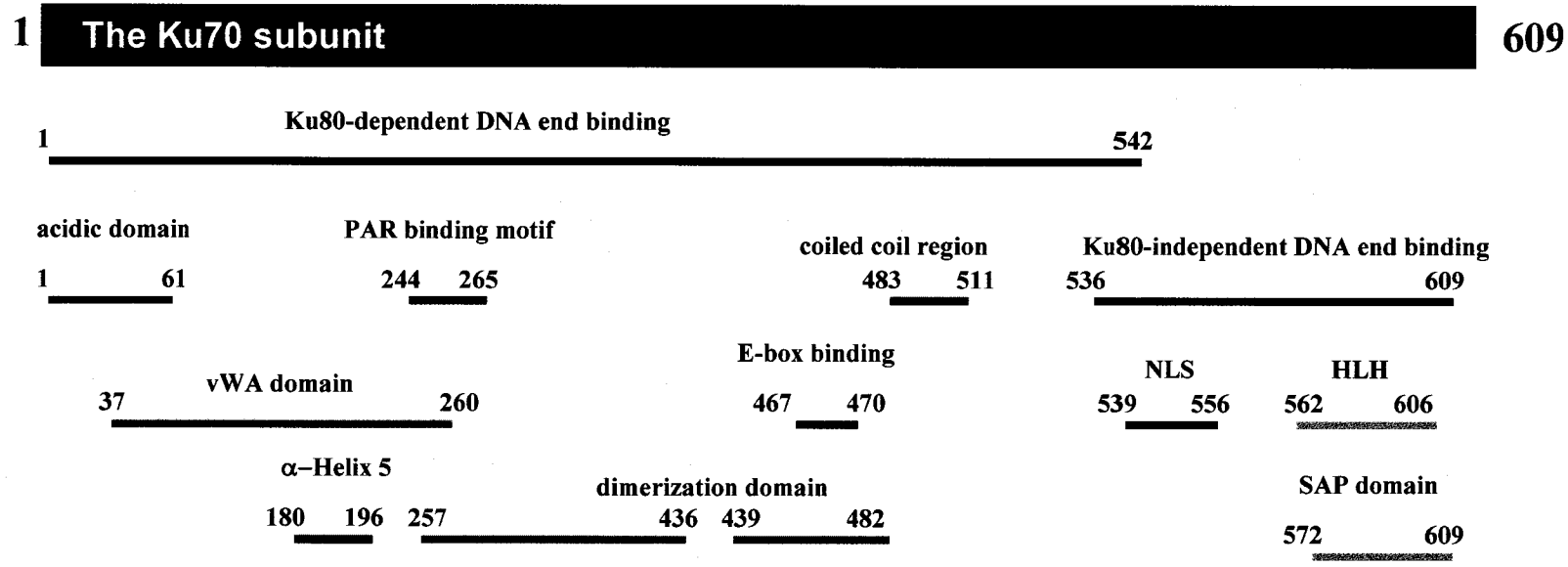
1
The Ku70 subunit
609
Ku80-dependent DNA end binding
1
542
acidic domain
1
61
PAR binding motif
244
265
coiled coil region
483
511
Ku80-independent DNA end binding
536
609
vWA domain
37
260
E-box binding
467
470
NLS
539
556
HLH
562
606
α–Helix 5
180
196
dimerization domain
257
436
439
482
SAP domain
572
609

b.

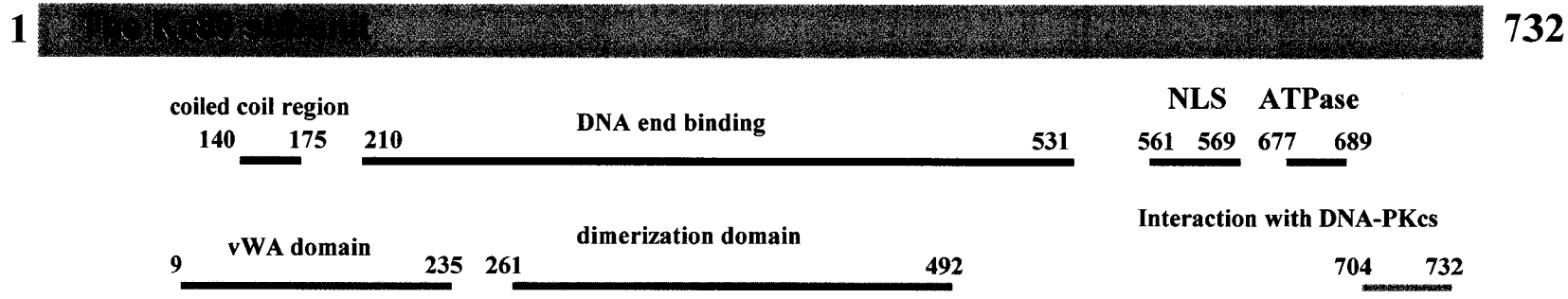
1
732
coiled coil region
140
175
DNA end binding
210
531
NLS
561
569
ATPase
677
689
vWA domain
9
235
dimerization domain
261
492
Interaction with DNA-PKcs
704
732

the vWA domains of Ku70 and Ku80 are required for the heterodimerization of the Ku antigen (58; 59). While each subunit of the Ku autoantigen contains its own NLS (60; 61; 62), it is unclear whether the subunits translocate to the nucleus separately, each utilizing their own NLS, or whether they are translocated together as a heterodimer (62).

The vWA domain of each subunit is proposed to be involved in the protein-protein interactions, however the set of proteins and function of these interactions differs between the two subunits. The vWA domain of Ku70, specifically the α-helix 5, is proposed to be involved in mediating protein-protein interactions with other members of the NHEJ apparatus since mutations within α-helix 5 of Ku70 greatly impaired NHEJ function (33). The vWA domain of Ku80 is required for telomere silencing and mutations in the α-helix 5 resulted in disruption of telomere silencing but did not effect NHEJ function (33).

The DNA binding activity of the Ku heterodimer is attributed to the central β-barrel domain in each subunit, which constitutes a heterodimer-dependent DNA binding domain. The C-terminal arm of Ku70 constitutes an additional DNA binding domain which is suggested to promote Ku80-independent binding (67). Upon formation of the heterodimer, the central β-barrel domain forms a symmetrical round barrel in each subunit and the two β-barrel domains together form a relatively flat base that holds approximately two turns of DNA (65).

The C-terminal domains of Ku70 and Ku80 mediate DNA recognition and protein-protein interactions, respectively. The C-terminal arm of the Ku70 subunit has been characterized as the SAP domain, named after SAF-A/B, Acinus and PIAS motifs (67). The SAP domain is a nucleic acid binding motif which has been identified in RNA-processing factors, scaffold attachment factors, and a variety of DNA repair and chromosome

maintenance proteins, such as PARP1, and is suggested to be involved in the sequence- or structure-specific RNA/DNA binding of these proteins (70). Upon binding of Ku to DNA, the SAP domain translocates from the base of the heterodimer to a come in contact with the DNA, potentially stabilizing Ku on the DNA. Meanwhile, the C-terminal region of Ku80 is implicated in protein-protein interactions, specifically in the recruitment of DNA-PK_{cs} to sites of DNA damage (71). Additionally it has also been shown to interact with the Werner's syndrome protein (64; 71).

The Ku70 subunit also contains a putative poly(ADP-ribose) (PAR) binding zinc finger motif, which is present in proteins that have been shown to bind free PAR polymers in solution (72; 73). This domain was identified in a number of proteins involved in the DNA damage response and checkpoint regulation and binding to PAR is believed to regulate functioning of the protein (73). In isolation this domain was shown to bind purified PAR polymers, and its presence within Ku70 suggest that Ku may be able to bind PAR polymers in solution (72; 73).

1.2.2 The DNA binding activity of Ku is complex

The Ku heterodimer was originally identified as an autoantigen in the sera of patients with the scleroderma-polymyositis overlap syndrome and was characterized as a DNA end binding protein (14; 15; 74). By examining the binding properties of Ku it was been shown that the minimum length of DNA to which a single Ku may bind to is 14 base pairs (bp) (25; 75), while a minimum of 50 bp has been shown to be the required to accommodate two Ku protein molecules (76). Ku is a versatile DNA binding protein: it binds non-specifically to ds DNA ends (14; 15), DNA nicks, gaps or bubbles, and to single-to-double strand

transitions in DNA (31; 75). Ku has also been shown to preferentially bind specific DNA sequences such as the negative regulatory element 1 (NRE1) in the long terminal repeat of mouse mammary tumor virus (77), the early-replicating origin-enriched sequences (*ors*) (40; 78), and the GATA motif of the Glycophorin B (GPB) promoter (79). Once bound to DNA, Ku is able to translocate along DNA in a Mg^{2+}-dependent manner, stalling at internal sites of DNA molecules, possibly these preferential binding sites, in a so-called "bind-and-slide" mechanism (80; 81; 82). While the binding of Ku to these specific sequences has been shown to affect the transcriptional regulation of the genes associated with these sequences (77; 78; 79), the mechanism by which the Ku protein recognizes the sequences has yet to be determined.

Crystallographic analysis of the Ku heterodimer both in the presence and absence of DNA has provided insight into how Ku binds to DNA ends (Figure 4a). Crystallographic structure studies of a truncated form of the Ku protein indicated that Ku loads onto DNA by threading the DNA through the central cavity of the ring-structure, with the Ku70 N-terminal vWA domain oriented toward the DNA terminus, and the vWA domain of Ku80 oriented internally (33; 65; 83). While the crystallographic structural studies show Ku binds to DNA in a specific orientation, they also show that the truncated form of Ku does not form specific contacts with any bases of the DNA duplex, and there are limited contacts with the DNA backbone (65; 84; 85). While these initial crystallographic studies were performed with a truncated form of Ku, which lacked the C-terminal helical arm of both Ku70 and Ku80 (65), further studies have since been performed with the complete Ku heterodimer both in the presence and absence of DNA (Figure 4b). Upon binding to DNA, the C-terminal SAP

Figure 4. The structure of the Ku heterodimer bound to DNA. (a) The crystal structure of the Ku heterodimer bound to a structured 14 bp duplex DNA molecule. The Ku heterodimer binds to DNA in a specific orientation, with the Ku70 subunit oriented toward the free end of the DNA, at outward face of the heterodimer, while the Ku80 subunit is oriented toward the interior of the DNA. The orientation of the heterodimer on the DNA correlates with the proposed roles of each subunit. The Ku70 subunit is proposed to be required for the involvement of Ku in DNA repair, while the Ku80 subunit and the inward face of the heterodimer is proposed to be involved more in the telomeric functioning of the heterodimer. The view from the free end of the DNA helix is shown on the left and the side view on the right. Ku70 is shown in red and Ku80 in yellow and the duplex DNA in gray. The crystal structure was resolved without the C-terminal domains of either the Ku70 or Ku80 subunit. (b) The globular structure of the Ku heterodimer free in solution and bound to DNA. Upon binding to DNA the SAP domain of Ku70 translocates from the base of the heterodimer to come into contact with the DNA. Ku70 is shown in red and Ku80 in blue and the duplex DNA in yellow. The crystal structure model (a) was adapted from (65) and the globular structure (b) was modified from (83).

a.

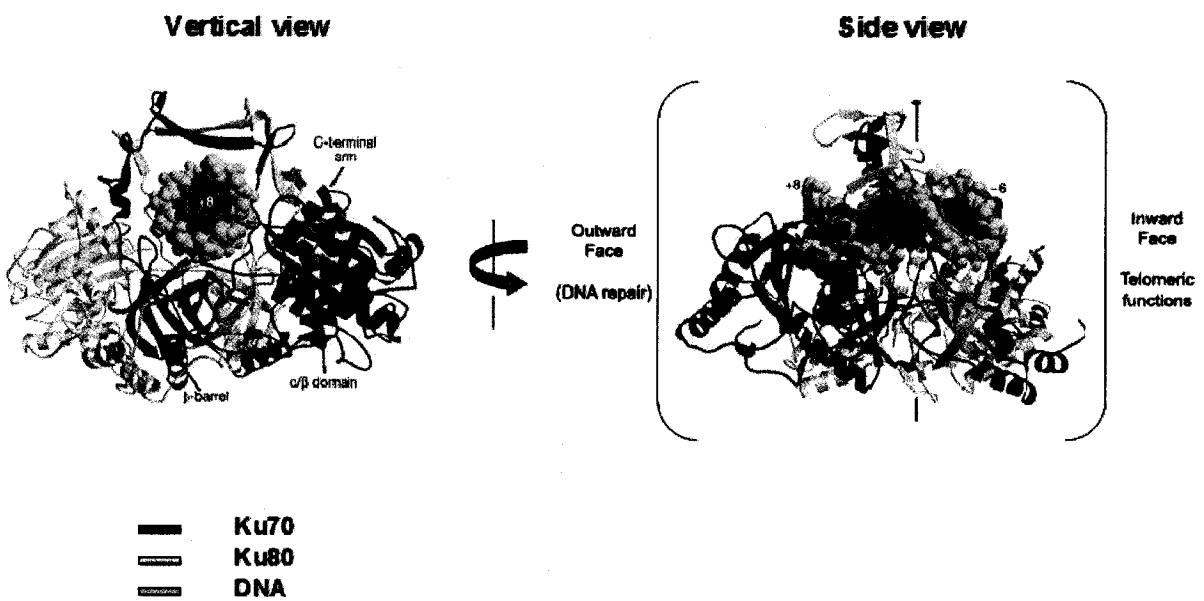
Vertical view
Side view
C-terminal arm
β-barrel
α/β domain
Outward Face
(DNA repair)
Inward Face
Telomeric functions
Ku70
Ku80
DNA

b.

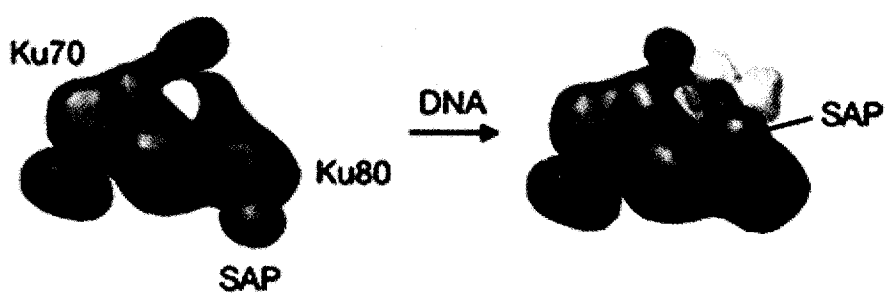
Ku70
Ku80
SAP
DNA
SAP

domain of Ku70 appears to move away from the base of the dimer to being proximal to the ring closing the central cavity and interacting with the DNA, potentially stabilizing the binding of Ku to the DNA and favoring interaction with other DNA repair proteins, such as DNA-PK_{cs} (67; 83). The significance of the presence of a separate DNA binding domain in the C-terminus in Ku70 remains to be established.

The structure of the DNA-PK complex (containing both the Ku heterodimer and DNA-PK_{cs}) on DNA has been resolved using transmission electron microscopy (83; 86; 87). These studies have provided evidence confirming the previous models of NHEJ which suggest that upon recruitment of DNA-PK_{cs} to the DNA end, Ku shifts to the interior of the DNA, allowing access to the end. However, a major question which has continuously resonated throughout the NHEJ process and is amplified by these crystal structures is that of how the threaded Ku complex becomes dissociated from the DNA once the DNA has religated. The crystal structure does not indicate the presence of a hinge-region in the dimerization interface of Ku, nor is there a sequence within either Ku subunit that bears resemblance to a hinge-region, that could readily allow for the release of Ku when it has encircled the DNA. The Ku heterodimer is very stable, both free in solution and bound to DNA, and the crystal structures of Ku in its DNA-free and DNA bound forms are highly similar. However, the structural evidence directly showing that Ku translocates to the interior of the DNA upon recruitment of DNA-PK_{cs} suggests that an active mechanism should exist to allow the removal of Ku from the DNA once repair has been accomplished. This mechanism would seem to require at least a temporary structural rearrangement of the protein, to allow for the escape of the heterodimer from the threaded DNA molecule.

1.3 Ku is integral to V(D)J recombination during lymphocyte development

1.3.1 An overview of V(D)J recombination

In addition to its roles in DNA damage repair, the NHEJ apparatus is utilized in V(D)J recombination, the process by which the antigen receptor genes, immunoglobulins, and T-cell receptors are assembled in the vertebrate immune system (88). The NHEJ apparatus works in collaboration with two lymphocyte-specific *r*ecombination *a*ctivating *g*ene (RAGs) proteins, RAG1 and RAG2, during the V(D)J recombination process (89; 90; 91). This site-specific recombination reaction generates a diverse repertoire of T cell receptor (TCR) and immunoglobulin (Ig) molecules that are necessary for the recognition of diverse antigens from pathogenic invaders and from dysfunctional cells, such as tumor cells. This process is essential for acquired immunity, and animals without it have severe combined immune deficiency (SCID) (32; 92).

This process couples "variable" (V), "diversity" (D), and "joining" (J) coding segments which when assembled together create the variable domain exon of a B-cell immunoglobulin or T-cell receptor genes (Figure 5). Since this variable region encodes the binding pocket for antigens, error-prone repair in V(D)J recombination is beneficial in that it maximizes diversity in the coding sequence of these genes. Thus the utilization of NHEJ contributes to the diversity in the resulting coding sequence.

Within the genome there are multiple copies of the V, D, and J coding segments, each flanked by a conserved recombination signal sequence (RSS). The RSS is comprised of a conserved heptamer sequence (CACAGTG), a conserved nonamer sequence (ACAAAAACC) and a spacer sequence (Figure 5). The spacer sequences are either 12- or 23 bp in length and recombination will only occur between a 12 and 23 spaced RSS, which

Figure 5. Schematic representation of V(D)J recombination and the enforcement of the 12/23 rule. (a) V(D)J recombination brings together the variable (V), diversity (D), and joining (J) gene segments and follows the strict 12/23 rule. Each gene segment is flanked by a recombination signal sequence (RSS) comprised of a conserved heptamer sequence, a conserved nonamer sequence, and a spacer region. The heptamer sequence (CACAGTG) and nonamer sequence (ACAAAAACC) are highly conserved and 5'→3' directionally oriented. The spacer region is either 12 or 23 bp long, and recombination will only occur between a 12-spaced RSS and a 23-spaced RSS, hence the 12/23 rule. (b) The V(D)J pathway. RAG1/2 recognizes and binds to the nonamer of the recombination signal sequences (RSS) and nicks DNA at the coding region 5' of the RSS heptamer. The exposed 3'-hydroxyl group then attacks the other strand with the formation of hairpin-ended coding ends and blunt-ended signal ends. The hairpin-ended coding ends are opened by Artemis following activation by DNA-PK_{cs}. The coding ends and signal ends are subsequently ligated by the NHEJ apparatus including Ku70/80, DNA-PK_{cs}, XRCC4, and DNA ligase IV with the formation of coding joints and signal joints, respectively. Figure has been modified from (100).

a.

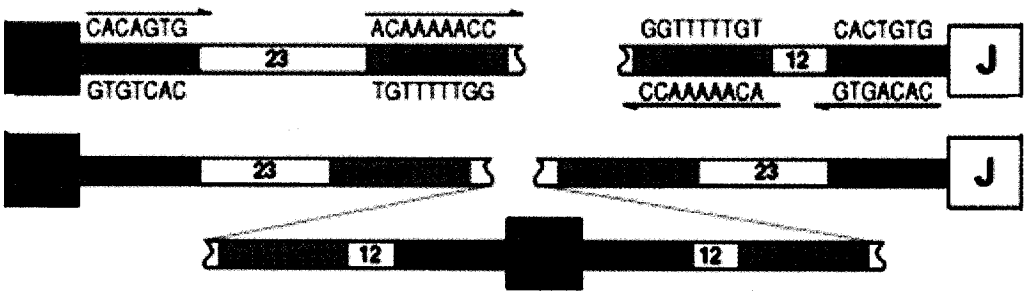

b.

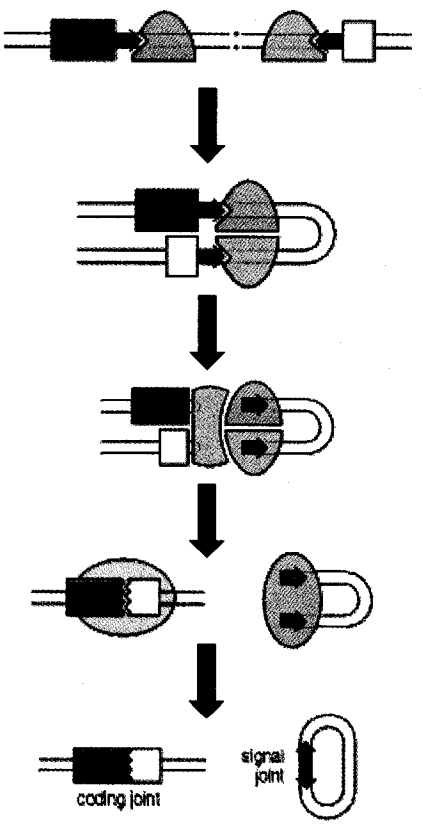

RAG complexes bind to RSSs

Protein complexes bring together gene segments and nick the DNA

NHEJ apparatus bind to the hairpins and the cleaved RSSs

Hairpins are cleaved and ends are processed

The ends are joined to form the coding and signal joints

is referred to as the 12/23 rule. Although the sequence of the spacer is not conserved, the length of the spacer sequence is conserved. The length represents one or two turns of the DNA double-helix, and in turn position the heptamer and nonamer on the same face of the DNA allowing for the enforcement of the 12/23 rule (93; 94; 95). Because V(D)J recombination involves the cleavage and reassortment of genes within the genome, it is important that the process be tightly regulated such that rearrangements occur only within desired cells at desirable times. Restricting V(D)J recombination to lymphoid cells is achieved by restricting the expression of the RAG1 and RAG2 proteins, as well as restricting the accessibility of the RSSs of Ig gene segments (96; 97; 98; 99). Throughout the development of the lymphocytes the levels of RAG2 protein fluctuate in a cell cycle dependent manner, accumulating in the G_0/G_1 phase, coordinating with the initiation of V(D)J recombination, and is degraded at the transition from G1 to S phase (101; 102; 103; 104; 105; 106).

Recombination is initiated by RAG1 and RAG2, which form a complex with the ubiquitously expressed HMGB1 (High mobility group B1) protein, forming a complex that binds to the heptamer/nonamer sequences of a 12- or 23-RSSs. Once bound, the RAG complexes bring together the bound RSSs and nick the DNA at the 5' end of the RSS, and the RAG complex uses the 3'-hydroxyl of the V, D, or J coding end to carry out a nucleophilic attack on the anti-parallel strand to create a hairpin at the coding end, thereby resulting in a blunt signal end that has a 5'-phosphate and 3'-hydroxyl (Figure 5) (107).

The resolution of the V(D)J intermediates can be broken down into two substeps, one that is specific for coding ends and one that is specific for signal ends. The evidence for this is that signal ends almost invariably are joined together in a head-to-head fashion without the

loss or addition of even a single nucleotide while coding ends are often highly modified, with the loss or addition of 1 to 10 nucleotides (108). The opening of the coding end hairpins requires components of the NHEJ apparatus, including Ku, Artemis and DNA-PK_{cs} (26). Further evidence of the roles of the NHEJ apparatus in V(D)J recombination continues to mount, as more and more reports continue to suggest that NHEJ factors, Ku and DNA-PK_{cs} specifically, are present and modulate the cleavage step of V(D)J recombination (38; 69).

1.3.2 The Ku protein is integral to V(D)J recombination

The Ku heterodimer plays an obligatory role in V(D)J recombination as loss of either subunit results in decreased recombination efficiency and accuracy. In $Ku70^{-/-}$ mice, the formation of signal joints and coding joints were each reduced 10- to 100-fold when compared with the wild-type (WT) counterparts and those signal joints recovered were imprecise (29; 49). While in $Ku80^{-/-}$ mice over 80% of thymocytes were arrested at the double negative stage and B cells from the bone marrow were arrested at the immature pro-B cell stage (56). Of the few coding joints formed in $Ku80^{-/-}$ mice, 90% displayed sequence homology suggesting that HR, or another backup repair pathway, was employed for the resolution of the recombination products (109). Furthermore, when *in vivo* transient V(D)J recombination assays using extrachromosomal recombination DNA substrates were performed in Ku80-deficient xrs-6 cells or in V15B fibroblasts, signal and coding joints were rarely formed and of the signal joints recovered from these cells, over 80% were imprecise with large deletions from both RSSs; furthermore, no coding joints were recovered (35; 51; 52; 110).

Although Ku has primarily been implicated in being involved in V(D)J recombination as a component of the NHEJ apparatus, its role does not appear to be limited to the NHEJ apparatus as DNA-PK_{cs}-deficient cells exhibit a distinct and less severe phenotypes from that of Ku70- or Ku80-deficient cells. In both DNA-PK_{cs}-null mice and DNA-PK_{cs}-deficient malignant glioma cell lines M059J, the formation of signal joints occurred at WT levels while no coding joints were detected (54; 111; 112; 113; 114). The severe phenotypes observed in Ku70- or Ku80-deficient cells suggest that the role of the Ku heterodimer extends beyond its functioning within the NHEJ apparatus. It has previously been shown that the Ku heterodimer is able to interact with RAG1/2 and this interaction may facilitate the cleavage of the RSS by RAG1 (69).

1.4 Involvement of the Ku heterodimer in telomere maintenance

Paradoxically, while Ku is required for double-stranded break repair by non-homologous end-joining, in many organisms Ku is also associated with telomeres whose function is to protect chromosomes from end-to-end fusions, a process that is promoted by Ku and NHEJ (44; 45; 115; 116). While located at telomeres, Ku appears to play several important roles, including: regulating telomere addition (117; 118; 119), protecting telomeres from recombination and nucleolytic degradation (120), transcriptional silencing of telomere-proximal genes (119; 121) and nuclear positioning of telomeres (122). The importance of Ku in maintaining telomeres is illustrated by the various morphological abnormalities observed in the chromosomes and telomeres of Ku-deficient cells such as telomere shortening, telomere fusions, and chromosomal translocations (115; 123).

The Ku heterodimer is localized to human telomeric DNA repeats independently of DNA-PK_{cs} (124; 125). Instead its telomere localization is mediated by its interactions with the telomeric-repeat binding factor 1 (TRF1) (126; 127; 128). In addition to the protection of telomeres, Ku recruits telomerase to telomeres and promotes telomerase-mediated lengthening of telomeres by stabilizing the association of TLC1 telomerase (129). This stabilization is mediated through the binding of the stem-loop region of the TLC1 telomerase-associated RNA by the Ku heterodimer (129).

The presence of Ku on the telomere is dynamic, and the levels of Ku associated with the telomere fluctuate with the cell cycle, with Ku being absent from the telomeres during late G2/M phase (129). The disruption of this fluctuation and the persistent residency of Ku on the telomeres during the alignment and separation of sister chromatids has been shown to result in telomere fusions and missegregation of chromosomes (130). Interestingly, while chromatin immunoprecipitation (ChIP) results show that the presence of Ku on the telomeres decreases during late G2/M phase, immunofluorescence (IF) studies show that the net local Ku content does not change (129; 131). This would suggest that Ku is removed from the telomeric DNA through a mechanism which allows Ku to remain in the local environment, without altering the total amount of Ku. Again the exact mechanism by which Ku is removed from the telomeres has yet to be elucidated.

1.5 Poly(ADP-ribosyl)ation and poly-ADP ribose polymerases

Poly(ADP-ribosyl)ation is a post-translational modification catalyzed by a family of conserved cell signaling enzymes called poly-ADP ribose polymerases (PARPs). To date 18 proteins have been classified as members of the PARP family, with the central feature being

Figure 6. The domain architecture of the 17 members of the poly(ADP-ribose) polymerase (PARP) superfamily and of poly(ADP-ribose) glycohydrolase (PARG). The central uniting feature of the PARP superfamily is the presence of a conserved catalytic PARP domain (residues 859–908 of PARP1) that mediates the polymerization of ADP-ribose polymers. Of all the PARP family members, PARP1 and PARP2 are the only members that have been identified as being involved in DNA repair and are the only PARPs whose catalytic activity is dependent upon the protein being associated with DNA. The catalytic activities of other PARPs remain to be fully characterized. The DNA binding activity of PARP1 is direct through two N-terminal zinc (Zn) finger-motifs, while a DNA binding domain (DBD) of unknown structure mediates the DNA binding in PARP2. The remaining members of the PARP family have been shown to catalyze mono- and poly(ADP-ribosyl)ation reactions but may not all be able to carry out the branching reaction, as has been described for PARP1. Of the remaining 15 PARP family members PARP5a and PARP5b (which are also described as Tankyrase-1 and Tankyrase-2, respectively) are the best understood. These two PARPs are active at the telomeres, regulating telomere associated proteins (130; 131; 137). Although not a member of the PARP family, poly(ADP-ribose) glycohydrolase (PARG) is the only identified enzyme which can catabolize the PAR polymers formed by the PARP enzymes. Although splicing variants are known for several members of the PARP family only one variant is illustrated. For complete list of identified domains and their proposed function see Reference (138). Figure has been modified from (138).

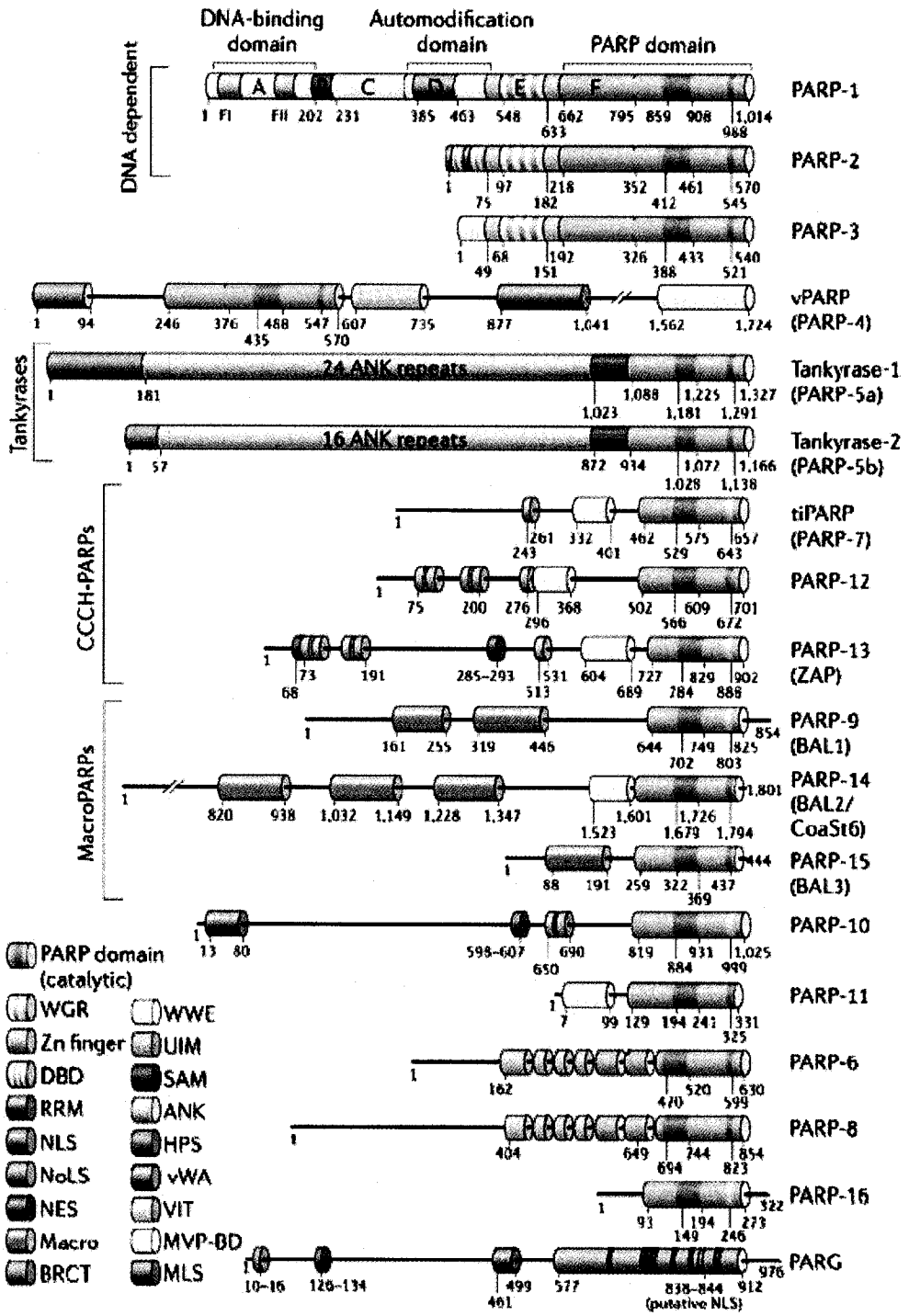
DNA-binding domain
Automodification domain
PARP domain
DNA dependent
A
B
C
D
E
F
PARP-1
PARP-2
PARP-3
vPARP (PARP-4)
Tankyrases
24 ANK repeats
Tankyrase-1 (PARP-5a)
16 ANK repeats
Tankyrase-2 (PARP-5b)
CCCH-PARPs
tiPARP (PARP-7)
PARP-12
PARP-13 (ZAP)
MacroPARPs
PARP-9 (BAL1)
PARP-14 (BAL2/ CoaSt6)
PARP-15 (BAL3)
PARP-10
PARP-11
PARP-6
PARP-8
PARP-16
PARG
PARP domain (catalytic)
WGR
Zn finger
DBD
RRM
NLS
NoLS
NES
Macro
BRCT
WWE
UIM
SAM
ANK
HPS
vWA
VIT
MVP-BD
MLS
(putative NLS)

the presence of a conserved catalytic domain that for some family members mediates the polymerization of ADP-ribose polymers (Figure 6) (132).

When active, PARP enzymes cleave nicotinamide adenine dinucleotide (NAD^+) into nicotinamide and ADP-ribose moieties, and subsequently bind the ADP-ribose to acceptor proteins (Figure 7) (132; 133). Glutamate, aspartate and carboxyterminal lysine residues of target proteins are covalently modified by the addition of an ADP-ribose subunit, via formation of an ester bond between the protein and the ADP-ribose residue (134; 135). Subsequently PARPs can also catalyse the elongation and branching of PAR chains using additional ADP-ribose units from NAD^+ of moieties onto existing protein-bound ADP-ribosyl moieties (136).

The metabolism and catabolism of PAR polymers are dynamic processes and while several enzymes are known to catalyze the synthesis of PAR polymers, there is only one known to catalyze the hydrolysis of PAR to free ADP-ribose: poly(ADP-ribose) glycohydrolase (PARG) (139; 140; 141). PARG exhibits both endoglycosidic and exoglycosidic activity, cleaving the glycosidic bonds between ADP-ribose subunits and degrading both free- and protein associated-PAR polymers into free ADP-ribose (Figure 7; green arrows). While the glycosidic activity of PARG is able to degrade polymers of PAR, it is unable to remove the protein-proximal ADP-ribosyl group from the acceptor protein (133). This primary ADP-ribosyl group is removed by ADP-ribosyl protein lyase, which functions only on mono(ADP-ribose) groups (142). Because of the proficient glycosidic activity of PARG, the PAR polymers have a rather short lifespan, from a few seconds to several hours, and therefore the accumulation of PAR polymers is a transient event (143).

Figure 7. Metabolism and catabolism of poly(ADP-ribose). In the event of DNA breaks, PARP1 binds to the free DNA ends and becomes catalytically active. Once active, PARP1 hydrolyzes NAD^+ to polymerize poly(ADP-ribose) chains onto specific amino acid side chains of the target protein, with the associated release of nicotinamide. The metabolism of poly(ADP-ribose) and ribosylation of target proteins by PARP1 occurs in the three steps of (red part of the cycle): (1) mono(ADP-ribosyl)ation of the glutamate or aspartate residue of the target protein; (2) elongation and (3) branching of the poly(ADP-ribose) chain. Branching occurs on average every 20-50 ADP-ribose units (153). The negatively charged poly(ADP-ribose) has a short half-life owing to PARG (green side of the cycle) that is activated by an increase in the cellular concentration of poly(ADP-ribose). PARG carries exo- and endoglycolytic activities that cleave the glycosidic bonds between ADP-ribose subunits (green arrows) (142; 154). Figure modified from (155).

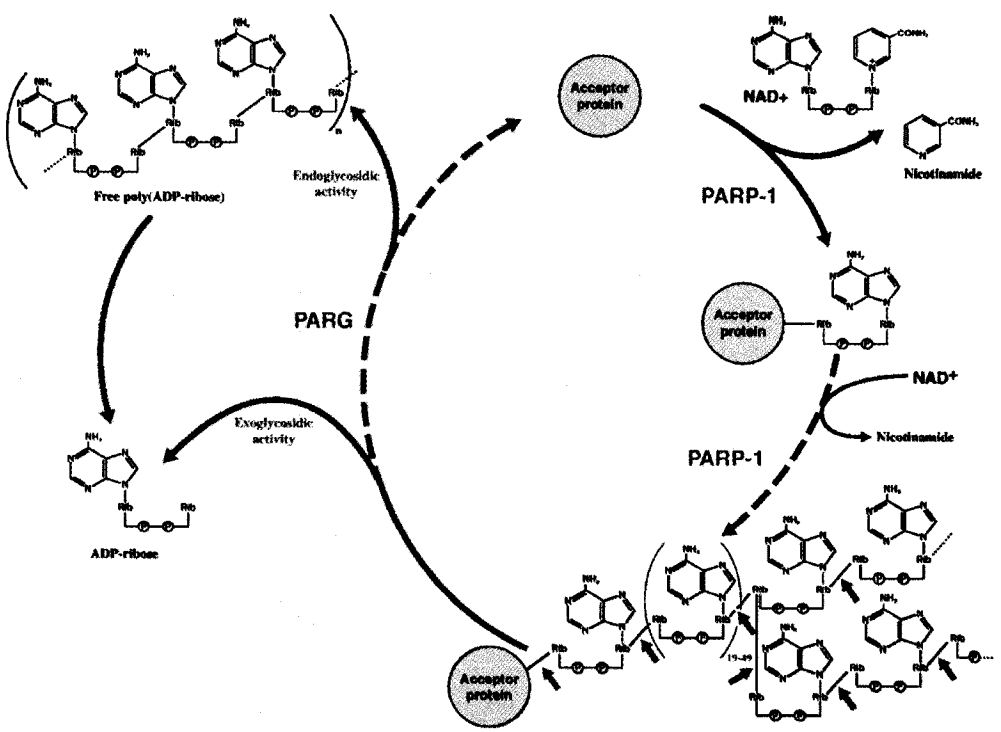
Free poly(ADP-ribose)
Endoglycosidic activity
Acceptor protein
NAD+
Nicotinamide
PARP-1
PARG
Acceptor protein
NAD+
Nicotinamide
PARP-1
Exoglycosidic activity
ADP-ribose
Acceptor protein

Many nuclear proteins have been identified *in vitro* and *in vivo* as being modified by PARPs, with the autoribosylation of PARP1 itself being the primary target for ribosylation (144). The proteins which have been shown to be ribosylated including histones (134; 135), DNA polymerases (145), DNA repair enzymes (146; 147), topoisomerases (148; 149), DNA ligases (150), and transcription factors (151). As opposed to many other post-translational modifications, ribosylation can greatly vary in its chain length and its complexity, with chain lengths extending up to 200 units and with multiple branch points (152). The functionality of ribosylation is not only mediated through the sheer size of the complex PAR chains, but also with the ensuing accumulation of negative charges which in turn will result in alterations in the activity of the ribosylated target protein, or its association with DNA (133).

1.5.1 PARP1

Of the PARP family members, PARP1, is the most abundant and catalyzes over 90% of the PAR synthesis that occurs in response to DNA strand breaks (156). PARP1 is a 113 kDa protein, with three functional domains: an N-terminal DNA binding domain (DBD), a central automodification domain, and a C-terminal catalytic domain (Figure 6) (132). In addition to the two zinc fingers, the DBD of PARP1 contains helix-turn-helix (HTH) motifs that are suggested to bind secondary structures in DNA (132; 136; 138). PARP1 contains an NLS which is located within the DBD, between the zinc fingers and the HTH motif. The C-terminal catalytic domain, the common domain of all members of the PARP family, is required for the formation of branched ADP-ribose polymers from NAD^+. The automodification of PARP1 occurs mostly in the central region of the enzyme that

contains 15 conserved glutamate residues (155; 157). In addition to being the site of automodification, this central region also contains a BRCT protein-protein interaction motif, which has been shown to interact with the BRCT domain of XRCC1 (147).

PARP1 binds to single- or double-strand DNA breaks via two amino-terminal zinc finger domains, which in turn stimulates its catalytic activity 500-fold (144). It is the induction of this robust catalytic activity that has implicated PARP1 and the formation of PAR polymers in many roles in the cell: regulation of transcription, genome stability, initiation of apoptosis, chromatin remodeling, and DNA break repair and protection (136; 158). PARP1 may transduce DNA strand break signals to downstream effectors by translating and amplifying the damage signal into an array of protein-bound PAR polymers (159).

1.5.2 PARP1 and DNA damage response

Of the 18 PARP family members, only PARP1 and PARP-2 have been shown to be stimulated by the presence of DNA breaks or strand interruptions (132; 159). Although PARP1 has been implicated as having multiple roles in the cell, its primary physiological role appears to be in DNA damage response. PARP1 is highly efficient in detecting DNA nicks, breaks and strand interruptions through its two zinc fingers domains and upon detecting these various forms of genotoxic stress PARP1 activity is robustly induced. This activation of PARP1, and the resulting synthesis of PAR, is believed to: 1 – relax the chromatin fibers and increases the access to breaks through ribosylation of histones H1 and H2B (134; 135) 2 – relay the signal of the occurrence and the extent of DNA damage so that

the cell can establish an adaptive response according to the severity of the injury (136; 160), and 3 – promote the recruitment of repair factors to the site of the lesion (161; 162).

Although loss of PARP1 is not lethal, chemical inhibition of PARP1 activity or dominant negative mutations within PARP1 compromise the repair of DNA damage (17; 156; 163). Additionally, PARP1 defective DT-40 cells show reduced levels of HR (164), and PARP1 knockout mice show an increased sensitivity to IR, an increased number of gene conversions and sister chromatid exchanges; which also highlights the importance of PARP1 in HR (165; 163). The deregulation of HR in PARP1 knock-out cells was restored by mutating components of the NHEJ pathway, including the Ku heterodimer (17; 164). These studies have lead to the suggestion that PARP1 plays a regulatory role in HR, directing DSB repair towards HR, however it is not clear whether PARP1 could also have a direct facilitatory role in NHEJ (166; 167).

1.6 Interaction of PARP1 and Ku

Given the high affinity that both PARP1 and Ku have for DNA strand breaks, their numerous overlapping roles in the cell (from DNA repair to chromatin maintenance), and their subcellular co-localization (matrix attachment regions, telomeres and DNA breaks), it is speculated that the interaction of the two proteins may be important for their functioning (168; 169), and there also may be some functional overlap between the two (17; 169; 170). Biochemical studies have shown that following DNA damage, PARP1 and Ku may compete for binding of DNA ends (17), and PARP1 and Ku co-immunoprecipitate from mammalian cell extracts (171; 172; 173). Several studies have shown that PARP1 and Ku co-localize to matrix attachment sequences suggesting a potential role in chromatin maintenance (171;

172). In PARP1 knock-out cells, the binding of Ku to DSBs prevents HR proteins from accessing and repairing the break site, and the ectopic expression of PARP1 re-establishes HR-mediated repair (17). While the concomitant decrease in binding affinity suggests ribosylation of Ku could mediate the release of DNA bound Ku, and the absence of PARP activity results in Ku-directed deregulation of repair, there has been no evidence showing that PARP1 is able to directly affect the presence of Ku at DSBs. Taken together these studies suggest that PARP1 and Ku interact *in vivo* in several cellular pathways, which is highlighted by the observation that mice containing a double mutant in both PARP1 and Ku80 die during early embryonic development, and cultured blastocysts display increased levels of apoptosis (169; 170).

While there is clearly a functional significance of the interactions between Ku and PARP1, little is known about the molecular nature of these interactions. *In vitro* studies using purified components in solution were able to show that PARP1 is able to ribosylate Ku (174; 175), and this ribosylation causes a decrease in the binding affinity of Ku (174). It is possible that one component of the interaction between PARP1 and Ku is the regulation of the DNA binding activity of Ku through ribosylation; however these studies did not address this possibility.

1.7 Principal objectives of the current research project

In vitro, Ku bound to DNA forms a very stable complex, remaining intact for over 24 hours (176; 177), however *in vivo* studies show that Ku on DNA ends is in a dynamic equilibrium with the Ku heterodimers in solution, cycling on and off the end with a half-life of 2 minutes (178). Additionally, in the presence of magnesium (Mg^{2+}), Ku is able to slide inward on the DNA, and can be entrapped on the DNA following ligation of the ends (81;

177; 77). When entrapped on closed circular DNA (ccDNA), these Ku:ccDNA complexes are very stable, even in the presence of 2M NaCl (81). Together these results suggest that Ku on its own is not sufficient to leave DNA and that a mechanism exists to remove Ku from the DNA – either when Ku is at the DNA ends, or when Ku is on the interior of DNA after ligation of the ends has occurred. Currently, there is no evidence describing a mechanism for either scenario, however the reports that PARP1 may influence the affinity of Ku for DNA suggests the potential for the involvement of PARP in the removal of Ku from DNA.

It is my hypothesis that: **1** - dissociation of Ku from DNA during NHEJ is a facilitated process and; **2** – ribosylation of Ku by PARP1 regulates the interaction of Ku with DNA.

My first objective was to determine whether the DNA-bound Ku could be released from the DNA by the activity of PARP1 *in vitro*, through electrophoretic mobility shift assays (EMSAs). This would be the first detailed investigation into the regulation of the DNA binding activity of Ku by another protein and should reveal whether PARP1 can regulate the association of Ku with DNA through ribosylation.

The second principal objective was to identify the mutations within the Ku heterodimer that abrogated the PARP1-mediate release of Ku from DNA and to determine the effect of these mutations on various roles of Ku *in vitro* and *in vivo.* This identification and characterization was performed through mutational analysis of the Ku subunits in concert with EMSAs, *in vitro* ^{32}P-NAD^{+} ribosylation assays, and *in vitro* binding assays. The generation of a novel binding assay allowed the analysis and manipulation of Ku on closed circular DNA, and should reveal whether PARP1 can regulate binding Ku in the

absence of a free DNA end. The *in vitro* characterization of the PARP1 insensitive mutants of Ku heterodimer will provide further information on the effect of PARP1 on the association of Ku with DNA.

The third principal objective was to determine the significance of the association of Ku with DNA *in vivo*. By utilizing the *in vitro* characterized mutations that prevent the loss of Ku from DNA, it will be possible to examine the *in vivo* effects of these mutations on the global functioning of Ku within the cell, with particular focus on the cell proliferation, cell survival following genotoxic stress, the retention of Ku at sites of DNA damage, and the ability of Ku to efficiently and accurately perform V(D)J recombination.

2. Materials and Methods

2.1 Chemicals, reagents and antibodies

The anti-Ku (p70/p80) Ab-3 (clone 162) antibody, used for immunoprecipitation, was purchased from Lab Vision Corporation (Fremont, CA). The anti-Ku80 Ab-2 (clone 111) antibody and the anti-Ku70 Ab-4 (clone N3H10) antibody, used for western blot analysis, were also purchased from Lab Vision Corporation (Fremont, CA). The anti-phospho-histone H_2AX (ser139), used for western blot analysis and immunofluorescence, was from Upstate Cell Signaling Solutions (Lake Placid, NY). The anti-GFP polyclonal antibody used for immunofluorescence was from Clontech (Mountain View, CA).

The PARP inhibitors 4-amino-1,8-naphthalimide (4-ANI) and 3-aminobenzamide (3-AB) were bought from Sigma-Aldrich (St-Louis, MO). Purified PARP1 and PARG were purchased from Trevigen (CAT#4668-100-01 and CAT#4680-096-01, respectively). The transition from 3-AB to 4-ANI was reflective of the transition from in vitro studies to in vivo studies. While 3-AB is a good inhibitor of PARP activity, the benzamide class of PARP inhibitors show limited intracellular accumulation and exert some non-specific actions. Therefore the concentration of 3-AB required to produce an adequate inhibitory effect on PARP would be overshadowed by the non-specific actions of the drug.

As an alternative I decided to use 4-ANI for the in vivo studies. In living cells, 4-ANI is about 1000-fold more potent at inhibiting PARP activity compared with 3-AB. Additionally, 4-ANI is less toxic than 3-AB. It was previously shown 4-ANI showed 3-4 fold more inhibitory potency against PARP1 than against other members of the PARP family.

2.2 Oligonucleotides, PCR primers, plasmids and vectors

2.2.1 Oligonucleotides and PCR primers

The oligonucleotides and PCR primers used in the experiments were purchased through Invitrogen as a lyophilized powder and were resuspended in TE buffer (10 mM Tris-HCl, 0.5 mM EDTA, pH 7.4) to a final concentration of 150 μM. The primer sequences, along with their annealing temperatures are listed in Appendix I and II.

2.2.2 Plasmids

The extrachromosomal recombination DNA substrates pJH200 and pJH290, were generously provided by Dr. M. Gellert (National Institute of Health, Bethesda, MD, USA), and are previously described (179; 180) as well as elsewhere in the text. Following amplification in *Escherichia coli* (*E. coli*) DH5α (Invitrogen, Cat#18258-012), large scale preparations of plasmids were purified using QIAgen Maxi prep Kit (QIAgen, Cat#12163) as per the manufacturer's instructions.

2.2.3 Expression vectors

The bicistronic bacterial expression vector pET70H80 encoding both the Ku70 and Ku80 subunits of the human Ku heterodimer, was a generous gift provided by Dr. L.A. Hanakahi (Johns Hopkins University, Baltimore, MD, USA). The mammalian expression vector EGFP-Ku70 was made previously in the laboratory (181). The EGFP-Ku70^{3E} expression vector was generated using EGFP-Ku70 as a template for Stratagene's PCR mutagenesis kit (CAT#200518), as described in detail elsewhere in the text; the PCR primers designed for the site directed mutagenesis are listed in Appendix I. The EGFP-Ku70

expression vectors were propagated in *E. coli* DH5α and large scale plasmid DNA was purified using QIAgen Maxi prep Kit (QIAgen, CAT#12162) as per the manufacturer's instructions.

The mammalian expression vectors pRAG1 (M2CD7) and pRAG2 (R2RCD2) encoding the full-length murine RAG1 and RAG2, respectively, were previously described and kindly provided by Dr. M.A. Oettinger (Harvard University, Boston, MA, USA). These expression vectors were grown in *E. coli* MC1061/P3 (Invitrogen, CAT#C663-03) and large scale plasmid DNA was prepared by using alkaline lysis followed by cesium chloride/ethidium bromide gradient centrifugation (182).

2.3 Expression and purification of recombinant proteins

2.3.1 Bacterial expression and purification of Ku

The expression and purification of the Ku heterodimer in BL21(DE3)pLysS Rosetta *E. coli* (Novagen, Cat#70956) cells was previously described (183). Briefly, Rosetta *E. coli* transformed with the pET70H80 construct were plated on Luria-Bertani (LB) broth plates containing ampicillin (Amp; 100 μg/mL) and chloramphenicol and grown at 37°C overnight. Single colonies were chosen to inoculate a large-scale culture (1 L) of LB containing Amp which was grown at 37°C until the culture reached OD_{600} 1.0. Expression of the Ku heterodimer was induced at 25°C with 0.3 mM IPTG and cultured for 18 hours. Cells were harvested by centrifugation at 4°C for 15 min at 8000 g. The resulting cell pellet was resuspended on ice in 25 mL of ice cold lysis buffer (50 mM Tris, pH 8.0, with 1 M NaCl, 0.4 M $(NH)_4OAc$, 10 mM imidazole and 2 mM 2-mercaptoethanol (BME), 5% glycerol and 1 mM phenylmethanesulphonyl fluoride (PMSF)) per gram of cells. The cell slurry was

sonicated with a Branson Sonifier 450 (20% output at 25% duty cycle 5 x 30 sec.) and insoluble material was removed by centrifugation at 4°C for 30 min at 25000 g. A Talon metal-affinity resin (Clontech, CAT#635501) column was prepacked and precleared with lysis buffer prior to addition of lysate. Lysate was passed through column at 4°C. After binding, the column was washed twice with lysis buffer followed by two washes with wash buffer (50 mM Tris, pH 8.0, 50 mM NaCl, 5% glycerol, 1 mM PMSF) at 4°C. Bound proteins were eluted from the column with 5 volumes of elution buffer (50 mM Tris, pH 8.0, 50 mM NaCl, 0.5 M imidazole, 5% glycerol and 1 mM PMSF). The eluted protein was loaded directly onto a 1 ml Hi-Trap heparin column (GE, CAT#17-0406-01) that had been equilibrated in HEq buffer (50 mM Tris, pH 8.0, 50 mM NaCl, 0.5 mM EDTA, 5% glycerol, 1 mM PMSF and 1 mM 1,4-dithiothreitol (DTT)) then eluted with HElu buffer (50 mM Tris, pH 8.0, 1 M NaCl, 0.5 mM EDTA, 5% glycerol, 1 mM PMSF, and 1 mM DTT). Peak fractions were pooled and dialyzed against buffer containing 50 mM Tris, pH 8.0, 50 mM NaCl, 0.5 mM EDTA, 20% glycerol, 1 mM PMSF and 1 mM DTT.

2.3.3 Generation of Ku deletions and point mutants

Deletions and point mutants within the Ku70 subunit were generated using Stratagene's PCR mutagenesis kit (CAT#200518) and using the pET70H80 construct as a template. The primer pairs employed are listed in Appendix I. Briefly, primers were designed for both DNA strands containing the desired mutation and 5' and 3' complementary sequence. Each reaction contained 125 ng of each primer, 50 ng of the template plasmid, 100 μM dNTP mix (0.2 mM of each dNTP), PfU reaction buffer, and 2 units (U) of the Pfu polymerase. Following completion of the PCR reaction, 10 U of *Dpn* I

was added directly to each reaction and incubated at 37^0C for 1 hour, to digest away the reaction template. The remaining PCR product was then transformed by electroporation into competent DH5α *E. coli*. In all cases, clones were screened using restriction enzyme digests to confirm the insert orientation followed by DNA sequencing. Upon sequence confirmation, mutant constructs were transformed and expressed in BL21(DE3)pLysS Rosetta *E. coli* as described previously.

2.4 Cells, infections and transfections

2.4.1 Cell culture

Human embryonic kidney 293T/17 cells (ATCC CRL-11268), and Chinese hamster ovary (CHO) fibroblasts $Ku80^{-/-}$ V15B (ATCC CRL-2349) were maintained in Dulbecco's Modified Eagle's medium (DMEM) (Gibco-BRL) supplemented with 10% fetal bovine serum (FBS) (JRH Biosciences), penicillin and streptomycin, at 37°C with 5% CO_2. Cells were passed at confluency in 1 to 4-8 dilutions for 293T cells and 1 to 8-12 dilutions for V15B fibroblasts.

Mouse embryonic fibroblasts (MEFs) and Ku70-/- MEFs were a generous gift from Dr. Matsuyama (184). Mouse embryonic fibroblasts (MEFs) were maintained at 37°C with 5% CO_2 in DMEM supplemented with 15% FBS in the presence of 50 μM BME (Sigma) and 1x antibiotic cocktail mixture (containing penicillin (50 μg/mL), streptomycin (100 μg/mL), and fungizone (100 μg/mL); Invitrogen). Cells were passed at confluency in 1 to 4-8 dilutions. Stably transfected MEFs were maintained in the presence of 1.0 μg/mL puromycin (Sigma).

2.4.2 Transient transfection of MEF cells

For transfection, MEFs were seeded at a density of 4.0 x 10^5 cells per 60 mm tissue culture dish and cells were transfected the following day. For the *in vivo* V(D)J recombination assays, MEF cells were co-transfected at 60 to 70% confluency with pRAG1, pRAG2, and either pJH200 or pJH290, in 6-well dishes using Lipofectamine 2000 Transfection Reagent (Invitrogen, CAT#11668-019) according to the manufacturer's instructions. Lipofectamine Transfection Reagent was used in a ratio of 3 µl of the reagent to 1 µg of total plasmid DNA. Briefly, 24 µl of Lipofectamine 2000 Transfection Reagent was added to 200 µl of serum-free DMEM and, after gently mixing, 2 µg of each plasmid were added followed by incubation for 20 min at room temperature. Thereafter, the mixture was transferred drop-wise to the tissue culture dish followed by 2 days of incubation at 37°C.

2.4.3 Transient transfection of 293T cells

For transient transfection of 293T cells with EGFP-Ku70 and EGFP-Ku70^{3E} constructs, transfection reaction was prepared as described above (Section 2.4.2) using 2 µg vector DNA and substituting FuGENE transfection reagent for the Lipofectamine 2000. Following transfection, 293T cells were washed twice with DMEM and incubated at 37°C for 18 hours, after which cells were split onto 18 mm cover slips.

2.4.4 Retroviral propagation and infection

Replication incompetent pBABE-puro-based (Clontech) retroviruses were generated by transfection of Phoenix Ampho (ATCC SD3443) packaging cells. Phoenix cells were

seeded at a density of 1.0 x 10^6 cells per 60 mm dish. The following day cells were transfected with 10 μg of the retroviral vector using FuGENE transfection reagent (Roche, CAT#1-814-443). In a 1.5 mL microfuge tube, 6 μl of FuGENE reagent was added to 94 μl room temperature serum-free DMEM, making sure that the undiluted FuGENE did not touch the walls of the microfuge tube. After incubating the FuGENE/DMEM mixture at room temperature for 5 min, 2 μg of vector DNA was added. The tube was mixed by tapping and the mixture was incubated at room temperature for 20 min. The mixture was added drop-wise onto the Phoenix cells. The cells were returned to the incubator for 18 hrs after which the media was changed. The following day the viral supernatants were collected and filtered through a 45 μM syringe filter. In 10 cm dishes, 1-2 x10^6 Ku70$^{-/-}$ MEF cells (20-30% confluent) were infected overnight using 1 ml of viral supernatant mixed with 4 ml of media containing 4 mg/ml polybrene. The infection was stopped by adding 6 ml of media to the plate. After 48 hr of infection the cells were selected in media containing 2.0 μg/ml puromycin for 10 days prior to ensure expression in all cells.

2.5 Preparation of whole cell extracts

Cells were rinsed twice with ice cold PBS and scraped in 500 μl PBS into 1.5 mL microfuge tubes using a rubber policeman. Cells were pelleted by centrifugation at 4°C for 5 min at 4000 g. For immunoprecipitation or direct Western analysis, cell pellets were resuspended in 100 ml of IPH buffer (50 mM Tris pH 7.4, 150 mM NaCl, 0.5% Nonidet P-40, 5 mM EDTA, 1 mM DTT, complete protease inhibitor cocktail). Cells were allowed to swell on ice for 10 min and were then sonicated for 10 s at a 30% duty cycle. Cell extracts were centrifuged at 13000 g for 5 min at 4°C to pellet cellular debris and the supernatants

were transferred to fresh tubes. For release assays, cells were resuspended in 300 µl whole cell lysis (WCL) buffer (25 mM *N*-2-hydroxyethylpiperazine-*N'*-2-ethanesulfonic acid (HEPES) pH 7.5, 300 mM NaCl, 1.5 mM $MgCl_2$, 0.5 mM EDTA, 5% glycerol, 0.5% Triton-X 100, 2 mM DTT and protease inhibitor cocktail) and allowed to swell on ice for 10 min. Extracts were produced using three cycles of freezing in methanol and dry ice followed by thawing at 37°C and vortexing. Cell extracts were centrifuged at 13000 g for 5 min at 4°C to clear cellular debris and the supernatants were transferred to fresh tubes. In both cases the concentration was determined using a Bradford Assay kit (BioRad; CAT#500-0006). Extracts were aliquoted and stored at -80°C for future use.

2.6 Electrophoretic mobility shift assays

Electrophoretic mobility shift assays (EMSAs) were performed using purified proteins and ^{32}P-labeled 30-mer oligonucleotides were used as a DNA probe (sequences are listed in Appendix I). The oligonucleotides were radiolabeled at 37°C for 30 min with [γ-^{32}P]-ATP by T4 polynucleotide kinase (New England BioLabs) in a 20-µl reaction containing 50 mM Tris-HCl (pH 7.5), 10 mM $MgCl_2$, 10 mM dithiothreitol (DTT), 1 mM ATP and 25 µg/ml bovine serum albumin (BSA) and purified using ProbeQuantT G-50 Micro columns (GE Healthcare, CAT#28-9034-08). DNA binding was performed in a 20 µl reaction mixture consisting of 21 ng of purified Ku was incubated with 2-5 pmol ^{32}P-labeled DNA probe (generally 10 000-30 000 c.p.m.) in EMSA Binding (EB) buffer (100 mM Tris pH 8.0, 5 mM $MgCl_2$, 6% glycerol, 50 mM NaCl, and 2 mM DTT) at room temperature for 30 minutes. Sheared calf thymus competitor DNA (200 ng; 200-500 bp), 150 µM of NAD^+, and 3-AB (2.5 mM) were included wherever described.

2.6.1 Release assays

Following prebinding incubation of Ku to DNA, dialyzed V15B extract (5 μg) or purified PARP1 (15 ng) was added to reaction mixture and the reactions were incubated at 30°C for indicated time. The reactions were separated on 5% non-denaturing polyacrylamide (29:1 Bis:Acrylamide) using 0.5x TBE running buffer. Following electrophoresis, the gel was dried on a gel dryer apparatus (BioRad; Model 583) and exposed to PhosphorImager screen (Molecular Dynamics) for 1 hour and retarded bands were quantified using IMAGEQUANT software (Molecular Dynamics).

2.6.2 Autoribosylation of PARP1

For assays performed with autoribosylated PARP1 purified PARP1 (50 ng) was incubated at 30°C with 200 ng unlabeled sheared calf thymus DNA in EB buffer containing 150 μM of NAD^+ for 30 minutes. Following the autoribosylation reaction, any further PARP activity was inhibited by the addition of 2.5 mM 3-AB and incubation at room temperature for 5 minutes. The autoribosylated PARP1 was then added to the Ku:DNA complex mixture and the reaction was incubated at 30°C for the indicated time. The reactions were separated on 5% non-denaturing polyacrylamide and the gel was dried and exposed to PhosphorImager screen and retarded bands were quantified using IMAGEQUANT software.

2.6.3 Rebinding reaction with PARG

Following prebinding incubation of Ku to DNA, purified PARP1 (50 ng) was added to the reaction mixture and the reactions were incubated at 30°C for 60 minutes. Further

PARP activity was inhibited by the addition of 2.5 mM 3-AB. PARG was then added to the reaction and the reaction was incubated for an additional 30 minutes at 30°C. For supershift of the complex, anti-Ku (p70/p80) Ab-3 (clone 162) antibody, was added following PARG treatment. The reactions were separated on 5% non-denaturing polyacrylamide and the gel was dried and exposed to a PhosphorImager screen and retarded bands were quantified using IMAGEQUANT software.

2.7 *In vitro* ribosylation of proteins

In vitro ribosylation assays were performed as described previously (185) with minor modifications. Briefly, purified proteins (1.5 μg) were incubated in the reaction buffer (100 mM Tris pH 8.0, 5 mM $MgCl_2$, 6% glycerol, 50 mM NaCl, and 2 mM DTT) with 0.5 μg of purified PARP1 (Trevigen, Gaithersburg, MD), 200 ng of sonicated calf thymus DNA, and 15 μCi ^{32}P-NAD^+ for 30 min at 30°C. Following incubation, the reaction mixtures were analyzed on 6% polyacrylamide-SDS gels then transferred to PVDF membrane. Membranes were exposed to PhosphorImager screen for autoradiography analysis and the resultant bands were quantified using IMAGEQUANT software. Membranes were subsequently used for western blot analysis.

2.8 Release of Ku from closed circular DNA

2.8.1 Binding and release reaction

To maximize the loading of Ku on the DNA, the binding reactions were performed with a 2:1 molar ratio of Ku to DNA ends. DNA binding was performed in a 20 μl reaction mixture consisting of 156 ng (1 pmol) of purified Ku incubated with 1 μg (0.5 pmol ends =

1 μg) of linearized DNA in binding buffer (100 mM Tris pH 7.5, 2 mM ATP, 10 mM $MgCl_2$, 6% glycerol, 50 mM NaCl, 150 μM of NAD^+ and 2 mM DTT) at room temperature for 30 minutes. To the binding reaction, 10 U of T4 DNA ligase were added and the reactions were incubated at room temperature for 90 minutes. Following ligation reaction, purified PARP1 (50 ng) and sheared calf thymus DNA (200 ng; 200-500 bp) were included wherever described, and reactions were incubated at 30°C for 1 hour. Reactions were stopped by the addition of 3-AB, and were placed on ice until later use.

2.8.2 Immunoprecipitation and co-immunoprecipitation

Binding/release reactions were diluted in IP buffer (12 mM HEPES pH7.9, 25 mM KCl, 0.5 mM EDTA, 6% glycerol, 0.1% NP-40, 0.2 mM DTT, complete protease inhibitor cocktail) to a final volume of 500 μl to which 10 mg of the anti-Ku (p70/p80) Ab-3 (clone 162) antibody was added and allowed to incubate at 4°C with rotation for 2 hrs. Following incubation with antibody 60 μl of Protein G sepharose beads (Sigma, CAT#P7700), equilibrated in IP buffer, were added to the reactions and the reactions were returned to 4°C with rotation for 1 hr. Immunoprecipitates were washed twice by collecting the beads after centrifugation at 2000 g for 2 min at 4°C, and gently adding 1 ml of wash buffer (50 mM Tris pH 7.4, 300 mM NaCl, 5 mM EDTA, 0.1% Triton X-100).

2.8.3 PCR analysis

One tenth of the recovered immunoprecipitation productions and one tenth (~2 μL) of the reactions (pre-immunoprecipitation) were employed for PCR analysis. DNA Taq Polymerase (Invitrogen) was utilized for all PCR reactions. The control primers set (Appendix I) amplified a region located approximately 2 kb from the DNA ends and

generated a 256 bp fragment regardless of ligation. The ligation primer set (Appendix I) was homologous to the regions flanking the ends of the linear DNA and amplified the region spanning the ligation site and would only generate a 550 bp fragment following ligation of the ends. The primer sets were employed within the same PCR reaction allowing the concurrent evaluation of both the immunoprecipitation and ligation reactions. The PCR was run for 25 cycles of 95°C for 10 sec, 58°C for 0.5 min and 72°C for 1 min followed by incubation at 72°C for 10 min. The PCR products were resolved on 2% agarose gels stained with Sybr Green (Sigma, CAT#S9430) and visualized with the GelDoc system (BioRad) and analyzed using IMAGEQUANT software (Molecular Dynamics). Typically, ½ of each sample was analyzed in each PCR reaction.

2.9 Cell replication and survival assays

2.9.1 Cell replication assays

Stably transfected MEFs were passaged into 24-well dishes with 2,000 to 4,000 cells per well and were grown for 16 hours at 37°C and 5% CO_2 in growth media (DMEM supplemented with 10% FBS and antibiotic cocktail mixture). Cells were tryspinized and counted at 24 hours after initial plating. Cell counting was performed using hemocytometer, and counts were performed in triplicate. Cell counts for the 24 hour period following initial plating were used as the "Day 0" time point and remaining growth measurements were compared to that time point. Cell counts were repeated at each time point by trypsinizing cells, and counting total cell numbers using hemocytometer.

To examine the cell stage, asynchronous cells and cells which had been serum starved for 48 hours were trypsinized, then sent for FACS analysis at StemCore Laboratories

(Sprott Center, Ottawa, ON). All analysis was performed by the technicians at the StemCore Laboratories.

2.9.2 Cell survival assays following DNA damage

Stably transfected MEFs were passaged into 24-well dishes with 2,000 to 4,000 cells per well, and were grown for 16 hours at 37°C and 5% CO_2 in growth media (DMEM supplemented with 10% FBS and antibiotic cocktail mixture). For bleomycin treatment, bleomycin was added at various concentrations to each well in series, and cells were returned to the incubator for 1 hour. Following treatment, each well was washed twice with fresh DMEM, then 500 µl of growth media. Cells were recovered for 5 days in the incubator at 37°C and 5% CO_2, with growth media being replaced as necessary. Hydrogen peroxide (H_2O_2) and camptothecin (CPT) survival assays were performed similarly with treatment times lasting for 30 minutes and 1 hour, respectively.

To asses the survival of the cells following the 5 day recovery, CellTiter 96® Assay (Promega, CAT# G4000) was performed as per the manufacturer's instructions. The CellTiter Assay is a modified MTT colorimetric assay described by Mosmann (186). Following two washes with sterile PBS, 250 µl of the dye solution was added to cells. Cells were incubated for 5 to 10 minutes, after which the dye solution was transferred to 96-well dish and absorbance at 570 nm was measured using plate reader (Multiskan Spectrum; Thermo Electron Corporation). Survival was expressed as the percent activity compared to undamaged cells.

2.10 Immunofluorescence analysis of GFP-Ku following DNA damage

To visualize the mobility of Ku within the nucleus following DNA damage, 293T cells transfected with GFP-Ku or GFP-Ku^{3E} were grown on 18 mm cover-slips in DMEM supplemented with 10% FBS at 37°C and 5% CO_2 for 24 hours. To induce DNA damage, 3.0 μg/ml of bleomycin was added to each well and cells were returned to the incubator for 1 hour. Following treatment, each well was washed twice with fresh DMEM, then 1 ml of growth media and was recovered for indicated amount of time in the incubator at 37°C and 5% CO_2.

Cells were processed for immunofluorescence staining as previously described (178). Briefly, cells were washed twice with ice cold PBS and permeabilized by washing with PBS containing 0.1% Triton X-100 for 2 minutes. Cells were fixed at room temperature with PBS containing 4% paraformaldehyde and 0.75% Triton X-100. Cover slips were washed four times with PBS containing 0.1% Triton X-100 and then incubated for 30 minutes at room temperature with PBS+ (PBS containing 5% normal goat serum (NGS) and 0.1% Tween-20). Cells were incubated at room temperature with primary antibodies to phosphorylated histone H_2AX (γH_2AX) (Upstate Biotechnology) and polyclonal anti-GFP (LivingColors; Clontech) in PBS+ for 90 min at room temperature. After three washes with PBS with 0.1% Tween-20 and one with PBS+, coverslips were incubated for 30 minutes with secondary antibodies in PBS+. Excess antibody was washed away by two 10-min washes with PBS containing 0.1% Tween-20, and cells were mounted with Vectashield including DAPI (Vector Laboratories, Burlingame, CA). The cells were examined with an inverted fluorescence microscope (Zeiss Axiovert 135). GFP signals were obtained with an FITC-fluorescence filter set (Zeiss 09, excitation 450-490 nm, beam splitter 510 nm,

emission filter >520 nm). Microphotographs were taken using a 63x oil immersion objective.

2.11 *In vivo* V(D)J recombination assay

2.11.1 Transfection and recovery of recombination vectors

For *in vivo* transient V(D)J recombination assays, MEFs were transiently transfected as described above (Section 2.4.2). Two days following transfection, DNA recombination substrates were recovered using a QIAgen Miniprep kits (CAT# 27104), and were dissolved in 20 µl of TE buffer (pH 7.4).

2.11.2 Analysis of recombination efficiency

Electrocompetent DH5α *E. coli* were transformed with 20% of the abovementioned recombination substrates and plated on agar plates containing either 100 mg/ml of ampicillin, or 100 µg/ml of ampicillin and 50 µg/ml of chloramphenicol. Ampicillin plates were incubated at 37°C for 16 hours, while ampicillin + chloramphenicol plates were incubated at 37°C for 24 hours. Colonies on each plate were counted and recombination efficiency was calculated by comparing the number of colony forming units (CFUs) on the ampicillin + chloramphenicol plates with the CFUs on the ampicillin plates. These values were expressed as a percentage compared with the WT transformed bacteria.

2.11.3 Transfection and recovery of recombination vectors

One tenth of the recovered recombination substrates (section 2.11.1) were employed for PCR analysis. The primer set R3-200 and R14-200 as previously described (187)

(Appendix I) amplified the region spanning the signal joints in pJH200 generating a 460 bp fragment in the absence of RAG1 and RAG2 and an additional 256 bp fragment in the presence of RAG1 and RAG2. The primer set R3-290 and R14-290 (Appendix I) amplified the region spanning the coding joints in pJH290 generating a 1.8 Kb fragment in the absence of RAG1 and RAG2 and an additional 1.5 Kb fragment in the presence of RAG1 and RAG2. The control primer set R7 and R8 generated a 308 bp fragment more than 3 kb away from either the coding or joining segments and amplified both recombined and unrecombined vectors. The primer set was employed to confirm that equivalent amounts of DNA substrates were transfected into and recovered from MEF cells. When the R3 and R14 primer set was employed, PCR was run for 25 cycles of 95°C for 10 sec, 55°C for 0.5 min and 72°C for 1 min followed by incubation at 72°C for 10 min. When the primer set R7 and R8 was used, PCR was performed by incubating at 94°C for 5 min followed by 25 cycles of 94°C for 1 min, 58°C for 1 min and 72°C for 1 min with additional incubation at 72°C for 5 min. The PCR products were resolved on 2% agarose gels stained with Sybr Green (Sigma, CAT#S9430) and visualized with GelDoc system (BioRad) and analyzed using IMAGEQUANT software (Molecular Dynamics). Typically, ½ of each sample was analyzed in each PCR reaction.

2.11.4 Sequence analysis of recombination products

Sequence analysis of the recombination products was performed by subcloning the amplified PCR product of the recombination site. PCR products were resolved on 2% agarose gels stained with Sybr Green. Amplified bands were excised and gel purified using QIAquick Gel Extraction Kit (QIAgen, CAT# 28704). Using the TA cloning kit (Invitrogen,

CAT#K2000-01), PCR products were cloned into a TA cloning vector. Positive transformants were selected, amplified and plasmids were sequenced at StemCore Laboratories (Sprott Center, Ottawa, ON).

3. Results

3.1 PARP1 accelerates the off-rate of Ku from DNA ends

3.1.1 PARP1 causes the rapid release of Ku from DNA ends

Upon binding DNA, the Ku heterodimer threads the DNA end through the central channel and *in vitro*, this Ku:DNA complex is very stable, remaining intact for over 24 hours (176). However, the *in vivo* turn-over of Ku and repair processes occurs within 30 minutes (178), which suggests that a mechanism exists to remove Ku from the DNA. Although there is no direct evidence of a mechanism for the removal of Ku from either free ends or internally on DNA, there are indications from previous studies that would suggest PARP1 as a primary candidate for the release of Ku from DNA.

In order to determine whether it was possible to promote the release of Ku from DNA, electrophoretic mobility shift assays (EMSAs) were performed using purified Ku heterodimer and V15B whole cell extracts (WCE). For this work recombinant Ku was expressed in and purified from bacteria as described previously (183). V15B cells are deficient in Ku80 and do not produce functional Ku. Using extracts from these cells made it possible to manipulate the amount of interacting protein factors in the reaction without introducing additional Ku (Figure 8a, lane 3). Additionally, dialysis of the extracts ensured that the small molecules present were removed and the fluctuations in the amount of Ku bound to the DNA could be attributed solely to the proteins in the extract. The reactions were performed with 100-fold molar excess of unlabeled sheared calf-thymus DNA, driving the binding equilibrium to a single Ku bound per DNA molecule. Purified Ku was pre-bound to the ^{32}P-labeled oligonucleotides for 30 minutes (Figure 8a, lane 2). After the initial

Figure 8. PARP1 mediates the release of Ku from DNA. (a) Purified Ku heterodimer (21 ng) was pre-bound to ^{32}P-labelled double stranded oligonucleotide at room temperature for 30 minutes, then incubated with V15B cell extracts (WCE; 50 μg) or purified PARP1 (10 ng) for an additional 60 minutes at 30°C. Reactions were performed in the presence or absence of NAD^+; the PARP inhibitor 3-AB was included in reactions where indicated. Following the incubation reactions were resolved on 5% native polyacrylamide gel and visualized by exposing the dried gel to PhosphoImager. (b) PARP1-mediated release of Ku from DNA is rapid. After 5 minutes of co-incubation with PARP1, 20% of the Ku remained bound to DNA and less than 5% of the Ku remained bound after 120 minutes. Release reactions were repeated as described above. Following addition of PARP1, reactions were incubated for indicated time (min.), then resolved on 5% native polyacrylamide gel and visualized by exposing the dried gel to PhosphoImager. Resultant bands were quantified using ImageQuant software.

a.

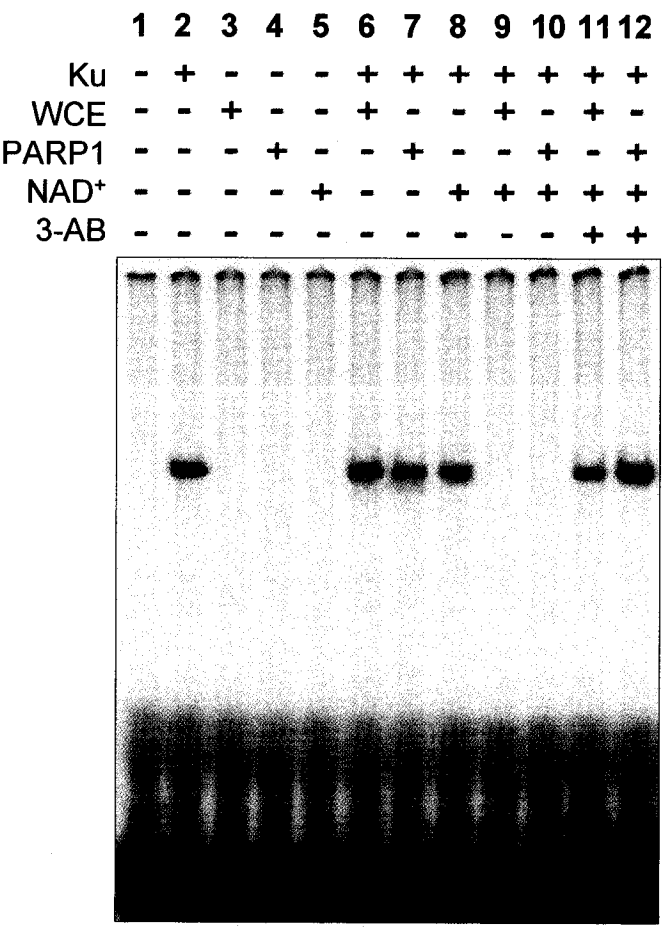
1 2 3 4 5 6 7 8 9 10 11 12
Ku - + - - - + + + + + + +
WCE - - + - - + - - + - + -
PARP1 - - - + - - + - - + - +
NAD+ - - - - + - - + + + + +
3-AB - - - - - - - - - - + +

b.

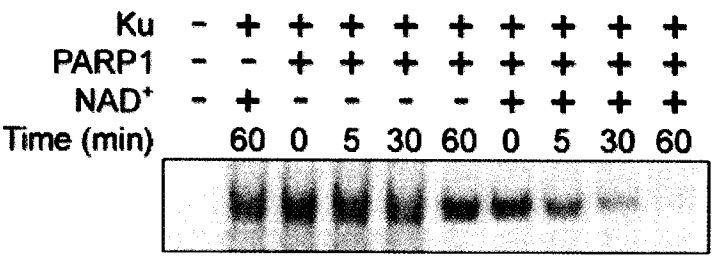
Ku - + + + + + + + + +
PARP1 - - + + + + + + + +
NAD+ - + - - - - + + + +
Time (min) 60 0 5 30 60 0 5 30 60

binding of Ku to the labeled oligonucleotides, the V15B WCE and unlabeled DNA were added to the Ku:DNA complexes and the reactions were incubated for an additional 60 minutes. Incubation of the Ku:DNA complex with the V15B WCE did not affect the amount of Ku bound (Figure 8a, lane 6). However, when the extracts were supplemented with NAD^+, the substrate for PARPs, and incubated with the Ku:DNA complex, Ku was lost from the labeled DNA, as the corresponding Ku:DNA complex was absent from the EMSA (Figure 8a, lane 9). To confirm that the loss of Ku from the DNA was the result of PARP activity, the PARP inhibitor 3-aminobenzamide (3-AB) was included in the reaction. Addition of 3-AB prevented the release of Ku from the DNA suggesting that one of the members of the PARP family was facilitating the release of Ku from DNA (Figure 8a, lane 11).

To determine whether PARP1 was able to elicit the release of Ku from the DNA, purified PARP1 was used in place of the V15B WCE, the release experiments were repeated. As seen in the reactions with the V15B extracts, purified PARP1 was able to cause the release of Ku from the DNA and this release was dependent on the presence of NAD^+ (Figure 8a, lane 7), and was prevented by the addition of the 3-AB inhibitor (Figure 8a, lane 12). Although previous studies have shown through EMSAs that PARP1 is able to bind DNA ends (188; 189), in my assays the DNA binding activity of PARP1 was not detectable under the conditions used (Figure 8a, lane 4). As compared to the conditions used here, the binding conditions of the previous studies did not contain Mg^{2+} and contained lower concentrations of Tris (tris(hydroxymethyl)aminomethane; 10 to 20 mM compared to the 100 mM used here). These alterations would increase the stringency of the binding conditions and could explain the absence of PARP1 binding in my reactions.

One of the limitations of EMSAs is that they provide only a snapshot in time of the reaction status and cannot portray the entire cycle of the reaction. Additionally, the presence of excess unlabeled DNA in the reactions prevents the detection of rebinding events. Consequently under the conditions used, it is not possible to determine whether the PARP1-mediated loss of Ku from the DNA is a transient state and Ku rebinds the unlabeled competitor DNA or whether PARP1 is altering the DNA binding ability of Ku. To address this problem, I examined the effect of PARP1 on Ku binding to the radiolabelled oligonucleotides in the absence of cold competitor DNA. The release of Ku from the DNA was rapid, with only 20% of the Ku remaining bound to DNA after 5 minutes of incubation with PARP1 (Figure 8b). Over time, Ku continued to be released from the DNA, so that less than 5% remained bound after 1 hour. Taken together, these results suggest that PARP1 induces the loss of Ku from DNA in a NAD^+ dependent manner and following its release from DNA, Ku does not rebind to the same or related DNA molecules.

3.1.2 PARP1-mediated release of Ku is dependent upon the activity of PARP and not its ribosylation status

Structurally, the polymers of PAR show some similarity to the structure of ssDNA (153), to which Ku is readily able to bind (176). Additionally, the Ku70 subunit contains a putative PAR-binding motif which is present in proteins that were shown to bind PAR polymers (72; 73). When PARP1 undergoes autoribosylation, multiple PAR polymers are added to the protein and it is possible that these PAR polymers act as an outlet for Ku and lure it away from the DNA. Therefore I tested whether it is the Ku-directed enzymatic activity of PARP1, or presence of the PAR polymers formed during the autoribosylation of

PARP1 that provokes the loss of Ku from DNA. PARP1 was first autoribosylated by incubating purified PARP1 with unlabeled linear DNA and NAD^+ for 30 minutes. The autoribosylation reaction, and the activity of PARP1 was stopped by the addition of 3-AB, and the autoribosylated PARP1 was then added directly to the Ku:DNA complex. Following incubation with the autoribosylated PARP1 the Ku:DNA complex was still present (Figure 9) which suggests that the mere presence of PAR polymers is not sufficient to cause the release of Ku from DNA, but rather it is the enzymatic activity of PARP1 in the presence of Ku that is required for the release of Ku from DNA.

3.1.3 The release of Ku from DNA by PARP1 is reversible by PARG treatment

Like many other post-translational modifications, the ribosylation of target proteins is a non-permanent modification and can be removed by PARG allowing the ribosylated target proteins to return to their original status (167). If the DNA binding affinity of Ku is compromised because of its ribosylation by PARP1, then incubation of the ribosylated Ku with PARG might be expected to restore the DNA binding ability of Ku. In order to test this hypothesis, purified PARG was added to the previously performed release experiments in the absence of cold-competitor DNA (Figure 10). As in the previous experiments Ku was first bound to radio-labeled DNA (Figure 10, lane 2), then incubated with purified PARP1 for 60 minutes. As shown previously, the incubation of the Ku:DNA complex with PARP1 caused the release of Ku from the DNA (Figure 10, lane 3). Following the incubation with PARP1, 3-AB was added to the reaction to prevent further PARP activity (Figure 10, lane 4 confirms that PARP1 activity is blocked by the addition of 3-AB as the inhibitor was added

Figure 9. The release of Ku from DNA is dependent on the enzymatic activity of PARP1 and not the ADP-ribosylation of PARP1. Purified PARP1 (10 ng) was incubated with NAD^+ and sheared calf-thymus DNA (1 μg) at 30°C for 30 minutes. Meanwhile, purified Ku (21 ng) was pre-bound to ^{32}P-labelled double stranded oligonucleotide at room temperature. After incubation, the ribosylated PARP1 was added to the Ku:DNA complex in the presence of the PARP inhibitor 3-AB. After the indicated time (min.), samples were resolved on 5% native polyacrylamide gel and visualized by exposing the dried gel to PhosphoImager. Resultant bands were quantified using ImageQuant software.

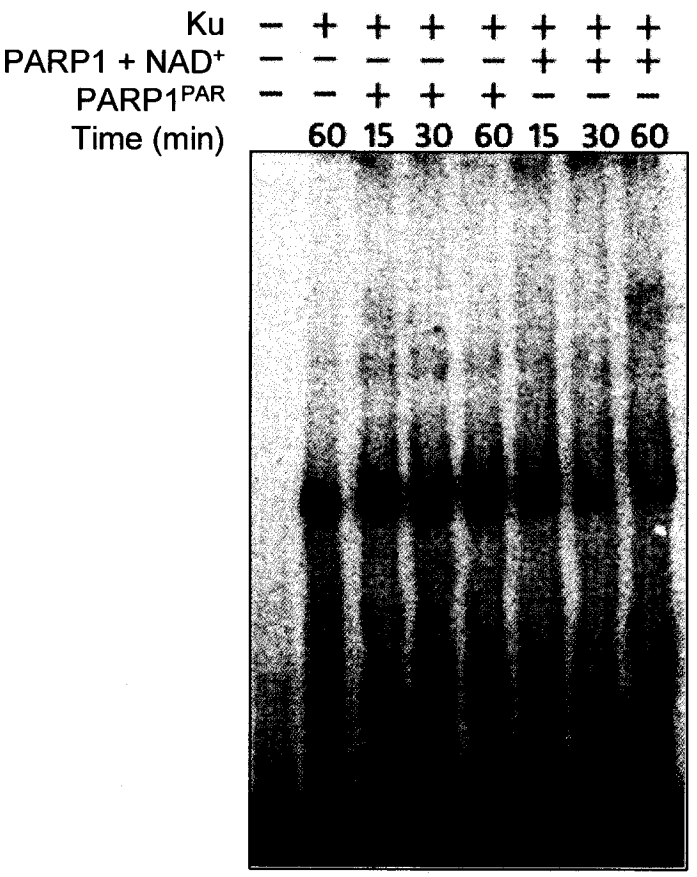
Ku − + + + + + + +
PARP1 + NAD+ − − − − − + + +
PARP1PAR − − + + + − − −
Time (min) 60 15 30 60 15 30 60

Figure 10. DNA binding is restored after PARG treatment. Double stranded oligonucleotide was ^{32}P-labelled (lane 1) and incubated with purified Ku (21 ng) (lane 2), then incubated with purified PARP1 (PARP; 10 ng) in the presence of NAD^+ for 30 minutes at 30°C (lane 3). The PARP inhibitor, 3-AB, was added to the reaction followed by purified PARG enzyme (25 ng) and the reaction was incubated for an additional 30 minutes at 30°C (lane 5). Ku specific antibody was added to confirm that the shifted complex was the result of Ku rebinding (lane 6). Inclusion of the PARP inhibitor (3-AB) prior to the addition of PARP1 prevented the loss of Ku from the DNA (lane 4). All samples were resolved on 5% native polyacrylamide gel and visualized by exposing the dried gel to PhosphoImager. Resultant bands were quantified using ImageQuant software.

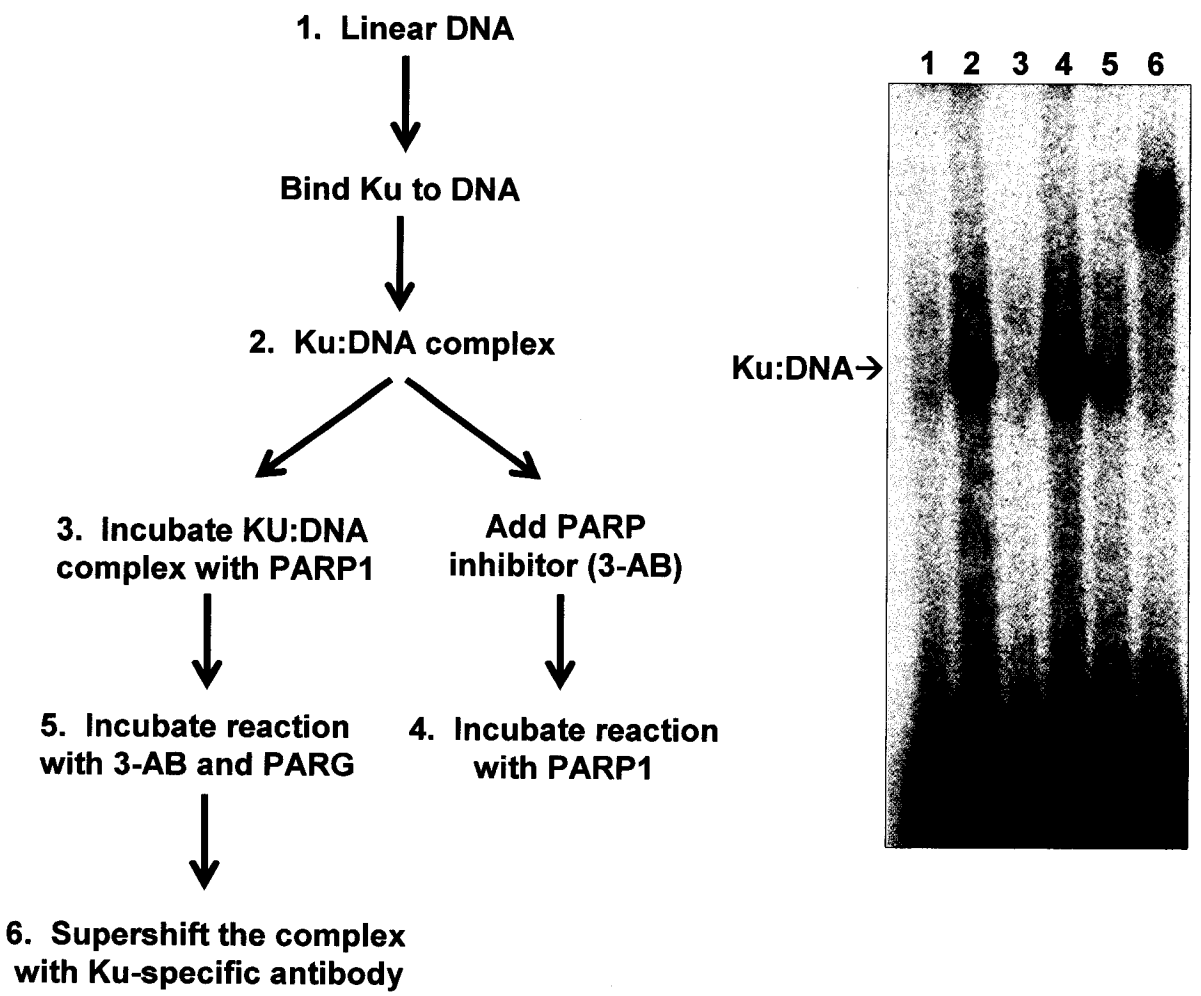
1. Linear DNA
Bind Ku to DNA
2. Ku:DNA complex
3. Incubate KU:DNA complex with PARP1
Add PARP inhibitor (3-AB)
5. Incubate reaction with 3-AB and PARG
4. Incubate reaction with PARP1
6. Supershift the complex with Ku-specific antibody
1 2 3 4 5 6
Ku:DNA→

to the reaction prior to the purified PARP1). Following the addition of 3-AB, purified PARG was added to the reactions and they were incubated for an additional 30 minutes. The addition of PARG to the reactions re-established Ku binding to the radio-labeled oligonucleotide (Figure 10, lane 5) and the addition of a Ku-specific antibody supershifted the complex (Figure 10, lane 6), confirming that it was Ku which had rebound the DNA. Together this supports the idea that PARP1 ribosylates Ku in order to release it from DNA ends and treatment with PARG removes the ADP-ribose modifications on Ku and re-establishing the DNA binding activity of Ku. Whether this loss of binding is mediated through a change in Ku's affinity for DNA or through an alteration of the structure of the heterodimer is yet to be determined. The amount of Ku rebinding DNA following PARG treatment represented only 30% of the total Ku binding prior to treatment with PARP1, suggesting that although PARG can restore the DNA binding activity of Ku, the restoration is incomplete. Since the PARG enzyme is unable to remove the protein-proximal ADP-ribosyl group from the acceptor protein (133), this would suggest that the Ku could still have a mono-ADP-ribosyl group associated with it, which may reconcile the incomplete restoration that was observed.

3.2 PARP1 ribosylates the Ku70 subunit of the heterodimer *in vitro*

Previous studies have shown that PARP1 is able to ribosylate the Ku heterodimer (174; 175), however these studies were performed with Ku in solution, not bound to DNA. All of the evidence presented herein provides a strong indication that PARP1 is able to ribosylate the Ku heterodimer when bound to DNA, and this ribosylation diminishes the DNA binding capabilities of the Ku heterodimer. To test whether DNA-bound Ku is a direct

enzymatic target of PARP1, *in vitro* ribosylation reactions were performed using purified Ku, PARP1 and ^{32}P-NAD^{+}. Purified Ku was prebound to linear DNA for 30 minutes, after which purified PARP1 and 15 μCi ^{32}P-NAD^{+} were added and the reactions were incubated at 30°C for indicated time. Following co-incubation there were three distinct bands present on the autoradiograph (Figure 11a). The predominant band in each reaction corresponded to full length PARP1, which is consistent with previous findings showing that the autoribosylation of PARP1 is the preferred ribosylation target (132; 144). In addition to the PARP1 band, there were two additional bands, 70 kDa and 80kDa in size, present in the reactions containing WT Ku. The corresponding western blot analysis identified these two radiolabelled bands as the Ku70 and Ku80 subunits. The ^{32}P-NAD^{+} incorporation of the Ku70 and Ku80 subunits was present after five minutes of co-incubation with PARP1 and continued to increase over the course of the reaction. Quantification of the ^{32}P-NAD^{+} incorporation into each of the Ku70 and Ku80 subunits represented about 5% of the total ^{32}P-NAD^{+} incorporation after 1 hour. These results demonstrate that DNA bound Ku is an enzymatic target of PARP1, which is consistent with previous studies that showed that both subunits of the Ku heterodimer are ribosylated by PARP1 (174; 175).

3.3 Ku70 amino acid requirements for Ku release from DNA ends and ribosylation

3.3.1 The SAP domain of Ku70 is required for PARP1-mediated release

In order to determine the region of the Ku heterodimer that is ADP-ribosylated by PARP1 *in vitro*, mutational analysis was performed. Although PARP1 is known to target glutamate and aspartic acid residues of target proteins, there is no identified consensus

Figure 11. PARP1 ribosylates the Ku70 subunit. (a) Purified Ku (1.5 μg) was bound to DNA then incubated with purified PARP1 (250 ng) in the presence of ^{32}P-NAD^{+} (1 μCi) at 30°C for indicated time. Reactions were separated on 6% SDS polyacrylamide gel and transferred to PVDF membrane. Radiolabelled bands were visualized by exposing membrane to PhosphoImager sceen. Resultant bands were quantified using ImageQuant software. (b) Corresponding western blot with antibodies specific for Ku70 and Ku80.

a.

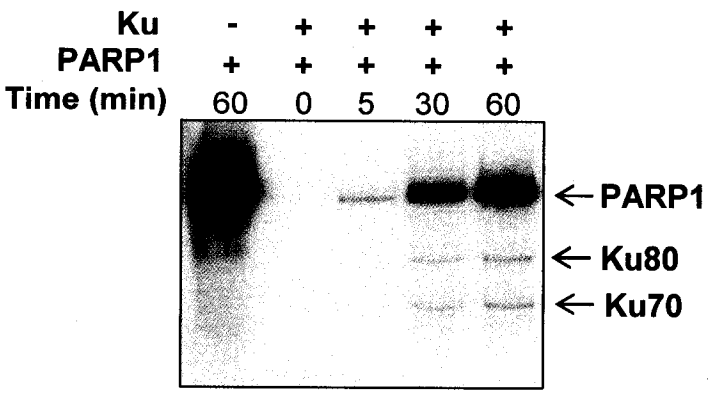
Ku - + + + +
PARP1 + + + + +
Time (min) 60 0 5 30 60
← PARP1
← Ku80
← Ku70

b.

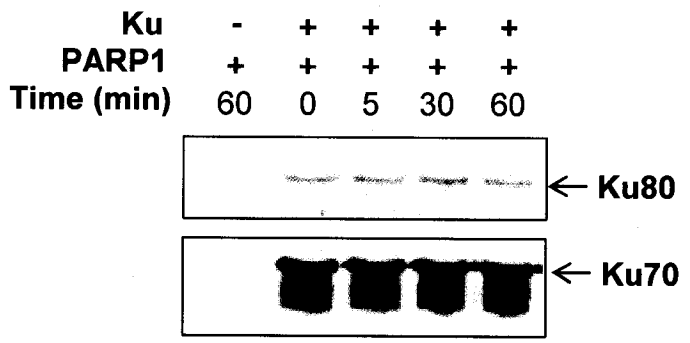
Ku - + + + +
PARP1 + + + + +
Time (min) 60 0 5 30 60
← Ku80
← Ku70

sequence for ribosylation. Given that the crystal structure of the Ku heterodimer bound to DNA is known, it was used to identify regions of the Ku heterodimer that could provide potential targets for ADP-ribosylation by PARP1. The crystal structure of the Ku heterodimer bound to DNA identifies the Ku70 subunit being oriented toward the free end of the DNA, while the Ku80 subunit is positioned towards the interior of the DNA (65; 87). Additionally the Ku70 subunit contains a putative PAR binding motif that on its own was shown to bind free PAR polymers (72; 73). It is for these reasons that the Ku70 subunit was the primary focus for the mutational analysis.

Using an *in silico* based approach three domains were identified as being potential target sites for PARP1 based on their proposed function and their accessibility when the Ku heterodimer was bound to DNA. These domains were the SAP domain, the proposed PAR binding domain, and α–helix 5 (Figure 12a). As previously described the SAP domain constitutes a potential DNA binding domain that contacts the exposed DNA end when Ku is bound to DNA and stabilizes the binding of Ku on the DNA end (67), and so the ribosylation of the SAP domain could conceivably destabilize its interaction with DNA and destabilize the binding of Ku to the DNA end. The PAR binding domain has been described as a conserved motif present in proteins that have been shown to bind free PAR polymers in solution (72; 73). Additionally, this motif has been shown to be targeted for ribosylation in two checkpoint proteins, APLF (aprataxin PNK-like factor) and CHFR (checkpoint protein with FHA and RING domains), which resulted in the abrogation of their functioning (73). The ribosylation of this domain in the Ku heterodimer could function in the same manner and abolish the DNA binding activity of Ku, especially since the domain is located within the Ku80-dependent DNA end binding domain of Ku70 (Figure 3a). The third domain,

Figure 12. Deletional analysis of the Ku70 subunit. (a) Schematic representation of the Ku70 subunit and the deletion mutations created. The α helix-5 (a.a. 180-196; green box), putative PAR binding motif (a.a. 244-265; red box), and SAP domain (a.a. 572-609; yellow box) were each deleted separately from the Ku70 subunit as described. (b) Deletion of the SAP domain prevents PARP1-mediated release of Ku. The described deletion mutants were expressed in *E. coli* and purified. After it was confirmed that the each deletion mutants were able bind DNA, they were used in the previously described release experiment. Each mutant was bound to ^{32}P-labelled double stranded oligonucleotide then incubated with purified PARP1 in the presence of NAD^+. Following incubation at 30°C for 60 minutes, samples were resolved on 5% native polyacrylamide gel and visualized by exposing the dried gel to PhosphoImager. Resultant bands were quantified using ImageQuant software.

a.

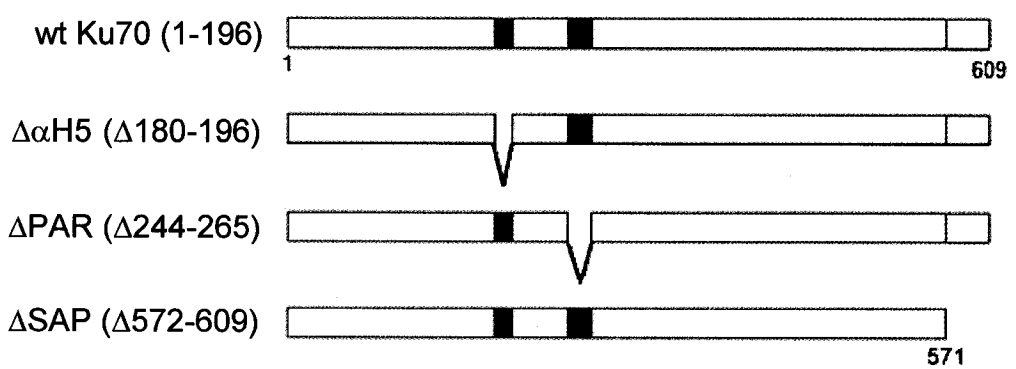
wt Ku70 (1-196)
1
609
ΔαH5 (Δ180-196)
ΔPAR (Δ244-265)
ΔSAP (Δ572-609)
571

b.

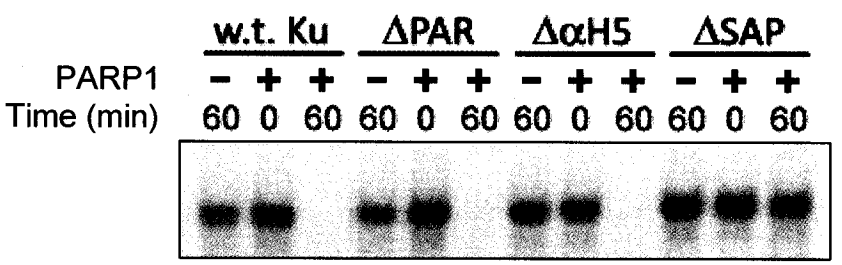
w.t. Ku
ΔPAR
ΔαH5
ΔSAP
PARP1
- + + - + + - + + - + +
Time (min)
60 0 60 60 0 60 60 0 60 60 0 60

α–helix 5 was described as the portion of Ku70 that interacts with other members of the NHEJ complex at the DNA end (44). Upon the recruitment of the NHEJ apparatus, Ku is proposed to undergo and inward translocation on the DNA, and the ribosylation of α–helix 5 might influence this inward shift of Ku disrupting the activity of Ku. Additionally, as with the PAR binding motif, α–helix 5 is also located within the Ku80-dependent DNA end binding domain of Ku70.

Deletion mutants for each of the Ku70 domains were created, expressed in bacteria together with WT Ku80, and purified. After it was established that deletion of the domains did not significantly influence the ability of Ku to bind to DNA, the mutants were used in the release experiment with purified PARP1. Deletion of either the PAR domain or of α-helix 5 did not affect the release of Ku from the DNA after incubation with PARP1 under release permissive conditions (Figure 12b). Deletion of the SAP domain (ΔSAP) however, did prevent the release of Ku from DNA after incubation with PARP1. Even after 60 minutes of incubation with PARP1 over 80% of the ΔSAP mutant remained bound to the DNA (Figure 12b).

The SAP domain is a highly conserved 35 amino acid domain located at the C-terminal end of the human Ku70 monomer and is conserved in the Ku70 sub-unit across higher eukaryotic species with 84% amino acid similarity (Figure 13a). Within the SAP domain of human Ku70 there are three glutamate residues, E583, E598, E601, which are conserved across species, and any variations are aspartate substitutions – the alternative target residue for PARP1 ribosylation (Figure 13a). In Ku the SAP domain is proposed to stabilize the dimer at the end of the DNA, capping the central cavity of Ku while coming in contact with the DNA (65).

Figure 13. Conserved glutamate residues within the SAP domain of Ku70 are involved in PARP1 regulation of Ku:DNA binding. (a) Sequence alignment of SAP domain from Ku70 of various species reveals three aspartate/glutamate residues (underlined) that are conserved across all species. (b) Point mutants were tested for resistance to PARP1-mediated release from DNA. The glutamate residues of the human Ku70 were mutated individually, and in combination with each other. The point mutants were expressed in *E. coli* and purified as described previously. Each of the point mutants were tested for their ability to be released by purified PARP1 through the release assay described. Following incubation with PARP1, samples were resolved on 5% native polyacrylamide gel and visualized by exposing the dried gel to PhosphoImager. Resultant bands were quantified using ImageQuant software. (c) Mutation of all three residues ($Ku70^{3E}$) confers resistance to PARP1-mediated release and remains bound to the DNA for up to 60 min. Time course analysis was performed with the $Ku70^{3E}$ mutant by incubating the DNA bound Ku with PARP1 for increasing amount of time (min), as indicated. Samples were resolved on 5% native polyacrylamide gel and visualized by exposing the dried gel to PhosphoImager. Resultant bands were quantified using ImageQuant software. (d) Comparison of the binding profile of the wild-type (black diamonds), ΔSAP mutant (blue circles) and $Ku70^{3E}$ mutant (green triangle) following incubation with purified PARP1. In the absence of PARP1, wild-type Ku remains bound to DNA for the duration of the experiment (open diamonds).

a.

Homo sapiens	573	LGKFTVPMLK**E**ACRAYGLKSGLKKQ**E**LL**E**ALTKHF	607
Macaca mulatta	573	LGKFTVPMLK**E**ACRAYGLKSGLKKQ**E**LL**E**ALTKHF	607
Canis lupus	573	LGKLTVPMLK**E**ACRVCGLKGGLKKQ**E**LL**D**ILTKHF	607
Rattus norvegicus	573	LGKLTVPALR**D**ICKAYGLKSGPKKQ**E**LL**E**ALSRHL	607
Mus musculus	573	LGKLTVPTLK**D**ICKAHGLKSGPKKQ**E**LL**D**ALIRHL	607
Xenopus laevis	573	LGKLTVPALK**E**ACRGYKLK-GSKKQ**E**LV**D**ALVEYF	606

b.

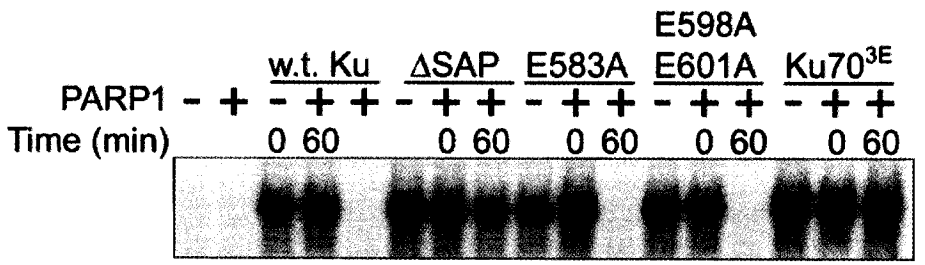

c.

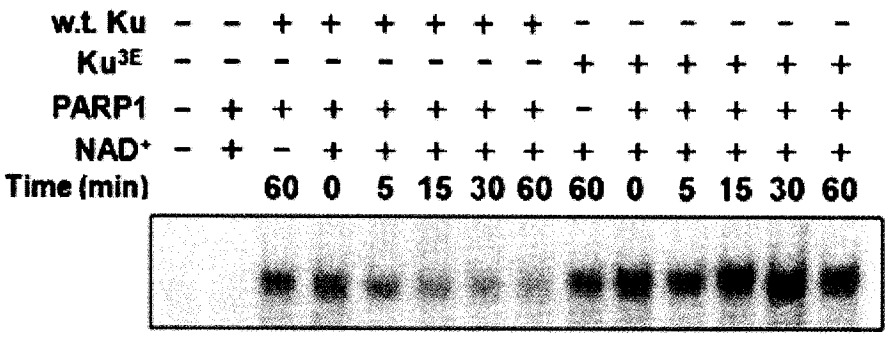

d.

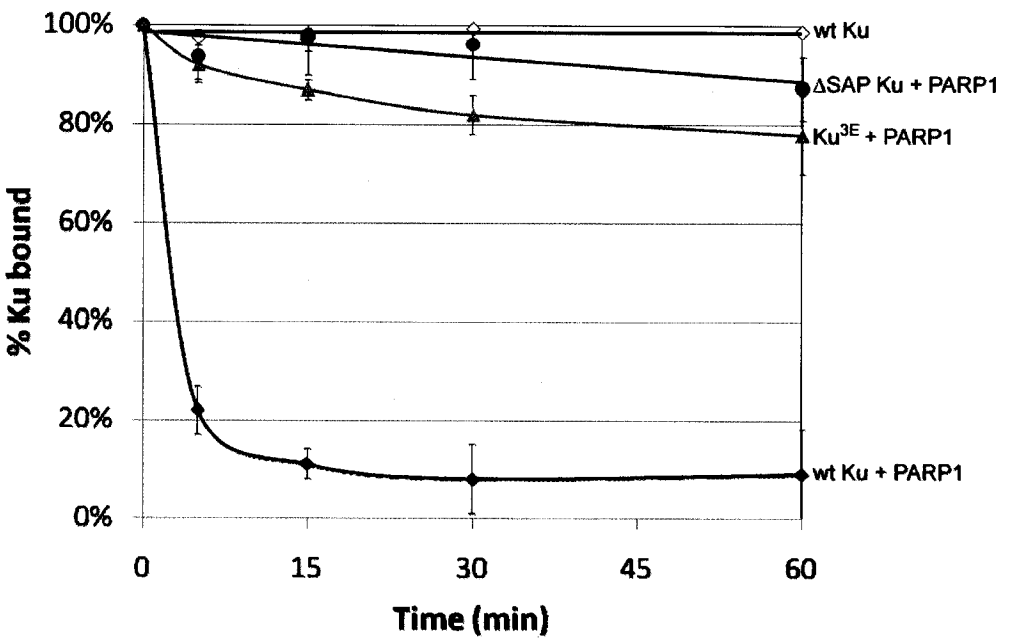

The three glutamate residues within the SAP domain of Ku70 were mutated to alanine residues, individually and in combination, using site-directed mutagenesis. The point mutants were expressed, purified and used in the previously described release assay with purified PARP1. Mutation of individual glutamate residues did not confer resistance to PARP1-mediated release since after 60 minutes the Ku was no longer bound to DNA (Figure 13b). Similarly, pairing the point mutations did not affect Ku retention and binding was abolished after 60 minutes of incubation with PARP. However, mutating all three glutamate residues within the SAP domain ($Ku70^{3E}$) prevented the release of Ku from DNA ends after incubation with PARP1 (Figure 13b).

As compared with the WT Ku, which is released after 5 minutes and continues to be released over the hour incubation of co-incubation with PARP1, the $Ku70^{3E}$ mutation remains bound throughout the incubation (Figure 13c). Indeed both the ΔSAP and $Ku70^{3E}$ mutants show resistance to PARP1-mediated release throughout the co-incubation, and after 1 hour about 80% of either mutant remains bound (ΔSAP - 87%; $Ku70^{3E}$ - 78%, Figure 13d). This all-or-none requirement is consistent with previous results for the ribosylation of p53, which showed that mutation of individual target residues was not sufficient to prevent ribosylation of p53 by PARP1, but mutation of all target sites within p53 prevented ribosylation (185).

3.3.2 Mutation of the SAP domain prevents ribosylation of Ku70 *in vitro*

To determine whether the $Ku70^{3E}$ mutations prevent ribosylation of Ku, the previously described ^{32}P-NAD^+ *in vitro* ribosylation reactions were repeated with purified

Figure 14. Mutation of conserved glutamate residues within the SAP domain of Ku70 prevents ribosylation by PARP1. (a) Purified wild-type Ku or purified $Ku70^{3E}$ were subjected to *in vitro* ^{32}P-NAD^+ ribosylation assay as described in Figure 11. Reactions were separated on 6% SDS polyacrylamide gel and transferred to PVDF membrane. Radiolabelled bands were visualized by exposing membrane to PhosphoImager screen. Resultant bands were quantified using ImageQuant software. (b) Corresponding western blot with antibodies specific for Ku70 and Ku80.

a.

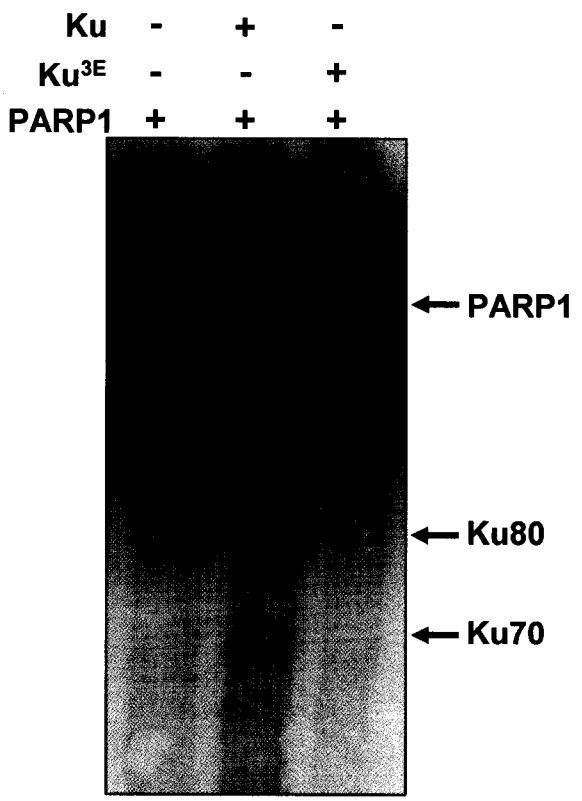

b.

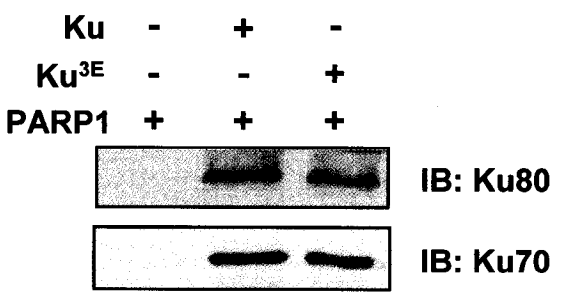

Ku^{3E} and purified PARP1 (Figure 14). Consistent with the previous ^{32}P-NAD^+ ribosylation reactions, the predominant band on the resulting autoradiograph corresponded to the autoribosylation of PARP1. In the reaction containing purified $Ku70^{3E}$ there were no 70 kDa bands present on the resulting autoradiograph, whereas there was a distinct band present in the reaction containing WT Ku. Additionally, there also appeared to be a reduction in the amount of ^{32}P-NAD^+ incorporation around the 80 kDa position as compared to the WT Ku reaction. Together this suggests that the $Ku70^{3E}$ mutations prevent not only the ribosylation of the Ku70 subunit, but may also reduce the overall ribosylation of both subunits of the Ku heterodimer.

3.4 PARP1 treatment promotes the release of Ku from closed circular DNA

Previous studies have shown Ku can slide inward on the DNA in an Mg^{2+}-dependent manner (81; 177; 77), independent of DNA-PK_{cs}. Utilizing this ability of Ku to translocate inward on the DNA, it was shown that Ku-bound linear DNA can be circularized by the addition of T4 DNA ligase (31; 81), entrapping the Ku on a covalently closed circular DNA (ccDNA) molecule. This Ku:ccDNA complex is very stable and it remains intact even in the presence of 2M NaCl (81). Similarly, the current model of NHEJ proposes that Ku translocates to the interior of the DNA upon recruitment of DNA-PK_{cs} to allow the other proteins of the NHEJ apparatus access to the DNA end and to repair the DNA break (24; 25; 190; 191). This model implies that following NHEJ, free DNA ends would no longer be present and this may jeopardize the ability of PARP to release the entrapped Ku. To date, there have been no reports demonstrating the release of Ku from either ccDNA, or from DNA following ligation.

All of the previously described experiments performed in this thesis were performed with linear DNA and it is possible that the ribosylation of Ku by PARP1 is causing Ku to slide off the free end of the DNA. While the current experiments explain the dissociation of Ku from DNA ends, they do not in their present form offer a comment on whether, or how Ku may be released from DNA in the absence of a DNA end as is perceived to occur during NHEJ. In order to address whether PARP1 plays a role in promoting the release of Ku from DNA in the absence of a free DNA end, an *in vitro* assay was developed which would allow the detection and measurement of the release of Ku from ccDNA (Figure 15a).

In this assay purified Ku was first bound to a 5 kb linear DNA fragment for 30 minutes. To maximize the loading of Ku on the DNA, the binding reactions were performed with a 2:1 molar ratio of Ku to DNA ends. Following the loading of Ku onto the DNA, T4 DNA ligase was added to the reactions to entrap Ku on the DNA. The Ku:ccDNA complex was incubated with PARP1 and additional linearized DNA, to permit PARP activation, in ribosylation permissive conditions for 60 minutes. After incubation, Ku was immunoprecipitated from the reactions, and using the DNA that was associated with the Ku as a template, PCR reactions were performed. Two unique primer sets were used in the PCR reactions; one set of primers amplified a control region on the DNA backbone 3 kb away from the ligation site and was used to detect the total DNA, and the second set of primers were specific for regions flanking the ligation site and only amplified a product following ligation. These experiments were performed using the previously described purified WT Ku, as well as the ΔSAP Ku, and Ku^{3E} mutants.

Figure 15. Ku is released from closed circular DNA by PARP1. (a) Schematic of the experimental progression. Purified Ku (1.5 μg) was pre-bound to linearized DNA (500 ng) for 30 minutes. Following Ku binding, T4 ligase (10 U) was added and the reaction was incubated at room temperature for 90 minutes. After ligation of DNA ends, Ku:DNA complex was incubated with PARP1 (50 ng) in the presence of NAD^+ and additional linear DNA for 60 minutes at 30°C. After incubation, Ku was immunoprecipitated as previously described. (b) DNA which was associated with Ku after immunoprecipitation was used as a template for PCR reactions to detect the DNA backbone and successful ligation. Reaction 1: DNA ligated with T4 ligase; Reaction 2: Ku bound to linear DNA; Reaction 3: Ku bound to linear DNA followed by PARP1; Reaction 4: Ku entrapped on closed circular DNA; Reaction 5: Ku entrapped on closed circular DNA and incubated with PARP1. PCR template derived from input reaction is designated as "In", while PCR template derived from immunoprecipitation reaction is designated as "IP".

a.

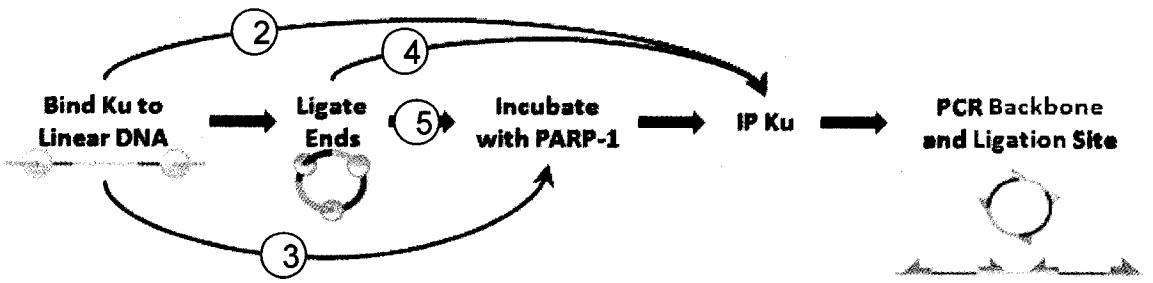
2
4
Bind Ku to Linear DNA
Ligate Ends
5
Incubate with PARP-1
IP Ku
PCR Backbone and Ligation Site
3

b.

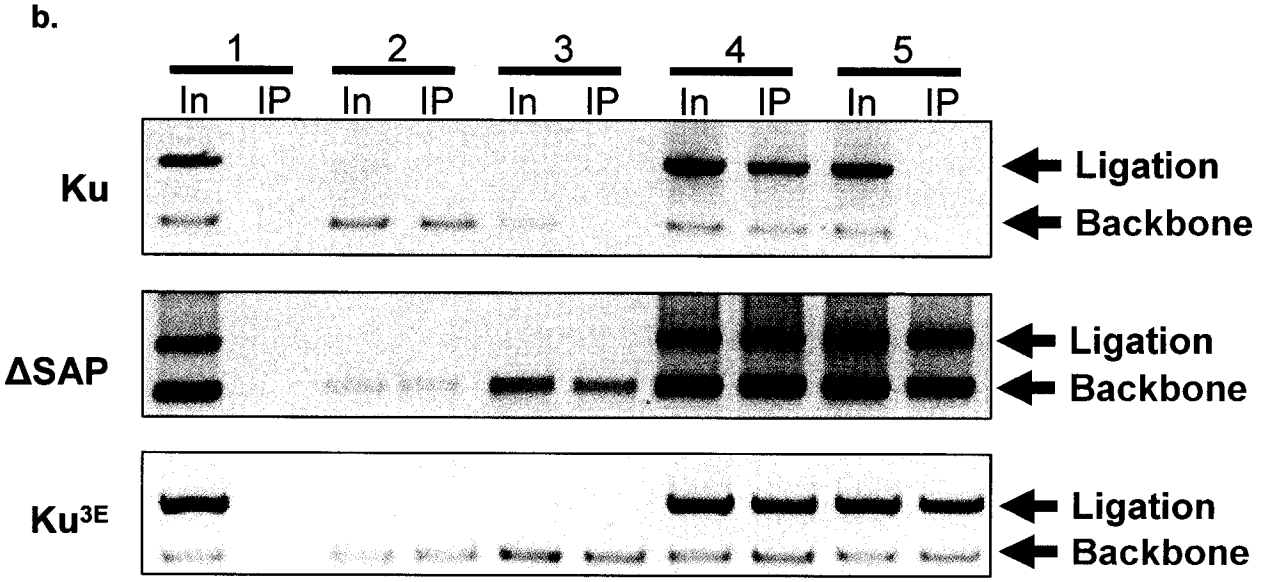
1
2
3
4
5
In
IP
In
IP
In
IP
In
IP
In
IP
Ku
ΔSAP
Ku3E
Ligation
Backbone
Ligation
Backbone
Ligation
Backbone

To confirm that the products from the PCR reactions were amplified from the DNA that was associated with Ku and not from excess unbound DNA, the reaction was performed in the absence of the Ku heterodimer. When Ku was omitted from the reactions, the PCR reactions failed to amplify either the control or ligation product following immunoprecipitation (Figure 15b, lane 1). To establish that the immunoprecipitation of Ku did not destabilize the Ku:DNA complex and cause dissociation of Ku from the linear DNA, the Ku:DNA complex was immunoprecipitated and analyzed through PCR. Immunoprecipitation of Ku did cause Ku to dissociate from the linear DNA as the "control" PCR fragment was present when the immunoprecipitation reaction was used as a template (Figure 15b, lane 2).

The addition of PARP1 to the Ku:linear DNA complex caused the release of the WT Ku from the DNA, as no products were formed from the PCR reaction, whereas both of the ΔSAP Ku and Ku^{3E}, remained bound to the linear DNA, as indicated by the control fragment from the resulting PCR reaction (Figure 15b, lane 3). These results were consistent with the previous results from the EMSAs and confirm the results seen therein.

To determine whether Ku could be trapped on ccDNA, the Ku:DNA complex was incubated with ligase, and Ku was immunoprecipitated. When the PCR products from these immunoprecipitation reactions were analyzed, both the control and the larger "ligation" PCR product were present indicating that the ligated DNA had immunoprecipitated with Ku (Figure 15b, lane 4). Similarly, both the ΔSAP Ku and Ku^{3E} mutants were entrapped on ccDNA as indicated by the presence of the "ligation" PCR product. As compared to the reactions performed in the absence of Ku, both the WT, ΔSAP Ku and Ku^{3E} mutants reduced

the ligation efficiency of the assay similarly (data not shown); however this was compensated for by performing the reactions with additional ligase.

In order to address whether PARP1 plays a role in promoting the release of Ku from DNA in the absence of a free DNA end, the Ku:ccDNA complex was incubated with PARP1 (Figure 15b, lane 5). When WT Ku entrapped on ccDNA was incubated with PARP1, no PCR products were detected, indicating that in addition to causing the release of Ku from linear DNA, PARP1 can initiate the release of Ku from ccDNA. This is the first such demonstration of release of Ku from ccDNA. By contrast, both the ΔSAP Ku and Ku^{3E} mutants remained entrapped on the ccDNA following incubation with PARP1 as the subsequent PCR reactions yielded both the "control" and "ligation" products. This shows that the mutants are resistant to the release of PARP1 from both linear and ccDNA.

3.5 Characterization of the Ku70 mutants *in vivo*

3.5.1 Establishment of Ku mutations in MEFs

While the *in vitro* results describe a novel mechanism for regulating the DNA binding activity of Ku, it was necessary to establish the effect of the mutations on Ku functioning *in vivo* by examining the impact on 1 - growth rate, 2 - NHEJ/DSB response, and 3 – fidelity of recombination through V(D)J recombination. To validate the *in vitro* results mouse embryonic fibroblast (MEF) cells that were Ku70-deficient were stably restored with either the WT human Ku70 subunit or either of the Ku70 SAP mutants (Figure 16a). The restoration of Ku70 with WT, or the mutant forms of Ku70 in the Ku70-deficient MEF cells resulted in expression levels comparable to the WT MEFs and resulted

Figure 16. The restoration of SAP mutants in Ku70$^{-/-}$ MEFs reduces cell proliferation. (a) Using replication incompetent retroviruses Ku70$^{-/-}$ MEFs were restored to stably express wild-type human Ku70 (WT), or either the ΔSAP Ku70 or Ku70^{3E} mutant. Equal levels of Ku were detected in all restored cells as determined by DNA pull-down assays. (b) Cells that were stably expressing the mutant forms of Ku70 displayed reduced growth rates as compared to the WT-restored MEFs. Cells (3 x 10^3) were seeded in 6-well plates and grown in DMEM plus 10% FBS. Cell proliferation was evaluated by counting cells following trypsinization and was plotted on log scale. Day 0 cell counts were performed 24 hours after initial plating of cells. All cell counts were normalized to Day 0. Data are means from three independent experiments, each carried out in quadruplicate and standard deviation are shown. * indicates P=0.01.

a.

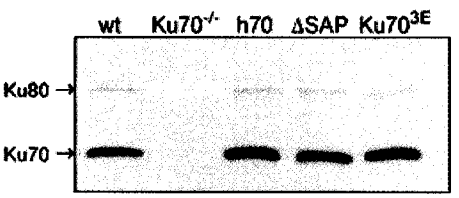
wt
Ku70-/-
h70
ΔSAP
Ku703E
Ku80
Ku70

b.

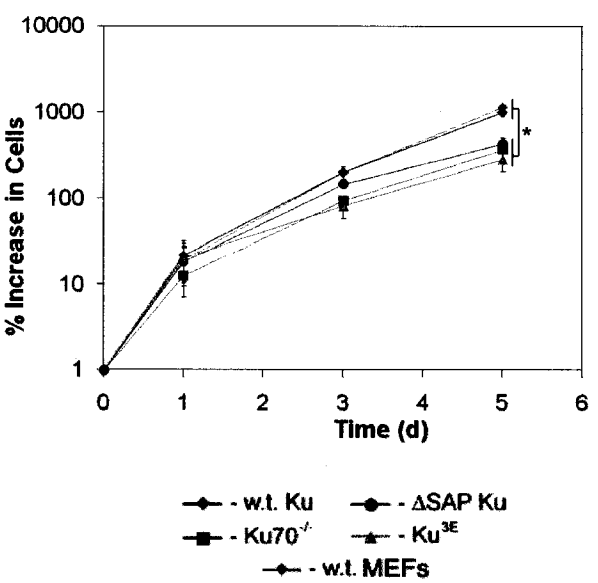
10000
1000
100
10
1
% Increase in Cells
0
1
2
3
4
5
6
Time (d)
*
- w.t. Ku
- ΔSAP Ku
- Ku70-/-
- Ku3E
- w.t. MEFs

in the stabilization of the Ku80 subunit, which was undetectable in the Ku70-deficient MEFs prior to restoration (Figure 16a).

Previous studies showed that Ku-deficient cells display growth defects, slowed cell proliferation and premature entry into cellular senescence (29; 48; 49; 56). Although these studies suggest that the growth defects observed in the mutant cells was likely due to a deregulation of the roles of Ku beyond DSB repair, they did not investigate further the mechanism by which the senescence was stimulated (49). To examine the effect of the mutations on growth rate, the cell proliferation of the stably transfected MEF cells were analyzed (Figure 16b). Consistent with previous findings, the $Ku70^{-/-}$ MEFs had a slower proliferation than their WT counterparts, with a growth rate that was about 5 times slower than the WT MEFs (P=0.01). Growth of the WT Ku70 restored MEFs was comparable to the WT MEFs, suggesting that the restoration of WT Ku70 in these cells was able to rescue the growth defects in these cells. The MEF cells that were stably expressing either ΔSAP Ku70 or $Ku70^{3E}$ had slower proliferation and 4 times slower growth rate than the WT-restored MEFs. Examination of asynchronous and G1 arrested cells did not identify any differences between the cells lines (data not shown). Further studies are needed to examine whether all of the cell types progress through the cell cycle at a similar rate, or if the mutant cells are progressing slower or are stalled at a certain stage of the cell cycle.

3.5.2 Mutations in the SAP domain of Ku70 sensitizes cells to DNA damage

To examine the ability of the restored cells to respond to DSBs, cells were treated with DNA damaging agents, such as bleomycin, hydrogen peroxide (H_2O_2), and camptothecin (CPT). While all of these chemical agents have been shown to induce both

double stranded and single stranded DNA breaks, bleomycin- and H_2O_2-induced breaks induce NHEJ-mediated repair (192) while CPT-induced breaks are repaired through NHEJ-independent processes, such as HR (164; 193; 194). Bleomycin is the most potent DSB inducing agent, with double-strand DNA lesions constituting 10-20% of the induced breaks (195; 196). Bleomycin mediates the production of superoxide and hydroxide free radicals which cleave DNA, producing both ss- and ds-DNA breaks (192; 197; 198). Similarly, H_2O_2 induces both ss- and ds-DNA breaks through the production of reactive oxygen species (197; 199; 200). Camptothecin induces replication-dependent DNA lesions by stabilizing the topoisomerase I/DNA complex and preventing religation of the DNA (201). Topoisomerase I relaxes super-coiled DNA generated through replication by binding to and cutting one strand of the DNA helix, permitting the helix to unwind. Once relaxed, topoisomerase I reconnects the broken strands. However in the presence of CPT, topoisomerase I cannot religate the DNA and the DNA that was cleaved is processed into DNA breaks and lesions as a consequence of encounters with replication forks (201). The repair of CPT-induced breaks and lesions is typically HR-directed and the involvement of the NHEJ apparatus during the processing of CPT-induced breaks is suggested to be detrimental to the repair process (193).

To examine the survival of the mutant cells in response to NHEJ-dependent DSBs, cells were treated with increasing doses of either bleomycin (Figure 17a) or H_2O_2 (Figure 17b), and, following recovery, an MTT assay was performed to measure cell viability. Treatment of both the ΔSAP and $Ku70^{3E}$ mutants with either bleomycin or H_2O_2 resulted in a dose-dependent reduction of survival that was intermediate between the WT-restored and $Ku70^{-/-}$ MEFs. This sensitivity was immediately visible at relatively low doses

Figure 17. Inhibition of Ku ribosylation results in increased sensitivity to DNA damage. Ku70-restored MEFs were treated with increasing doses of (a) bleomycin for 1 hour, (b) hydrogen peroxide (H_2O_2) for 30 minutes, or (c) camptothecin (CPT) for 1 hour. Following treatment with DNA damaging agent, cells recovered for 5 days and survival was determined via an MTT proliferation assay. Survival was normalized to untreated cells. The means of four independent experiments and standard deviation are shown. * indicates P=0.05.

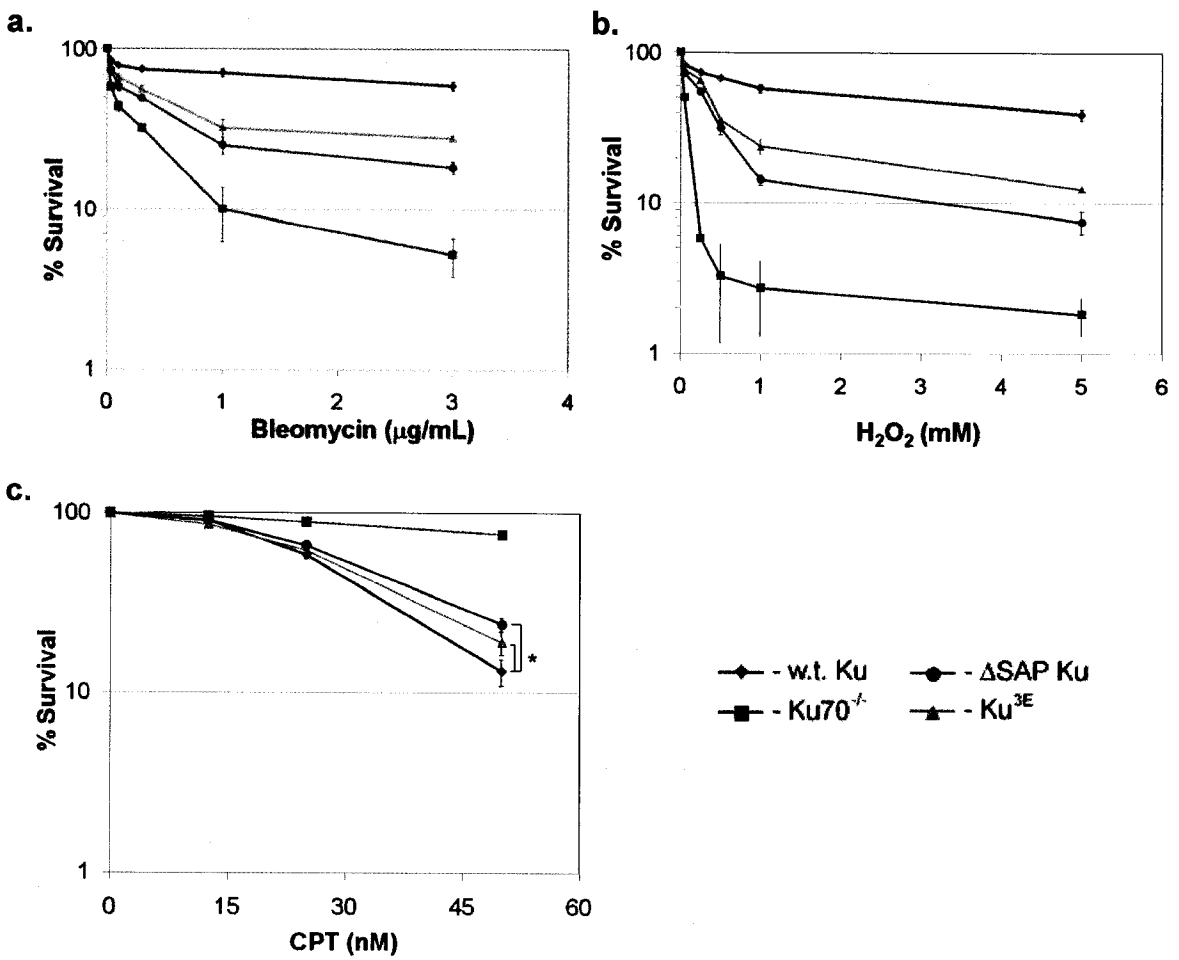
a.
100
10
1
% Survival
0
1
2
3
4
Bleomycin (μg/mL)
b.
100
10
1
% Survival
0
1
2
3
4
5
6
H2O2 (mM)
c.
100
10
1
% Survival
0
15
30
45
60
CPT (nM)
*
- w.t. Ku
- ΔSAP Ku
- Ku70-/-
- Ku3E

of both agents. Following bleomycin treatment the WT Ku70-restored MEFs show a median lethal dose (LD_{50}) of 0.75 μg/mL, while the ΔSAP mutants show an LD_{50} of 0.3 μg/mL, and the $Ku70^{3E}$ mutant had an LD_{50} of 0.48 μg/mL. Treatment of mutant cells with H_2O_2 resulted in a dose dependent decrease in cell survival compared with the WT-restored cells, with the $Ku70^{-/-}$ cells displaying the greatest sensitivity (LD_{50} = 0.05 mM). The WT Ku70-restored cells showed an LD_{50} of 1.6 mM. Both of the mutant-restored cell lines show similar sensitivity to H_2O_2 with ΔSAP-restored cells having an LD_{50} of 0.3 mM, and the $Ku70^{3E}$-restored cells had an LD_{50} of 0.4 mM.

To examine whether the Ku mutations influence the survival of the cells in response to NHEJ-independent DSBs, cells were treated with increasing doses of CPT. Consistent with previous studies that showed NHEJ-deficient cells were insensitive to CPT induced damage (17; 202), the Ku70 knockout cells were insensitive to CPT treatment showing only 24% reduction in survival at the highest doses used (Figure 17c). By contrast, the WT-restored cells were significantly more sensitive to CPT treatment than the $Ku70^{-/-}$ cells, displaying a dose dependent decrease in cell survival, with 87% reduction in survival for the WT-restored MEFs at the highest dose of CPT used. The Ku70-mutant-restored cells were similarly sensitive to the CPT treatment with an 81% and 76% reduction in survival at the highest dose of CPT used for the $Ku70^{3E}$- and ΔSAP- restored MEFs, respectively. The survival of the mutant-restored MEFs was significantly less (P=0.05) than the observed survival of the WT-restored MEFs.

To confirm that the reduced survival of the SAP mutants - following bleomycin or H_2O_2 treatment - was due to preventing the ribosylation of Ku by PARP1 and not due to the inhibition of additional functions of Ku, cells were treated with the PARP1 inhibitor 4-ANI

(4-Amino-1,8-naphthalimide) prior to-, during-, and for the first 24 hours following treatment with bleomycin. In the absence of DNA damaging agents, the inhibition of PARP activity with 4-ANI reduced the survival of all cells by 15-20%, representing the basal toxicity for 4-ANI treatment (Figure 18). Following treatment with 4-ANI and bleomycin, the WT-restored MEFs displayed recovery levels below those observed at the same dose points of bleomycin alone. Interestingly, the $Ku70^{-/-}$ MEFs showed a similar response until survival decreased below 10% when the cell survival was equal to that of bleomycin alone. By contrast, inhibition of PARP activity in the SAP mutant MEFs did not markedly affect their recovery following bleomycin treatment. Together these results establish a role for PARP1 in modulating Ku function in response to DSBs and this role is dependent on the SAP domain of Ku70.

3.5.3 $Ku70^{3E}$ mutants are proficient in γH_2AX signaling

One of the central roles of PARP1 is to act as a signal relay, amplifying the DNA damage signal to other co-factors within the cell, eliciting an appropriate damage response. H_2AX is one of several histone 2A variants and becomes phosphorylated on serine residue 139, then called γH_2AX, in response to DSBs (203). The γH_2AX is commonly used as a marker for the signaling and repair of DNA damage (203). It is possible that the reduction in cell survival observed in the ΔSAP- and $Ku70^{3E}$-restored MEFs is due to inadequate signaling of the DNA damage to other repair factors and processes. To determine whether the $Ku70^{3E}$ are able to elicit an appropriate γH_2AX response, the γH_2AX signal in the Ku70-restored MEFs was analyzed following bleomycin treatment (3 μg/mL; Figure 19). Both the

Figure 18. Inhibition of PARP activity with 4-ANI sensitizes wild-type Ku70 MEFs to bleomycin induced DNA damage. PARP activity was inhibited in Ku70-restored MEFs by treating the cells with 4-ANI prior to, during, and following treatment with bleomycin for 1 hour. Following treatment with bleomycin, cells recovered for 5 days and survival was determined via an MTT proliferation assay. Survival was normalized to untreated cells. Solid markers treatment with bleomycin; open markers were treated with 4-ANI and bleomycin. The means of four independent experiments and standard deviation are shown.

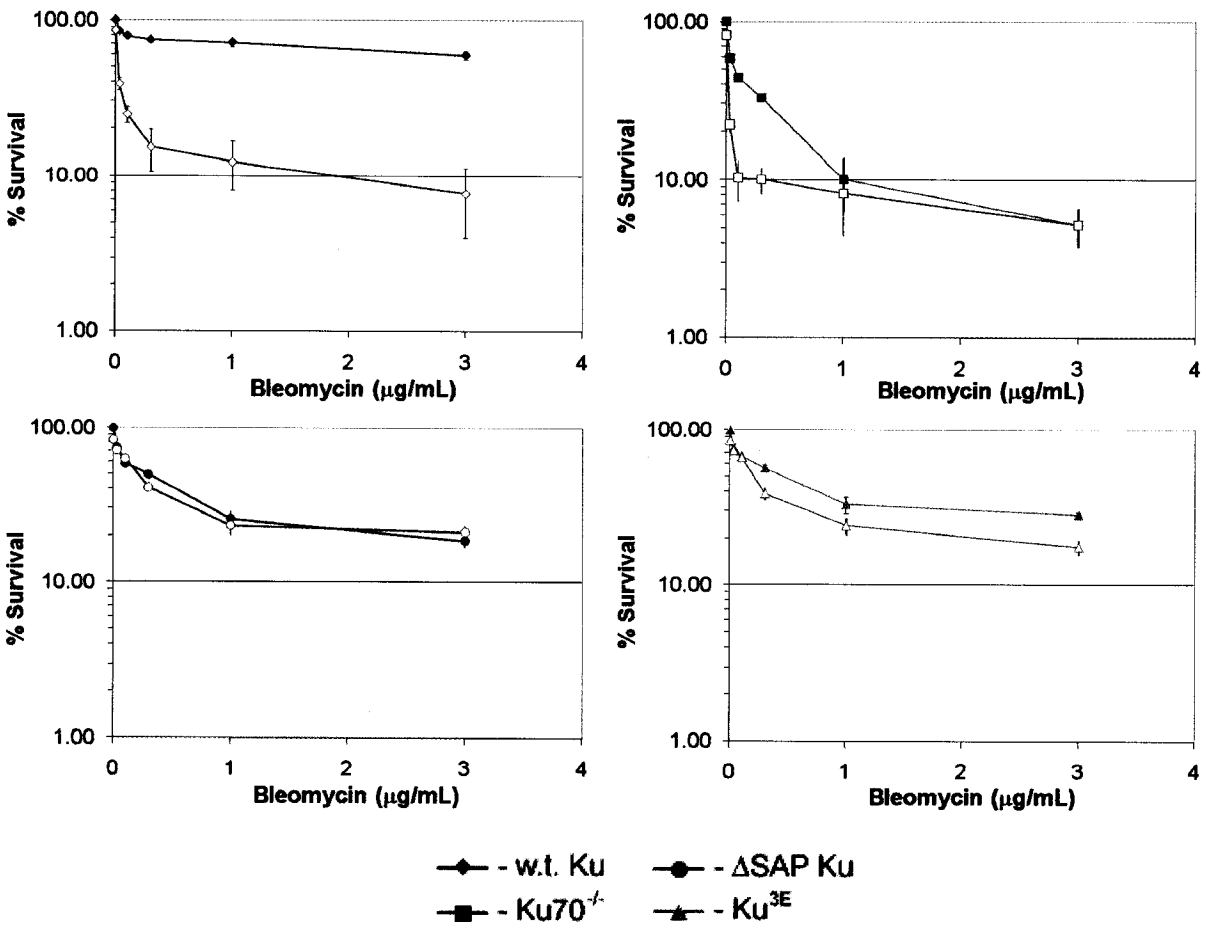
100.00
10.00
1.00
% Survival
0
1
2
3
4
Bleomycin (μg/mL)
- w.t. Ku
- ΔSAP Ku
- Ku70-/-
- Ku3E

Figure 19. Ku70^{3E} mutation does not impair γH$_2$AX signaling. Restored MEFs were treated with bleomycin (3 μg/mL) for 1 hour, then allowed to recover for indicated time (hours). Following recovery, cell extracts were resolved on 15% SDS polyacrylamide gel and transferred to PVDF membrane. Western blot analysis was performed using γH$_2$AX and histone 4 (H4) specific antibodies. Undamaged cells (U) were analyzed as a background control while histone 4 was used to control for variations in sample loading.

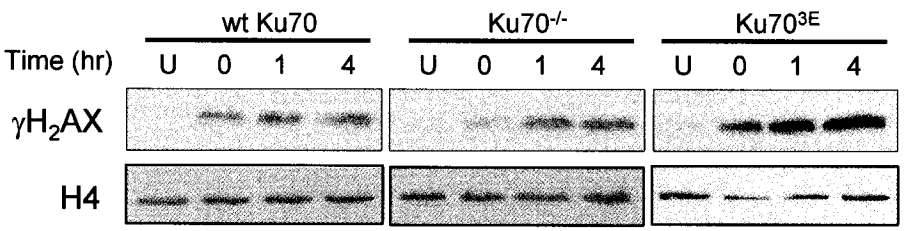
wt Ku70
Ku70-/-
Ku703E
Time (hr)
U 0 1 4 U 0 1 4 U 0 1 4
γH2AX
H4

WT- and Ku70^{3E}-restored cells show induction of γH_2AX immediately following treatment with bleomycin, and the γH_2AX levels remained elevated for 4 hours following treatment. This data suggests that DNA damage signaling is not overly compromised by the mutations within the SAP domain.

3.6 Ku70 SAP domain mutants display increased retention at foci following DNA damage

The use of concentrated localized damage – laser scissors, ionizing radiation induced foci (IRIF), low-/high-LET (high linear energy transfer) γ-radiation – in live cells has provided other groups the opportunity to examine the sequential recruitment of repair factors to sites of DNA damage, and subsequently delineate the order of their departure (16; 178; 204; 205). Other groups have tracked the coordinated arrival and leaving of repair factors at damage sites by examining their retention at heterochromatic foci following mild nuclear extractions (206). By using either of these methods, groups have determined that Ku is recruited to the damage sites immediately following the formation of DSBs and is retained at the site of DNA damage for over 2 hours, but is dispersed from the break site after 4 hours (16; 207). If the ribosylation of Ku by PARP1 contributes to the release of Ku from the DNA during or following repair of the break then the described SAP mutations might be expected to show an alteration in the rate at which Ku is released from sites of DNA damage.

To examine whether the SAP mutations cause a delayed retention at damage sites 293T cells were transfected with GFP-tagged WT Ku70 or GFP-tagged Ku70^{3E}. Once it was determined that the transfection efficiency of the two constructs was similar (data not

shown), the transfected cells were treated with bleomycin for 1 hour, at a dose sufficient to cause significant nuclear retention of Ku following a mild nuclear extraction, and then recovered (R_t) for up to 4 hours (Figure 20a). The retention of GFP-Ku in the nucleus was tracked by using a mild nuclear extraction followed by immunofluorescent staining using GFP-specific antibodies, and counterstained with 4'-6-diamidino-2-phenylindole (DAPI) to detect nuclei (Figure 20a).

In naive cells, the WT-Ku70 and $Ku70^{3E}$ were retained in fewer than 5% cells following the mild nuclear extraction (Figure 20b). Following treatment of the cells with bleomycin, the amount of Ku retained in the nucleus increased immediately in both cell types, reaching a maximal level after 1 hour of recovery from damage. Immediately following bleomycin treatment, both the WT and $Ku70^{3E}$ transfected cells displayed nuclear retention of Ku, with both reaching a maximal number of positive cells (cells with significant nuclear staining of GFP-Ku) after 1 hour of recovery (Figure 20b). After 1 hour of recovery, 59.1% of the cells transfected with WT GFP-Ku70 and 66.8% of the cells transfected with GFP-$Ku70^{3E}$ showed nuclear retention of Ku.

The nuclear retention of Ku following recovery from bleomycin treatment was also examined. As the recovery progressed, the staining of the nuclear retained Ku in the cells transfected with WT Ku70, transitioning from a punctate nuclear stain to a diffuse pan-nuclear stain, with only 16% of the cells having a detectable Ku signal within the after 4 hours of recovery (Figure 20c). While the amount of nuclear retained Ku in the $Ku70^{3E}$ cells also decreased, the nuclear retention of WT-Ku was lost almost twice as fast as that of the $Ku70^{3E}$. After 4 hours of recovery, 39.8% of the $Ku70^{3E}$ cells had detectable levels of nuclear retained Ku, with some cells still having Ku localized to a punctate nuclear stain.

Figure 20. $Ku70^{3E}$ is retained in the nucleus longer following bleomycin treatment. (a) The nuclear retention of Ku was examined by immunofluorescence (scale bar = 2 μm) in 293T cells transfected with GFP-Ku70 or GFP-$Ku70^{3E}$. Transfected cells were treated with 3.0 μg/mL bleomycin for 1 hour, and then allowed to recover for indicated time (R_t; hours). After recovery, cells were permeabilized with 0.1% Triton-X then fixed with paraformaldahyde. Using GFP-specific antibodies, immunflourescent staining was performed. Cells were counterstained with DAPI. (b) The number of cells with Ku retained in the nucleus increased to a maximal after 1 hour of recovery and was similar for both the WT-Ku70 and $Ku70^{3E}$. The nuclear retention of Ku was evaluated by counting the number of fluorescent positive cells and normalized against total number of cells as determined by DAPI stain. (c) The $Ku70^{3E}$ is retained in the nucleus longer than WT-Ku. The nuclear retention of Ku was evaluated as in (b) over the course of 4 hours post-damage. Retention was normalized to 1 hour post-damage, the maximal retention for both WT-Ku70 and $Ku70^{3E}$. The means of four independent experiments and standard deviation are shown. * indicates P=0.05.

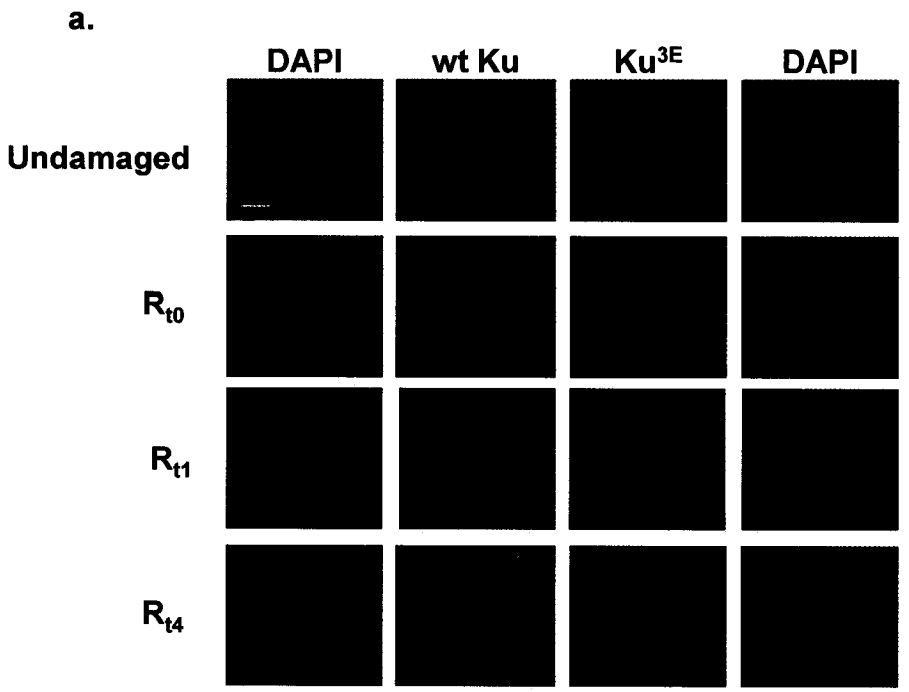
a.
DAPI
wt Ku
Ku3E
DAPI
Undamaged
Rt0
Rt1
Rt4

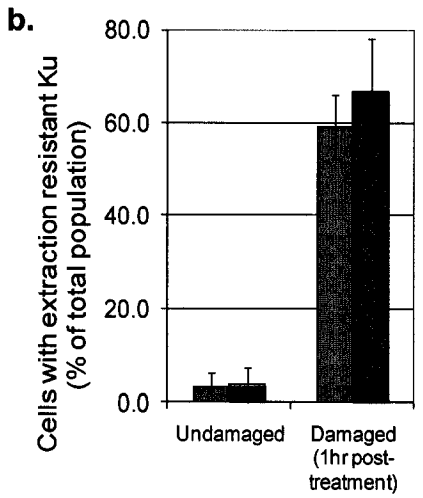
b.
Cells with extraction resistant Ku (% of total population)
80.0
60.0
40.0
20.0
0.0
Undamaged
Damaged (1hr post-treatment)

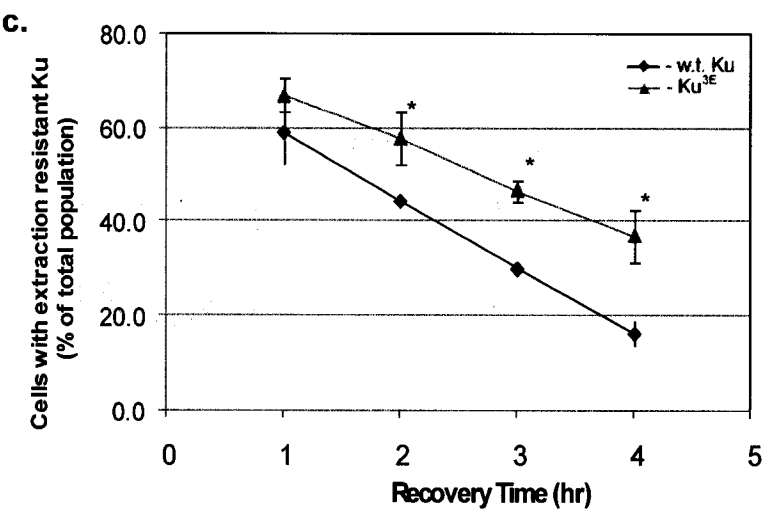
c.
Cells with extraction resistant Ku (% of total population)
80.0
60.0
40.0
20.0
0.0
0
1
2
3
4
5
Recovery Time (hr)
- w.t. Ku
- Ku3E
*
*
*

These results show that while the $Ku70^{3E}$ mutation does not compromise the recruitment of Ku to the DSB, it does cause Ku to be retained at the DSB for almost twice as long as WT Ku, this prolonged retention could have a negative effect on cell survival following DNA damage.

3.7 *In vivo* V(D)J recombination

3.7.1 Mutation of SAP domain reduces recombination efficiency

In addition to its roles in DNA damage repair, NHEJ plays a critical role in V(D)J recombination. A functional NHEJ apparatus is required for the processing and ligation of the V(D)J recombination products and dysfunction in the NHEJ apparatus leads to immunodeficiency (32). Previous work in our lab and others has demonstrated that Ku plays an essential role in V(D)J recombination, as Ku-deficient cells display reduced recombination efficiency and accuracy (38; 69). In Ku-deficient mice, the formation of signal joints has been shown to be reduced up to 100-fold and those recovered show massive deletions of the joined RSS sequences (29; 49). Thus, in order to test the functionality of the SAP mutations in V(D)J recombination, a vector-based *in vivo* V(D)J recombination assay was employed that would provide a direct measurement of the V(D)J products and in turn, the efficiency and accuracy of recombination.

The *in vivo* V(D)J recombination assay is a vector-based RSS system, whereby a vector containing two RSSs is transfected into cells in conjunction with plasmids encoding RAG1 and RAG2 (Figure 21a). Following transfection and expression of the RAGs, the recovered recombination vector is transformed into *E. coli* then grown on LB plates in the presence of either ampicillin or ampicillin and chloramphenicol. The recombination vector

Figure 21. Mutation of the SAP domain causes errors in V(D)J recombination. (a) The schematic representation of the extrachromosomal recombination substrate pJH200 used in the V(D)J recombination assays. pJH200 contains a 12RSS cassette in the orientation of the nonamer-12 bp spacer-the heptamer and a 23RSS cassette in the orientation of the heptamer-23 bp spacer-the nonamer. In the presence of the RAG1/2 protein, pJH200 can undergo deletional recombination with the intervening sequences between the two heptamers deleted from the plasmid substrates. The primer set R7 and R8 generates a 308 bp fragment more than 3 kb from the 12RSS or 23RSS and amplifies both unrecombined and recombined pJH200. The primer set 200-R3 (R3) and 200-R14 (R14) generates by PCR a 460 bp fragment spanning the region containing the 12RSS and 23RSS before recombination and a 256 bp fragment containing the fused RSSs in the configuration of the nonamer-12 bp spacer-the heptamer-the heptamer-23 bp spacer-the nonamer after recombination (187). The pJH200 vector contains a gene encoding chloramphenicol acetyltransferase (CAT). The CAT gene is interrupted by the intervening sequences between the two heptamers and upon RAG-mediated deletional recombination the CAT gene can be functionally expressed. The pJH200 vector also contains an ampicillin resistance gene. Thereby, recombination efficiency can be determined comparing the growth of *E. coli* transformed with the pJH200 vector on LB plates containing either ampicillin or chloramphenicol and ampicillin. (b) Ku70 restored MEFs were transfected with pJH200 V(D)J recombination assay plasmid, and/or RAG1 and RAG2. After 48 hours, plasmid was isolated and recombination efficiency was examined as previously described. (c) To analyze the recombination sites the recovered pJH200 vector samples were amplified by PCR using the primer set 200-R3 and 200-R14 or the primer set R7 and R8. The amount of recombined template DNA (Input DNA) used for individual PCR reactions was standardized based on the recombination efficiency (b). The PCR products were resolved on a 2% agarose gel stained with Sybr Green. (d) Aberrant signal joint structures from stably transfected MEFs. The amplified recombination products from the signal joints were subcloned into TA cloning vector and individual clones sequenced. On average, 30 recombination products were sequenced for each cell type; frequency of each recombination event is indicated.

a.

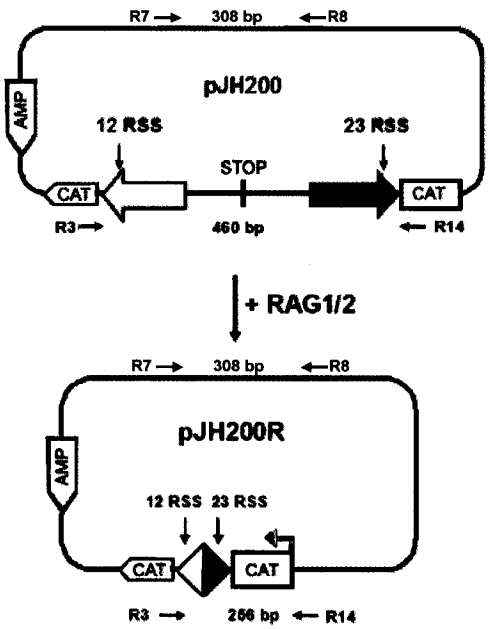

b.

	Relative Recombination Efficiency	
	Signal Joint	Coding Joint
WT	1.00 ± 0.03	1.00 ± 0.04
Ku70$^{-/-}$	0.02 ± 0.02	0.01 ± 0.02
ΔSAP	0.19 ± 0.04	0.09 ± 0.03
Ku70^{3E}	0.25 ± 0.02	0.16 ± 0.03

c.

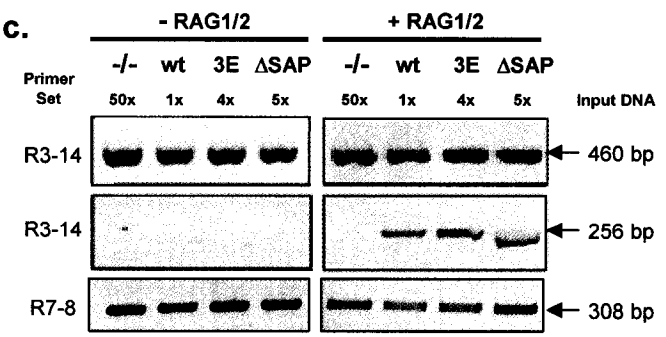

d.

WT	0.96	TGTTTTTGTTCCAGTCTGTAGCACTGTG	CACAGTGGTAGTACTCCACTGTCTGGCTGTACAAAAACC
	0.02	TGTTTTTGTTCCAGTCTGTAGCACTGTG	ACAGTGGTAGTACTCCACTGTCTGGCTGTACAAAAACC
	0.02	TGTTTTTGTTCCAGTCTGTAGCACTG	CACAGTGGTAGTACTCCACTGTCTGGCTGTACAAAAACC
ΔSAP	0.20	TGTTTTTGTTCCAGTCTGTAGCACT	GTGGTAGTACTCCACTGTCTGGCTGTACAAAAACC
	0.17	TGTTTTTGTTCCAG	CACAGTGGTAGTACTCCACTGTCTGGCTGTACAAAAACC
	0.13	TGTTTTTGTTCCAGTC	TGTACAAAAACC
	0.10	TGTTTTTGTTCCAGTCTGTAGCACTGTG	
	0.07	TGTTTT	AAACC
	0.07	TG	GTCTGGCTGTACAAAAACC
	0.03		CACAGTGGTAGTACTCCACTGTCTGGCTGTACAAAAACC
	0.23	Translocations & Rearrangements	
Ku70^{3E}	0.30	TGTTTTTGTTCCAGTCTGTAGCACTGTG	CAGTGGTAGTACTCCACTGTCTGGCTGTACAAAAACC
	0.30	TGTTTTTGTTCCAGTCTGTAGCACTG	AGTGGTAGTACTCCACTGTCTGGCTGTACAAAAACC
	0.24	TGTTTTTGTTCCAGTCTGTAGCA	TGGTAGTACTCCACTGTCTGGCTGTACAAAAACC
	0.07	TGTTTTTGTTCCAGTCT	GGTAGTACTCCACTGTCTGGCTGTACAAAAACC
	0.03	TGTTTTTGTTCCAGTCTGT	CCACTGTCTGGCTGTACAAAAACC
	0.03	TGTTTTTGTTCCAG	ACTCCACTGTCTGGCTGTACAAAAACC
	0.03	TGTTTTTGTTCCAGTCTGTA	TGTCTGGCTGTACAAAAACC

contains resistance markers for both ampicillin and chloramphenicol, however the chloramphenicol acetyltransferase (CAT) gene is only expressed after recombination removes a transcriptional terminator (179). Thus, the recombination efficiency can be assessed by comparing growth on the two selectable plates.

There are two separate vectors available for this analysis which allows the analysis of either the signal or coding joints following recombination. The pJH200 vector retains two signal joints following recombination, with the coding gene segments being removed. Alternatively, the pJH290 recombination vector retains the coding gene segments while the signal joints are lost following recombination. These two recombination vectors allow a thorough analysis of both of the products of V(D)J recombination. The recombination analysis was performed using the previously described restored MEFs and both pJH200 and pJH290 recombination vectors.

When the recombination efficiency of the WT Ku70-restored MEFs was examined, the vector containing signal joints recovered 1.5% recombination, while 0.8% of the recovered coding joint vector was recombined. These values were standardized as 100% for the remaining analysis (Figure 21b). Consistent with previous studies, each of the recovered vectors from the $Ku70^{-/-}$ MEFs had almost 100-fold reduction in the recombination efficiency, with 1 % recombination efficiency for the coding joints and 2 % efficiency for the signal joints, as compared to the WT MEFs. When the transformants from the ΔSAP and $Ku70^{3E}$ MEFs were analyzed, there was a reduction in the recombination efficiency for both mutants as compared to the WT MEFs. The $Ku70^{3E}$ mutants showed 25% recombination efficiency for the signal joints and 16% recombination efficiency for the recovered coding joints. The recombination efficiency in the ΔSAP MEFs was even further reduced with 19%

recombination efficiency for the signal joints and 9% recombination efficiency for the recovered coding joints. Although both mutants had a greater recombination efficiency as compared with the Ku70-deficient cells, suggesting they were able to complete recombination, the amount of recombination was severely impaired as indicated by their reduced recombination efficiency as compared to the WT-restored MEFs.

3.7.2 V(D)J recombination in SAP mutants is imprecise

The reduced recombination efficiency in the mutant cell lines compared with the WT cells could result from the failure to form a functional NHEJ complex. By understanding whether those recombination events that did occur were occurring accurately, it may be possible to discern where in the process the efficiency of recombination was deteriorating.

Although NHEJ is an error-prone mechanism of DNA repair, often processing the DNA ends prior to ligation, it can directly ligate compatible ends, like blunt ends, without any processing. Serendipitously, the cleavage of the RSS to generate the signal ends results in the formation of blunt ends, to which the NHEJ apparatus repairs without the need for processing, to form the signal joints. This direct ligation of the signal joints provides a means for measuring the accuracy of recombination. By utilizing PCR primers which bind to the signal joint recombination vector (pJH200) and amplifying both RSSs and the region between them (Figure 21a) it is possible to measure the accuracy of recombination. If recombination has occurred, the region between the RSSs will be removed and the PCR reaction will yield a 256 bp "recombined" fragment. In the event recombination does not occur, a larger 460 bp "unrecombined" fragment will be produced as the region between the two RSSs will be present and amplified. In order to standardize the amount of recombined

template used for individual PCR reactions, the amount of recombined template DNA added to each reaction was adjusted based on the recombination efficiency.

PCR analysis of the recovered recombination vector from WT Ku70-restored MEFs yielded only the unrecombined fragment when transfected with the recombination construct alone. When the constructs encoding RAG1 and RAG2 were co-transfected with the recombination vector both the unrecombined and recombined fragments were amplified (Figure 21c). Regardless of the presence or absence of RAG1 and RAG2, PCR analysis of recovered recombination vector from the Ku70-deficient MEFs did not produce the 256 bp recombination fragment and only amplified the larger unrecombined fragment. When the ΔSAP MEFs were co-transfected with the recombination vector and the RAG1 and RAG2 constructs, the resulting PCR products from the recovered vector contained the larger 460 bp unrecombined fragment, but also contained smaller products of various sizes, as a smear was present when the reactions were resolved, with the average size of the amplified product being approximately 200 bp – 56 bp shorter than the 256 bp recombined fragment. The PCR analysis of the recovered recombination vectors from the co-transfected $Ku70^{3E}$ MEFs yielded the recombined fragment, and did not appear to differ noticeably in size from the predicted 256 bp.

In order to characterize the nature of the recombination products, the amplified recombination products were subcloned into a TA cloning vector, and individual clones were sequenced. Sequence analysis indicated that accurate recombination had occurred in 96% of the clones recovered from the WT Ku70-restored MEFs (Figure 21d). A minor fraction of the sequences analyzed (4%) contained deletions of one or two nucleotides.

Sequence analysis of the recombination products recovered from the ΔSAP MEFs showed large egregious errors present in all of recombination products analyzed, with deletions present in 77% of the recombination products while the remaining 23% of the recombination products analyzed contained translocations and other rearrangements (Figure 21d). While the deletions ranged from short deletions of both heptamers to almost the entire deletion of both RSSs, larger deletions that removed 12 nucleotides (or more) of either RSS constituted the majority of the sequences analyzed (57%). In addition to the deletions in the RSSs, 23% of the recombination products analyzed contained rearrangements of the recombination vector itself and in some instances (3), the translocation of chromosomal DNA.

Sequence analysis of the recombination products of the $Ku70^{3E}$ MEFs also identified deletions in 70% of the samples analyzed, however these deletions were less severe than those recovered from the ΔSAP MEFs, often with no more than 15 nucleotides deleted, and there were no translocation events detected.

Altogether the examination of the V(D)J recombination events in MEF cells restored with the ΔSAP and $Ku70^{3E}$ mutations suggest that although these cells can process recombination events, these events are rare and those that do occur contain errors in the rejoined products. Assuming that the cleavage of the RSS by the RAGs occurs equally between cell types, the errors observed in the rejoined products must be the result of a deficient NHEJ process. Given the previously shown *in vitro* and *in vivo* data that shows the described mutations in Ku70 affect the ability of Ku to respond to ribosylation by PARP1, then these effects within V(D)J recombination may be the result of this inability of the Ku

heterodimer to respond to PARP1. This is the first description of PARP1 having an effect on a component of the NHEJ apparatus in the V(D)J recombination process.

4. Discussion

The structure of the Ku heterodimer provides an elegant solution to recognizing and binding DNA breaks. The intricate folding of the two subunits results in the formation of a central cavity in which the DNA is threaded through, providing for a stably bound protein:DNA complex. Ku binds to DNA in a specific orientation to DNA ends with Ku70, which is suggested to be the subunit required for the involvement of Ku in DNA repair, oriented toward the free end of the DNA, and Ku80, which is suggested to be the subunit involved in protein-protein interactions, oriented toward the interior of the DNA (33; 65; 83). The formation of a Ku:DNA complex is highly stable and is able to remain intact for over 24 hours *in vitro* (177). Following binding to the DNA, Ku is able to slide inward on the DNA in a so-called "bind-and-slide" mechanism stalling at internal sites of DNA molecules (80; 81; 82). This complex, yet elegant method that Ku employs to bind DNA has been described in numerous studies yet only a of them few studies have investigated the manner in which Ku is removed from the DNA once repair has been completed. The data presented herein is the first known description of an active dissociation of Ku from DNA, independent of free DNA ends. I have demonstrated that PARP1 is able to mediate the active dissociation of Ku from DNA regardless of the presence of DNA ends. Mutation of specific glutamate residues within the C-terminal SAP domain of Ku70 results in the inhibition of Ku ribosylation and the PARP1-mediated release from DNA. Furthermore, the mutation of these residues *in vivo* results in the prolonged retention of Ku at sites of DNA damage, increased sensitivity to bleomycin and H_2O_2, and a decrease in the proliferation and growth rate of cells. Given its abundance within the cell and the numerous roles it undertakes, understanding the fundamental mechanisms regulating the DNA binding of Ku

provides a more robust knowledge about the functioning of the heterodimer. The results presented in this study suggest that the deregulation of the DNA binding activity of Ku impacts several aspects of the function of Ku in the cell, and ultimately the cell's survival.

4.1 PARP1 ADP-ribosylates the SAP domain of Ku70

Previous studies have suggested that aside from the autoribosylation of PARP1 itself, the predominant targets for ribosylation by PARP1 are DNA bound proteins, such as histones (134; 135), DNA repair factors (146; 147), DNA ligases (150), and DNA polymerases (145). Consistent with this trend, *in vitro* studies using purified components in solution were able to show that PARP1 is able to ribosylate Ku (174; 175), and this ribosylation causes a decrease in the binding affinity of Ku (174). While these studies showed that Ku in solution was able to be ribosylated by PARP1, they failed to ascribe the ribosylation to a specific domain within the heterodimer. In addition to confirming that PARP1 is able to ribosylate both subunits of the Ku heterodimer *in vitro*, I have also been able to identify mutations within the SAP domain of Ku70 that prevent ribosylation of the Ku heterodimer. Interestingly, while these mutations were within the Ku70 subunit of the heterodimer, they appear to prevent the ribosylation of both the Ku70 and Ku80 subunits. The results of the present study cannot address whether the ribosylation of Ku80 is dependent upon the ribosylation of Ku70, or the mutations in Ku70 are directly inhibiting the ribosylation of Ku80. In order to address this, mutations within the Ku80 subunit which prevent its ribosylation by PARP1 would need to be identified. The same candidate domain approach used here could be applied to the Ku80 subunit, identifying domains in the Ku80 subunit which, given their location in the Ku heterodimer bound to DNA, could be

accessible and targeted by PARP1. While the mutations in the SAP domain were shown to prevent the release of Ku, it is possible that this retention was not a result of preventing the ribosylation of Ku70 directly, but moreover an effect of preventing the ribosylation of the entire heterodimer. The active release of Ku from DNA by PARP1 might require the ribosylation of both subunits, and identifying the mutations within the Ku80 subunit that prevent its ribosylation would provide a more detailed description of how PARP1 mediates the active dissociation of Ku from DNA.

4.2 PARP-1 manipulates the interaction of Ku with DNA

The *in vitro* and the immunofluorescence data presented here show that the inhibition or prevention of the ribosylation of Ku results in prolonged residency of Ku on DNA. The SAP domain of Ku70 is defined as a DNA binding domain that, upon binding of Ku to DNA, transitions from the base of the heterodimer to being proximal to the central cavity and interacting with the DNA, potentially stabilizing the binding of Ku to the DNA (67; 83). The accumulation of negative charges associated with ribosylation has been shown to influence the association of proteins with DNA (133), and it is possible that the ribosylation of the SAP domain specifically, destabilizes the binding of the SAP domain to the DNA, permitting Ku to slide more freely on the DNA. If the loss of ribosylation results not only in the retention of Ku on DNA, but also in an impediment of the inward translocation of Ku on the DNA, then this may help reconcile the errors V(D)J attributed to a defective NHEJ apparatus. Previous studies have shown that the DNA ligase IV-dependent ligation is stimulated by Ku independent of DNA-PK_{cs}, but requires the inward translocation of Ku on DNA (31; 212). Additionally, Ku has been shown to inhibit HR repair at I-SceI-generated

DSBs in PARP1 deficient DT-40 chicken cells (17), at RAG-generated breaks in mouse embryonic stem cells (213), and at telomeres (214). Taken together, these results suggest that if the ability of Ku to be removed from the DNA end (either by inward translocation or by dissociation) is inhibited, then Ku at the DNA end prevents either HR- or NHEJ-mediated repair from occurring by restricting access to the DNA ends; which is the suggested role that Ku plays while located on the telomeres. The ribosylation of Ku by PARP1 would cause the removal of Ku from the end – either through the inward translocation on DNA or the altogether loss of Ku from the DNA – and in turn, providing the repair proteins access to the ends.

It was previously shown that the Ku heterodimers on DNA ends *in vivo* is in a dynamic equilibrium with the Ku heterodimers in solution, cycling on and off the end with a half-life of 2 minutes (178). This however is in stark contrast to the *in vitro* observations that the Ku heterodimer is stable on linearized DNA for over 24 hours, and does not transfer between DNA molecules (81; 176; 177) with the measured dissociation constant (k_d) of Ku ranging in the nano- to picomolar range (31; 76; 215; 216). This *in vivo* cycling of Ku molecules on the DNA end observed by Mari *et al.* (178) could result from the turn-over of the Ku resident on the DNA end through ribosylation, and subsequent deribosylation. The glycosidic activity of PARG is highly proficient and *in vivo* PAR polymers have a rather short lifespan and the accumulation of PAR polymers is a transient event (143). Additionally, I have shown *in vitro* that following treatment with PARG the DNA binding ability of ribosylated Ku was restored. Taken together this supports the notion of PARP1 accelerating the turn-over of Ku at the DNA end, and the same molecule of Ku could rebind the DNA end following catabolism of the PAR chains by PARG. Alternatively, given the

abundance of Ku within the nucleus it is conceivable that the release of one Ku molecule would be immediately replaced by another. Either case would suggest that the mutations in the SAP domain of Ku70 that prevent PARP1-mediated release of Ku from the DNA would also prevent the shuttling observed by Mari and colleagues (178).

While it is conceivable that the ribosylation of Ku increases the mobility of Ku on the DNA, allowing Ku to translocate to the interior of the DNA or slide off the free end of the DNA, this mechanism is not sufficient to explain the observations that PARP1-mediated release of Ku also occurs in the absence of DNA ends. Therefore the release of Ku is likely to involve alterations in the heterodimer that extend beyond translocation of the SAP domain, involving an opening of the heterodimer and possibly the dissociation of the Ku70 and Ku80 subunits. The extent to which the two subunits progress from an opened state that slides freely on the DNA, to a complete dissociation of the Ku from the DNA may be a function of the amount of ribosylation imposed on the heterodimer, suggesting that the ribosylation of Ku may progress in a step-wise fashion (Figure 22). As discussed previously, this is supported by the *in vitro* ribosylation experiments which show that both subunits of the heterodimer are ribosylated by PARP1, and mutation of the SAP domain prevents ribosylation of the entire heterodimer. Additionally, the rebinding experiments with PARG would suggest that removal of the PAR groups would allow Ku to re-establish its "closed" structure and rebind the DNA.

It appears contradictory that the role of PARP1 (whose enzymatic activity is stimulated by its binding to DNA) is to help initiate the inward translocation of Ku from the DNA end by ribosylating the SAP domain of Ku70, and yet Ku, localized to the DNA ends,

Figure 22. Model of PARP1-mediated regulation of Ku binding activity. (**1.**) Following formation of DSB, (**2.**) Ku binds to the free DNA ends and is stabilized by the translocation of the SAP domain which binds to the threaded DNA. (**3.**) PARP1 is recruited to the DNA end and ribosylates the SAP domain of Ku70. (**4.**) Ribosylation of the SAP domain destabilizes its association with the DNA and causes the SAP domain to move away from the DNA. (**5.**) This repositioning of the SAP domain places the heterodimer in the "open" position and allowing it to move more freely on the DNA, either translocating inward away from the end, or sliding off of the end itself. (**6.**) Further ribosylation of the heterodimer (Ku80 in particular) is possible, which could cause additional structural alterations to the heterodimer resulting in the release of Ku from the DNA, regardless of DNA ends.

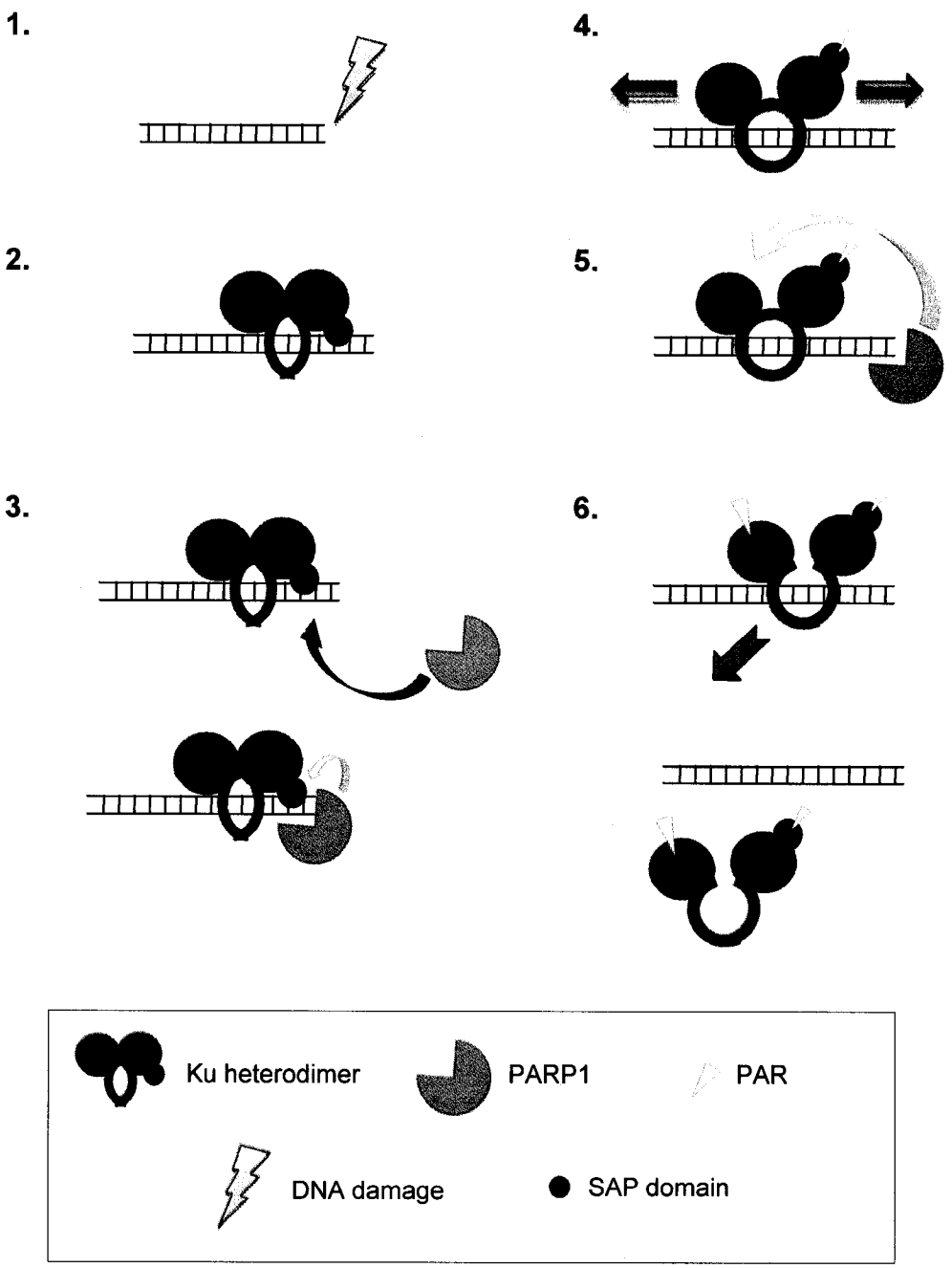
1.
2.
3.
4.
5.
6.
Ku heterodimer
PARP1
PAR
DNA damage
SAP domain

prevents access of other proteins to the DNA. However, these apparent conflicting observations may be reconciled by further examining the structure of the Ku heterodimer bound to DNA. As mentioned previously, the Ku heterodimer forms a cradle-like structure, with a relatively flat base that holds the DNA, while a bridge-like structure encircles the DNA (Figure 4a). Much of the DNA surface facing away from the cradle base is exposed except the 3 to 4 bp of DNA encircled by the bridge-like structure (217). This arrangement with the bulk of the Ku protein on one side of the DNA helix allows other proteins access to the contralateral, exposed surface of the DNA helix (24), and may provide a solution to how PARP1 becomes activated at DNA ends occupied by Ku.

In order to form a functional NHEJ complex, Ku at some point must be stable on the DNA end so that DNA-PK_{cs} can be recruited and NHEJ can proceed. The recruitment of DNA-PK_{cs} to the damage site may alter the ribosylation of Ku, either by preventing the initial ribosylation from occurring, or by stabilizing the ribosylated Ku on the DNA. The recruitment of DNA-PK_{cs} to the site of DNA damage occurs within minutes of the damage occurring (213), which is similar to the recruitment of PARP1 to DSBs (16). If DNA-PK_{cs} prevents the ribosylation of Ku by PARP1, then a competition between DNA-PK_{cs} and PARP1 for Ku at the DNA end may exist, and the outcome of this competition would determine the mechanism of repair. This idea is supported by the observations that by preventing procession through NHEJ by either inhibiting the catalytic activity of the early components (DNA-PK_{cs}) (205) or deleting the latter components (XRCC4, DNA ligase IV) (178) the assembled DNA-PK complex (containing both Ku and DNA-PK_{cs}) is stable on the DNA end and is retained at the DSB. This stalled repair complex diminishes the repair capability of the cell, and the DNA lesions remain unrepaired. Conversely, cells lacking

DNA-PK$_{cs}$, the repair of DSBs through NHEJ is compromised, however repair is not absent and under these conditions HR or a back-up NHEJ (NHEJ-b) repair is suggested to repair the breaks (178). In both instances, Ku would be present at the DSB, however it may suggest that in cells lacking DNA-PK$_{cs}$, PARP1 is able to remove Ku from the DNA ends and other mechanisms can attempt repair. On the other hand, in cells where DNA-PK$_{cs}$ is present but lacks its catalytic activity, DNA-PK$_{cs}$ binds to Ku blocking it from PARP1 and preventing the ribosylation of Ku; as a result, a non-functional DNA-PK complex occupies the DNA preventing any form of repair from occurring.

4.3 Consequences of Ku70 ribosylation

The loss or inhibition of proteins involved in the detection and repair of DSBs consistently results in cells with an increased sensitivity to DNA damage. Studies have shown that cells lacking PARP1 are deficient in DSB repair and display increased sensitivity to ionizing radiation and alkylating agents (17; 157; 208; 209), while the loss of either subunit of the Ku heterodimer renders cells deficient in DSB repair and more sensitive to DNA damage (29; 49; 210). Interestingly, the experiments performed here show that cells expressing the mutant forms of Ku which are unable to be ribosylated by PARP1 *in vitro* also display an increased sensitivity to DNA damage. The MEF cells expressing either the ΔSAP or Ku70^{3E} mutants had a significantly increased sensitivity to bleomycin- or H_2O_2-induced DNA damage compared with the WT cells, however these cells were not as sensitive as Ku70-deficient cells. While this increased susceptibility to DNA damage was noticeable at all dose points, the intermediate phenotype of the SAP mutants was most noticeable at the highest doses used. This suggests that at low doses of DNA damage, the

mutant forms of Ku70 are able to elicit a DNA damage response and repair some of the breaks, however at higher doses of DNA damage this response is insufficient and results in an increased sensitivity to DNA damage as compared with the WT-restored cells. While this could be the result of a failure to activate proper repair pathways, such as HR, it may also be the result of the prolonged residency of Ku on the DNA following repair ultimately leading to a disruption in the post-repair processes. The reduction in survival and prolonged retention during the nuclear retention assays are not able to address whether these observations are the result of lower levels of repair, or a slower rate of repair. Further studies will be required to delineate exactly the how much repair is occurring and what stages of the NHEJ repair process are defective, however it may be possible to suggest at which stages the defects in repair may be occurring given the results obtained through the γH_2AX signaling and V(D)J recombination experiments. The induction of γH_2AX signaling and the immediate localization of Ku to foci following bleomycin treatment would argue that the initial repair signals are intact, while the aberrations observed in the V(D)J recombination assays suggest that errors occur later in the repair process, possibly during the processing of the break. Taken together, these results would suggest a novel role for PARP1 in the resolution of DSBs repaired through the NHEJ pathways. To date, PARP1 has not been suggested to play an active role in NHEJ but is believed to be important for the regulation of the repair pathway choice (17; 211). However, the results presented here implicate PARP1 as playing a more direct, active role for in NHEJ-mediated repair. It is my hypothesis that the role of PARP1 in NHEJ-mediated repair is to facilitate the translocation of Ku from the DNA end, and ultimately the release of Ku from the DNA.

Previous studies have shown that the presence of Ku at DNA ends inhibits the HR repair process, and this inhibition can be overcome by the deletion of various members of the NHEJ apparatus. DNA lesions formed by treatment with CPT are typically HR-directed and the involvement of the NHEJ apparatus during the processing of CPT-induced breaks is suggested to be detrimental to the repair process and the survival of the cell (193). Consistent with these studies, the Ku-restored MEFs (both WT and mutant forms) had a significantly reduced survival compared with the Ku-deficient MEF cells. Interestingly, the WT cells were the more sensitive to CPT exposure than the ΔSAP- and $Ku70^{3E}$-restored cells. Given that it is proposed that the presence of Ku and the NHEJ apparatus is detrimental to the recovery from CPT exposure by preventing HR from accessing the DSB, it might have been expected that the SAP mutants would have been more sensitive to CPT than the WT cells as they would bind to the DNA breaks and reside longer on the DNA than the WT Ku. This longer residence could be expected to make the mutant Ku a more potent inhibitor of HR than the WT Ku. However, the observed differences in survival may not reflect the true sensitivity to CPT-induced DNA damage, but may be suppressed by the differences in the growth rates between the WT and mutant cells. Double stranded DNA breaks induced by CPT are derived from the collision of the ongoing replication fork with the topoisomerase I-cleaved DNA complex (201; 219). If the WT-restored cells proliferate faster, then they will "experience" more CPT-induced DSBs for the same dose than the slower growing ΔSAP and $Ku70^{3E}$ cells. Therefore it may be that the mutant Ku is more detrimental to the repair of CPT-induced breaks, yet fewer breaks occur in these cells as a result of their reduced growth rate, compensating for the reduced repair.

4.4 The involvement of PARP1 in V(D)J recombination

V(D)J recombination is the process of introducing controlled, site-specific DSBs for the recombination of the genes involved in generating the diverse repertoire of T cell receptor (TCR) and immunoglobulin (Ig) molecules. The requirement of the Ku heterodimer and the NHEJ apparatus in V(D)J recombination has been well established and is involved in the resolution of both the coding ends and signal ends. Cleavage of the RSS to form the signal ends results in the formation of blunt ends which the NHEJ apparatus treats as a simple DSB, which the NHEJ apparatus can ligate together without the loss of nucleotides (108). However, cells with deficiencies in either the Ku heterodimer or in DNA-PK_{cs} display reduced recombination efficiencies and imprecise recombination events of the signal sequences (29; 49; 56; 109). Consistent with these previous studies, the $Ku70^{3E}$ and the ΔSAP mutant cells had decreased V(D)J recombination efficiency and display errors in the recombination products, with deletions of either the 12- or 23-RSS, vector rearrangements, and chromosomal translocations all taking place. While V(D)J recombination was not completely absent, these irregularities suggest a deregulation of the processing of the break and appear to be suggestive of erroneous cleavage events, which could suggest a defective NHEJ apparatus.

The role for PARP1 in V(D)J recombination is less defined and there are contradictory studies suggesting that PARP1 facilitates the resolution of coding end resolution (146), or acts as an antagonist to V(D)J recombination in DNA-PK_{cs}-deficient cells (218). Interestingly, the evidence presented in the current study may bridge these two seemingly contradictory results by suggesting that the role of PARP1 in V(D)J recombination reactions is in the regulation of Ku on the DNA; a function that is more a

characteristic of PARP1 function in NHEJ than in V(D)J recombination specifically. The proposed role for PARP1 in NHEJ repair is to mitigate the movement of Ku from the DNA end by ribosylating the DNA bound SAP domain. I have been able to show that preventing the ribosylation of Ku results in the prolonged residency of Ku on the DNA. The presence of an immobile Ku on the DNA following cleavage by RAGs is detrimental to the resolution of the breaks, as illustrated by the drastically reduced recombination efficiencies in the SAP mutant MEFs. In order to circumnavigate the immobile Ku on the DNA and repair the RAG-induced breaks, the repair apparatus could utilize the nuclease activity of Artemis, a protein known to be involved in V(D)J recombination (219; 220; 221; 222), to cleave the DNA occupied by Ku. Therefore, for appropriate V(D)J recombination to proceed, PARP1 regulates the association of Ku at the RAG-induced breaks. Inhibition or prevention of this regulation results in the prolonged residence of Ku at the repair site, which in turn inhibits the repair of the break.

4.5 Alternatives to ADP-ribosylation for regulating Ku binding?

Despite structural variations, the Ku heterodimer is functionally conserved in all eukaryotes. The conservation and the variations of the Ku heterodimer between species may reflect the differences between the roles and regulation of Ku in each organism. Homologous recombination-mediated repair dominates the DSB repair process in yeast, and while the NHEJ process exists, its roles, along with the roles of Ku, are minor in comparison to their mammalian counterparts.

Postow and colleagues have recently described the ubiquitylation of the Ku80 subunit as a mechanism for regulating the binding of the Ku heterodimer, specifically

directing Ku toward ubiquitin-mediated degradation (223). Under cellular conditions the subunits of the Ku heterodimer are always associated with each other within the nucleus; however the *in vitro* experiments presented by Postow and colleagues are focused primarily on the Ku80 subunit and not on the activity of the entire heterodimer. As opposed to the data presented within this thesis, the experiments presented by Postow were performed entirely in the presence of DNA ends. Their data did not address the instances where Ku was located on the interior of the DNA, nor did they examine significance of the ubiquitylation on the role of Ku in DSB repair.

However, the implication of ubiquitylation regulating Ku's association with DNA may still be valid, especially in cases where PARP activity may be compromised or absent, as it is in yeast. To date, no homologs for any of the PARP family members have been identified in yeast. Interestingly, the yeast homolog of Ku70 lacks both the PAR binding motif and the SAP domain, and these variations between species may reflect the differences between the regulation of Ku binding in each organism. Although the absence PARP and the Ku70 SAP domain may merely be coincidental, it does however suggest that an alternative mechanism for regulating the DNA binding of Ku exists in yeast with ubiquitylation being a possible candidate.

4.6 Future Studies

The data presented here describes the regulation of Ku binding through ribosylation by PARP1 and describes the *in vivo* implications of deregulating Ku binding, however this study is just the initial investigation into the role of Ku ribosylation and there is still a number of questions left to be answered. Future experiments are required to expand on the

findings presented here, as well as to address some questions which were raised as a result of these findings.

While this study has shown that the ribosylation of Ku will abolish its DNA binding ability and cause Ku to be released from both linear and ccDNA, the timing of the ribosylation was not investigated. The binding of Ku to DSBs is not a static event and although the initiation of NHEJ repair involves the binding of Ku to the DNA, other factors are recruited to the break site and Ku transitions to the interior of the DNA so that NHEJ may proceed. Although this study has shown that PARP1 regulates the DNA binding of Ku, it is important to further understand the impact of this interaction and modification in the context of the biologically relevant system. In order to do this, it would be interesting to reconstitute a complete *in vitro* NHEJ repair system to determine what influence the other members of the NHEJ apparatus, DNA-PK_{cs} in particular, have on the ribosylation of Ku; and to understand the timing of Ku ribosylation. The ccDNA release assay described within this study (Section 3.4) would provide an *in vitro* assay to which it would be possible to assess the impact of the NHEJ apparatus on the ribosylation and release of Ku during the NHEJ process. By supplementing the described system with purified components of the NHEJ apparatus, and then examining the ribosylation status of Ku it would be possible to determine when in the repair process Ku was being ribosylated.

The idea of dissociating subunits is supported by the results presented in the rebinding experiments performed with PARG, whereby Ku that had been ribosylated and released from DNA, was able to rebind DNA following treatment with PARG (Figure 10). In those experiments, the treatment of PARG allowed the rebinding of Ku to the DNA, however the amount of Ku that rebound the DNA represented only 30% of total amount of

Ku available in the reaction. Although it is possible that the catabolism of PAR by PARG was incomplete, it is also possible that the ribosylation of Ku causes a dissociation of the heterodimer. Since the formation of the heterodimer requires an intricate folding of the subunits, the reformation of the heterodimer may not have been complete in these reactions, thus the amount of rebound Ku is less than the total amount of Ku in the reaction. In order to test whether the ribosylation of Ku causes a complete dissociation of the heterodimer further experiments need to be conducted. These experiments could include immobilizing Ku on a resin by tagging one subunit of the heterodimer. Following ribosylation of the immobilized protein, western blot analysis of the untagged subunit would determine the extent of heterodimer dissociation.

The $Ku70^{3E}$ mutants were more sensitive to DNA damaging agents, which could reflect deficiencies in repair. Also the IF assays showed that the $Ku70^{3E}$ mutations remained at repair sites longer than their WT counterparts. While this result does not directly address whether the $Ku70^{3E}$ mutants are proficient in DNA repair, or whether the Ku is residing at internal sites on the repaired DNA, it does suggest that there are differences in the repair process. However the fundamental question as to whether Ku is proficient in DNA repair when its ribosylation is prevented remains to be addressed. Previous studies have examined the proficiency of repair by transfecting cells with linear DNA with non-compatible ends, and following transfection, examined the joined products through ligation mediated PCR (lmPCR), or through double selection in bacteria (224; 225). By transfecting the restored MEFs with various forms of linear DNA, it would be possible to evaluate their efficiency of repair. While some of the previous studies have shown distinguishable differences in repair following the transfection of linearized DNA, other studies have shown that the ligation of

the linearized DNA does not require a competent repair apparatus (224). If no notable differences are detected in the MEFs, it may be worthwhile to perform a modified ChIP assay, using the transfected DNA as a template following immunoprecipitation of the Ku. These assays would be an *in vivo* extension of the ccDNA release assays.

The V(D)J recombination process involves the introduction and repair of controlled, site-specific breaks in the genome, to which NHEJ is intimately involved. The Ku heterodimer is believed to have a critical contribution in the V(D)J recombination process, as illustrated by studies which showed that the loss of either subunit of the Ku heterodimer results in a severely reduced efficiency and proficiency of V(D)J recombination. The data presented herein suggests that the DNA binding activity of Ku greatly influences the V(D)J recombination capabilities of the cell and implicates a role for PARP1 in the resolution of the products of V(D)J recombination. While the mechanism by which PARP1 is involved in regulating the V(D)J process is unclear, there are a number of studies which continue to implicate the involvement of PARP1 in V(D)J recombination. Ongoing studies within our lab may provide some insight into the role that PARP1 play in regulating the involvement of Ku in V(D)J recombination. Through *in vitro* GST-pull-downs and *in vivo* IP assays, we have shown that RAG1 interacts with Ku and we have mapped this interaction to the SAP domain of Ku70. The significance of the interaction between RAG1 and the SAP domain of Ku70 needs to be further investigated and it is possible that PARP1 plays a role in modulating the Ku-RAG1 interaction. The recovered recombination products from the ΔSAP and Ku^{3E} mutants would suggest that the ribosylation of Ku may be effect the interaction between Ku and RAG1. As an initial investigation towards understanding these roles, it would be beneficial to determine whether the ribosylation of the SAP domain

disrupts the interaction of RAG1 and Ku70. Additionally, to further investigate the involvement of PARP1 in V(D)J recombination the *in vivo* recombination assay could be repeated in PARP1-deficient cells, or in the presence of PARP inhibitors.

Although it is necessary to develop a further understanding of the role that ribosylation plays in regulating Ku during DNA repair, it would be valuable to extend some of the future studies into examining whether ribosylation is involved in regulating other functions of Ku. This study has shown that rescuing Ku70 knock-out cells with $Ku70^{3E}$ or ΔSAP Ku results in differences in the growth rates compared to the WT Ku. As previously suggested, these differences may be due to the other roles of Ku within the cell, specifically the functioning of Ku at telomeres. Given the previous findings that suggest that by maintaining Ku's association with telomeric DNA results in shortened telomeres and telomere fusions (44), this may suggest that cells expressing ΔSAP or $Ku70^{3E}$ would have telomere aberrations. It would be interesting to study the effect of these mutations on Ku's telomere function. Although there are countless experiments which could be used to examine the integrity of the telomeres in the $Ku70^{3E}$ MEFs, these studies may include PCR based length analysis of telomere length, or fluorescent *in situ* hybridization (FISH) to identify telomere fusions.

4.7 Summary and Conclusions

The regulation of DNA repair pathways is believed to be directed by the binding of the initiation factors to the DNA ends, and it is the competition for the DNA ends and the interaction of the initiation factors at the DNA that ultimately determines which repair pathway is used for the repair of the break. Two key moderators in the regulation of the

repair processes in higher eukaryotes are PARP1 and the Ku heterodimer, and studies have shown that in some cell types, it is the competition between PARP1 and Ku for binding to the DNA ends that determines the pathway which is utilized (17; 188). The data presented here suggests that in addition to the competition for binding PARP1 can directly regulate Ku's binding to DNA by ribosylating the SAP domain of Ku70, and this regulation may ultimately influence the choice of repair pathway. The current study has shown that the ribosylation of Ku causes its release from DNA, either from the interior of DNA or at the DNA ends. The data presented in this study is the first demonstration and characterization of the regulation of Ku binding to DNA, and constitutes the first study showing the release of Ku from interior positions of DNA. The data contained within this study suggests that disrupting the ribosylation of Ku, and in turn preventing its release from DNA, impacts all of Ku's functions, including its retention at repair sites, and V(D)J recombination. These impacts need to be studied further to determine their magnitude as this initial work suggests that the interaction between Ku and PARP1 may extend beyond DSB repair.

5. References

1. Sancar, A., Lindsey-Boltz, L.A., Unsal-Kacmaz, K., and Linn, S. 2004. Molecular mechanisms of mammalian DNA repair and the DNA damage checkpoints. *Ann. Rev. Biochem.* 73:39-85.

2. Bartek, K., and Lukas, J. 2006. Balancing life-or-death decisions. *Science* 314:261-262.

3. Preston, C.R. 2006. Age-dependent usage of double-strand-break repair pathways. *Curr. Biol.* 16:2009-2015.

4. Rothkamm, K. 2003. Pathways of DNA double-strand break repair during the mammalian cell cycle. *Mol. Cell Biol.* 23:5706-5715.

5. Johnson, R.D., and Jasin, M. 2000. Sister chromatid gene conversion is a prominent double-strand break repair pathway in mammalian cells. *EMBO J.* 19:3398-3407.

6. Wang, H., Perrault, A.R., Takeda, Y., Qin, W., Wang, H., and Iliakis, G. 2003. Biochemical evidence for Ku-independent backup pathways of NHEJ. *Nucleic Acids Res.* 31:5377-5388.

7. Perrault, R., Wang, H., Wang, M., Rosidi, B., and Iliakis, G. 2004. Backup pathways of NHEJ are suppressed by DNA-PK. *J. Cell. Biochem.* 92:781-94.

8. Nussenzweig, A., and Nussenzweig, M. 2007. A backup DNA repair pathway moves to the forefront. *Cell* 131:223-225.

9. Rosidi, B., Wang, M., Wu, W., Sharma, A., Wang, H., and Iliakis, G. 2008. Histone H1 functions as a stimulatory factor in backup pathways of NHEJ. *Nucleic Acids Res.* 36:1610–1623.

10. Lieber, M.R., Ma, Y., Pannicke, U., and Schwarz, K. 2003. Mechanism and regulation of human non-homologous DNA end-joining. *Nat. Rev. Mol. Cell Biol.* 4:712-720.

11. Filippo, J.S., Sung, P., and Klein, H. 2008. Mechanism of eukaryotic homologous recombination. *Ann. Rev. Biochem.* 77:229-257.

12. van Gent, D.C., Hoeijmakers, J.H., and Kanaar, R. 2001. Chromosomal stability and the DNA double-stranded break connection. *Nat. Rev. Genet.* 2:196-206.

13. Koike, M. 2002. Dimerization, translocation and localization of Ku70 and Ku80 proteins. *J. Radiat. Res.* 43:223-236.

14. Mimori, T., Ohosone, Y., Hama, N., Suwa, A., Akizuki, M., Homma, M., Griffith, A.J., and Hardin JA. 1986. Isolation and characterization of cDNA encoding the 80-kDa subunit protein of the human autoantigen Ku (p70/p80) recognized by autoantibodies from patients with scleroderma-polymyositis overlap syndrome. *Proc. Natl. Acad. Sci. USA.* 87:1777–1781.

15. Mimori, T., and Hardin, J.A. 1986. Mechanism of interaction between Ku protein and DNA. *J. Biol. Chem.* 261:10375-10379.

16. Kim, J.S., Krasieva, T.B., Kurumizaka, H., Chen, D.J., Taylor, A.M., and Yokomori, K. 2005. Independent and sequential recruitment of NHEJ and HR factors to DNA damage sites in mammalian cells. *J. Cell Biol.* 170:341-347.

17. Hochegger, H., Dejsuphong, D., Fukushima, T., Morrison, C., Sonoda, E., Schreiber, V., Zhao, G.Y., Saberi, A., Masutani, M., Adachi, N., Koyama, H., de Murcia, G., and Takeda, S. 2006. PARP-1 protects homologous recombination from interference by Ku and Ligase IV in vertebrate cells. *EMBO J.* 25:1305-1314.

18. Strathern, J.N., Shafer, B.K., and McGill, C.B. 1995. DNA synthesis errors associated with double-strand break repair. *Genetics* 140:965-972.

19. de Jager, M., Dronkert, M.L., Modesti, M., Beerens, C.E., Kanaar, R., and van Gent, D.C. 2001. DNA-binding and strand-annealing activities of human Mre11: implications for its roles in DNA double-strand break repair pathways. *Nucleic Acids Res.* 29:1317-1325.

20. Kuznetsov, S., Pellegrini, M., Shuda, K., Fernandez-Capetillo, O., Liu, Y., Martin, B.K., Burkett, S., Southon, E., Pati, D., Tessarollo, L., West, S.C., Donovan, P.J., Nussenzweig, A., and Sharan, S.K. 2007. RAD51C deficiency in mice results in early prophase I arrest in males and sister chromatid separation at metaphase II in females. *J. Cell Biol.* 176:581-592.

21. Sharan, S.K., and Kuznetsov, S.G. 2007. Resolving RAD51C function in late stages of homologous recombination. *Cell Div.* 2:15.

22. Weterings, E., and van Gent, D.C. 2004. The mechanism of non-homologous end-joining: a synopsis of synapsis. *DNA repair.* 3:1425-1435.

23. Yano, K.I., Morotomi-Yano, K., and Akiyama, H. 2008. Cernunnos/XLF: A new player in DNA double-strand break repair. *Int. J. Biochem. Cell Biol.* E.-Pub.

24. Yoo, S., Kimzey, A. and Dynan, W.S. 1999. Photocross-linking of an oriented DNA repair complex. *J. Biol. Chem.* 274:20034-20039.

25. Yaneva, M., Yaneva, M., Kowalewski, T. and Lieber, M.R. 1997. Interaction of DNA-dependent protein kinase with DNA and with Ku: biochemical and atomic-force microscopy studies. *EMBO J.* 16:5098–5112.

26. Ma, Y., Pannicke, U., Schwarz, K. and Lieber, M.R. 2002. Hairpin opening and overhang processing by an Artemis/DNA-dependent protein kinase complex in nonhomologous end-joining and V(D)J recombination. *Cell* 108:781–794.

27. Budman, J., and Chu, G. 2005. Processing of DNA for nonhomologous end-joining by cell-free extract. *EMBO J.* 24:849-860.

28. McElhinny, S.A.N., Snowden, C.M., McCarville, J. and Ramsden, D.A. 2000. Ku recruits the XRCC4-ligaseIV complex to DNA ends. *Mol. Cell. Biol.* 20:2996-3003.

29. Gu, Y., Jin, S., Gao, Y., Weaver, D.T., and Alt, F.W. 1997. Ku70-deficient embryonic stem cells have increased ionizing radiosensitivity, defective DNA end-binding activity, and inability to support V(D)J recombination. *Proc. Natl. Acad. Sci. U.S.A.* 94:8076-8081.

30. Satoh, M., Wang, J., and Reeves, W.H. 1995. Roles of free p70 (Ku) subunit in posttranslational stabilization of newly synthesized p80 during DNA-dependent protein kinase assembly. *Eur. J. Cell. Biol.* 66:127-135.

31. Blier, P.R., Griffith, A.J., Craft, J., and Hardin, J.A. 1993. Binding of Ku protein to DNA. Measurement of affinity for ends and demonstration of binding to nicks. *J. Biol. Chem.* 268:7594-7601.

32. Doherty, A.J., and Jackson, S.P. 2001. DNA repair: How Ku makes ends meet. *Curr. Biol.* 11:R920-R924.

33. Ribes-Zamora, A., Mihalek, I., Lichtarge, O., and Bertuch, A.A. 2007. Distinct faces of the Ku heterodimer mediate DNA repair and telomeric functions. *Nat. Struct. Mol. Biol.* 14:301-307.

34. Lieber, M.R., Hesse, J.E., Lewis, S., Bosma, G.C., Rosenberg, N., Mizuuchi, K., Bosma, M.J., and Gellert, M. 1988. The defect in murine severe combined immune deficiency: joining of signal sequences but not coding segments in V(D)J recombination. *Cell* 55:7-16.

35. Smider, V., Rathwell, W.K., Lieber, M.R. and Chu, G. 1994. Restoration of X-ray resistance and V(D)J recombination in mutant cells by Ku cDNA. *Science* 266:288-291.

36. Roth, D., Menetski, J., Nakajima, P., Bosma, M. and Gellert, M. 1992. V(D)J recombination: broken DNA molecules with covalently sealed (hairpin) coding ends in scid mouse thymocytes. *Cell* 70:983-991.

37. Zhu, C., Bogue, M., Lim, D.S., Hasty, P. and Roth, D. 1996. Ku86 deficient mice exhibit severe combined immunodeficiency and defective processing of V(D)J recombination intermediates. *Cell* 86:379-389.

38. Sawchuk, D.J., Mansilla-Soto, J., Alarcon, C., Singha, N.C., Langen, H., Bianchi, M.E., Lees-Miller, S.P., Nussenzweig, M.C., and Cortes, P. 2004. Ku70/Ku80 and DNA-dependent protein kinase catalytic subunit modulate RAG-mediated cleavage: implications for the enforcement of the 12/23 rule. *J. Biol. Chem.* 279:29821-29831.

39. Shakibai, N., Kumar, V., and Eisenberg, S. 1996. The Ku-like protein from *Saccharomyces cerevisiae* is required *in vitro* for the assembly of a stable multiprotein complex at eukaryotic origin of replication. *Proc. Natl. Acad. Sci. U.S.A.* 93:11569-11574.

40. Schild-Poulter, C., Matheos, D., Novac, O., Cui, B., Giffin, W., Ruiz, M.T., Price, G.B., Zannis-Hadjopoulos, M., and Haché, R.J. 2003. Differential DNA binding of Ku antigen determines its involvement in DNA replication. *DNA Cell Biol.* 22:65-78.

41. Park, S.J., Ciccone, S.L., Freie, B., Kurimasa, A., Chen, D.J., Li, G.C., Clapp, D.W., and Lee, S.H. 2004. A positive role for the Ku complex in DNA replication following strand break damage in mammals. *J. Biol. Chem.* 279:6046-6055.

42. Idogawa, M., Masutani, M., Shitashige, M., Honda, K., Tokino, T., Shinomura, Y., Imai, K., Hirohashi, S., and Yamada, T. 2007. Ku70 and poly(ADP-ribose) polymerase-1 competitively regulate ß-catenin and T-cell factor-4–mediated gene transactivation: Possible linkage of DNA damage recognition and Wnt signaling. *Cancer Res.* 67:911-918.

43. Tanaka, Y., Imamura, J., Kanai, F., Ichimura, T., Isobe, T., Koike, M., Kudo, Y., Tateishi, K., Ikenoue, T., Ijichi, H., Yamaji, Y., Yoshida, H., Kawabe, T., and Omata, M. 2007. Runx3 interacts with DNA repair protein Ku70. *Exp. Cell Res.* 313:3251-3260.

44. Bertuch, A.A., and Lundblad, V. 2003. Which end: dissecting Ku's function at telomeres and double-strand breaks. *Genes Dev.* 17:2347-2350.

45. Fisher, T.S., and Zakian, V.A. 2005. Ku : A multifunctional protein involved in telomere maintenance. *DNA repair* 4:1215-1226.

46. Difilippantonio, M.J., Zhu, J., Chen, H.T., Meffre, E., Nussenzweig, M.C., Max, E.E., Ried, T., and Nussenzweig, A. 2000. DNA repair protein Ku80 suppresses

chromosomal aberrations and malignant transformation. *Nature* 404:510-514.

47. Ferguson, D.O., Sekiguchi, J.M., Chang, S., Frank, K.M., Gao, Y., DePinho, R.A., and Alt, F.W. 2000. The nonhomologous end-joining pathway of DNA repair is required for genomic stability and the suppression of translocations. *Proc. Natl. Acad. Sci. U.S.A.* 97:6630-6633.

48. Li, G., Nelson, C., and Hendrickson, E.A. 2002. Ku86 is essential in human somatic cells. *Proc. Natl. Acad. Sci. U.S.A.* 99:832-837.

49. Gu, Y., Seidl, K.J., Rathbun, G.A., Zhu, C., Manis, J.P., van der Stoep, N., Davidson, L., Cheng, H.L., Sekiguchi, J.M., Frank, K., Stanhope-Baker, P., Schlissel, M.S., Roth, D.B., and Alt, F.W. 1997. Growth retardation and leaky SCID phenotype of Ku70-deficient mice. *Immunity* 7:653-665.

50. Gu, Y., Sekiguchi, J.A., Gao, Y., Dikkes, P., Frank, K., Ferguson, D., Hasty, P., Chun, J., and Alt, F.W. 2000. Defective embryonic neurogenesis in Ku deficient but not DNA-dependent protein kinase catalytic subunit-deficient mice. *Proc. Natl. Acad. Sci. U.S.A.* 97:2668-2673.

51. Errami, A., Smider, V., Rathmell, W.K., He, D.M., Hendrickson, E.A., Zdzienicka, M.Z., and Chu, G. 1996. Ku86 defines the genetic defect and restores X-ray resistance and V(D)J recombination to complementation group 5 hamster cell mutants. *Mol. Cell. Biol.* 16:1519-1526.

52. Taccioli, G.E., Rathbun, G., Oltz, E., Stamato, T., Jeggo, P.A., and Alt, F.W. 1993. Impairment of V(D)J recombination in double-strand break repair mutants. *Science* 260:207-210.

53. Tacciolli, G.E., Gottlieb, T.M., Blunt, T., Priestly, A., Demengeot, J., Mizuta, R., Lehmann, A.R., Alt, F.W., Jackson, S., and Jeggo, P.A. 1994. Ku80: Product of the XRCC5 gene and its role in DNA repair and V(D)J recombination. *Science* 265:1442-1445.

54. Taccioli, G.E., Amatucci, A.G., Beamish, H.J., Gell, D., Xiang, X.H., Torres-Arzayus, M.I., Priestley, A., Jackson, S.P., Marshak-Rothstein, A., P.A., Jeggo, and Herrera, V.L. 1998. Targeted disruption of the catalytic subunit of the DNA-PK gene in mice confers severe combined immunodeficiency and radiosensitivity. *Immunity* 9:355-366.

55. Li, G.C., Ouyang, H., Li, X., Nagasawa, H., Little, J.B., Chen, D.J., Ling, C.C., Fuks, Z., and Cordon-Cardo, C. 1998. Ku70: a candidate tumor suppressor gene for murine T cell lymphoma. *Mol. Cell* 2:1-8.

56. Nussenzweig, A., Sokol, K., Burgman, P., Li, L., and Li, G.C. 1997. Hypersensitivity of Ku80-deficient cell lines and mice to DNA damage: The effects of ionizing radiation on growth, survival, and development. *Proc. Natl. Acad. Sci. U.S.A.* 94:13588-13593.

57. Aravind, L., and Koonin, E.V. 2001. Prokaryotic homologs of the eukaryotic DNA-end-binding protein Ku, novel domains in the Ku protein and prediction of a prokaryotic double-strand break repair system. *Genome Res.* 11:1365-1374.

58. Singleton, B.K., Priestley, A., Steingrimsdottir, H., Gell, D., Blunt, T., Jackson, S.P., Lehmann, A.R., and Jeggo, P.A. 1997. Molecular and biochemical characterization of xrs mutants defective in Ku80. *Mol. Cell. Biol.* 17:1264-1273.

59. Wang, J., Dong, X., Myung, K., Hendrickson, E.A., and Reeves, W.H. 1998. Identification of two domains of the p70 Ku protein mediating dimerization with p80 and DNA binding. *J. Biol. Chem.* 273:842-848.

60. Bertinato, J., Schild-Poulter, C., and Haché, R.J.G. 2000. Nuclear localization of Ku antigen is promoted independently by basic motifs in the Ku70 and Ku80 subunits. *J. Cell Sci.* 114:89-99.

61. Koike, M., Ikura, T., Miyasaka, T. and Shiomi, T. 1999. The nuclear localization signal of the human Ku70 is a variant bipartite type recognized by the two components of nuclear pore-targeting complex. *Exp. Cell. Res.* 250:401-413.

62. Koike, M., Shiomi, T., and Koike, A. 2001. Dimerization and nuclear localization of Ku proteins. *J. Biol. Chem.* 273:1167-1173.

63. Cary, R.B., Chen, F., Shen, Z., and Chen, D.J. 1998. A central region of Ku80 mediates interaction with Ku70. *Nucleic Acids Res.* 26:974-979.

64. Gell, D., and Jackson, S.P. 1999. Mapping of protein–protein interactions within the DNA-dependent protein kinase complex. *Nucleic Acids Res.* 27:3494–3502.

65. Walker, J.R., Corpina, R.A. and Goldberg, J. 2001. Structure of the Ku heterodimer bound to DNA and its implications for double-strand break repair. *Nature* 412:607-614.

66. Osipovich, O., Durum, S.K., and Muegge, K. 1997. Defining the minimal domain of Ku80 for interaction with Ku70. *J. Biol. Chem.* 272:27259-27265.

67. Aravind, L., and Koonin, E.V. 2000. SAP - a putative DNA-binding motif involved in chromosomal organization. *Trends Biochem. Sci.* 25:112-114.

68. Monferran, S., Muller, C., Mourey, L., Frit, P., and Salles, B. 2004. The membrane-associated form of the DNA repair protein Ku is involved in cell adhesion to fibronectin. *J. Mol. Biol.* 337:503-511.

69. Cui, B. 2004. Integration of NHEJ into V(D)J recombination via Ku70/80 binding to the RSS heptamer and RAG1/2. *Ph.D. Thesis*, University of Ottawa, Ottawa, ON.

70. Zhang, Z., Zhu, L., Lin, D., Chen, F., Chen, D.J., and Chen, Y. 2001. The three-dimensional structure of the C-terminal DNA-binding domain of human Ku70. *J. Biol. Chem.* 276:38231-38236.

71. Falck, J., Coates, J., and Jackson, S.P. 2005. Conserved modes of recruitment of ATM, ATR and DNA-PKcs to sites of DNA damage. *Nature* 434:605–611.

72. Pleschke, J.M., Kleczkowska, H.E., Strohm, M., and Althaus, F.R. 2000. Poly(ADP-ribose) binds to specific domains in DNA damage checkpoint proteins. *J. Biol. Chem.* 275:40974-40980.

73. Ahel, I., Ahel, D., Matsusaka, T., Clark, A.J., Pines, J., Boulton, S.J., and West, S.C. 2008. Poly(ADP-ribose)-binding zinc finger motifs in DNA repair/checkpoint proteins. *Nature* 451:81-85.

74. Mimori, T., Akizuki, M., Yamagata, H., Inada, S., Yoshida, S., and Homma, M. 1981. Characterization of a high molecular weight acidic nuclear protein recognized by autoantibodies in sera from patients with polymyositis-scleroderma overlap. *J. Clin. Invest.* 68:611-620.

75. Falzon, M., Fewell, J.W., and Kuff, E.L. 1993. EBP-80, a transcription factor closely resembling the human autoantigen Ku, recognizes single- to double-strand transitions in DNA. *J. Biol. Chem.* 268:10546-10552.

76. Arosio, D., Cui, S., Ortega, C., Chovanec, M., Di Marco, S., Baldini, G., Falaschi, A., and Vindigni, A. 2002. Studies on the mode of Ku interaction with DNA. *J. Biol. Chem.* 277:9741-9748.

77. Giffin, W., Torrance, H., Rodda, D.J., Préfontaine, G.G., Pope, L., and Haché, R.J.G. 1996. Sequence-specific DNA binding of Ku autoantigen and its effects on transcription. *Nature* 380:265-268.

78. Ruiz, M.T., Matheos, D., Price, G.B., and Zannis-Hadjopoulos, M. 1999. OBA/Ku86: DNA binding specificity and involvement in mammalian DNA replication. *Mol. Biol. Cell* 10:567-580.

79. Camara-Clayette, V., Thomas, D., Rahuel, C., Barbey, R., Cartron, J.P., and Bertrand, O. 1999. The repressor which binds the -75 GATA motif of the GPB promoter contains Ku70 as the DNA binding subunit. *Nucleic Acids Res.* 27:1656-1663.

80. DeVries, E., van Driel, W., Bersma, W.G., Amberg, A.C., and van der Viet, P.C. 1989. HeLa nuclear protein recognizing DNA termini and translocating on DNA forming a regular DNA-multimeric protein complex. *J. Mol. Biol.* 208:65-78.

81. Paillard, S., and Strauss, F. 1991. Analysis of the mechanism of interaction of simian Ku protein with DNA. *Nucleic Acids Res.* 19:5619-5624.

82. Yaneva, M., Kowalewski, T., and Lieber, M.R. 1997. Interaction of DNA-dependent protein kinase with DNA and with Ku: biochemical and atomic-force microscopy studies. *EMBO J.* 16:5098-5112.

83. Rivera-Calzada, A., Spagnolo, L., Pearl, L.H. and Llorca, O. 2007. Structural model of full-length human Ku70-Ku80 heterodimer and its recognition of DNA and DNA-PK_{cs}. *EMBO reports* 8:56-62.

84. Vivadiu, H., and Aggarwal, A.K. 2000. Structure of BamHI bound to nonspecific DNA: A model for DNA sliding. *Mol. Cell* 5:889-895.

85. Luscombe, N.M., Laskowski, R.A., and Thornton, J.M. 2001. Amino acid-base interactions: a three-dimensional analysis of protein-DNA interactions at an atomic level. *Nucleic Acids Res.* 29:2860-2874.

86. Leuther, K.K., Hammarsten, O., Kornberg, R.D., and Chu, G. 1999. Structure of DNA-dependent protein kinase: implications for its regulation by DNA. *EMBO J.* 18:1114–1123.

87. Spagnolo, L., Rivera-Calzada, A., Pearl, L. and Llorca, O. 2006. Three-dimensional structure of the human DNA-PKcs/Ku70/Ku80 complex assembled on DNA and its implications for DNA DSB repair. *Mol. Cell* 22:511-519.

88. Gellert, M. 1992. Molecular analysis of V(D)J recombination. *Annu. Rev. Genet.* 26:425-446.

89. Oettinger, M.A., Schatz, D.G., Gorka, C., and Baltimore, D. 1990. RAG-1 and RAG-2, adjacent genes that synergistically activate V(D)J recombination. *Science* 248:1517-1523.

90. Casillas, A.M., Thompson, A.D., Cheshier, S., Hernandez, S., and Aguilera, R.J. 1995. RAG-1 and RAG-2 gene expression and V(D)J recombinase activity are enhanced by protein phosphatase 1 and 2A inhibition in lymphocyte cell lines. *Mol. Immunol.* 32:167-175.

91. Swanson, P.C. 2004. The bounty of RAGs: recombination signal complexes and reaction outcomes. *Immunol. Rev.* 200:90-114.

92. Revy, P., Buck, D., le Deist, F., and de Villartay, J.P. 2005. The repair of DNA damages/modifications during the maturation of the immune system: lessons from human primary immunodeficiency disorders and animal models. *Adv. Immunol.* 87:237-295.

93. Early, P., Huang, H., Davis, M., Calame, K., and Hood, L. 1980. An immunoglobulin heavy chain variable region gene is generated from three segments of DNA: V_H, D and J_H. *Cell* 19:981-922.

94. Lewis, S.M., and Hesse, J.E. 1991. Cutting and closing without recombination in V(D)J joining. *EMBO J.* 10:3631-3639.

95. Steen, S.B., Gomelsky, L., and Roth, D.B. 1996. The 12/23 rule is enforced at the cleavage step of V(D)J recombination in vivo. *Genes Cells* 1:543-553.

96. Kwon, J., Imbalzanno, A.N., Matthews, A., and Oettinger, M.A. 1998. Accessibility of nucleosomal DNA to V(D)J recombination is modulated by RSS positioning and HMG1. *Mol. Cell* 2:829-839.

97. Kwon, J., Morshead, K.B., Guyon, J.R., Kingston, R.E., and Oettinger, M.A. 2000. Histone acetylation and hSWI/SNF remodeling act in concert to stimulate V(D)J cleavage of nucleosomal DNA. *Mol. Cell* 6:1037-1048.

98. Baumann, M., Mamais, A., McBlane, F., Xiao, H., and Boyes, J. 2003. Regulation of V(D)J recombination by nucleosome positioning at recombination signal sequences. *EMBO J.* 22:5197-5207.

99. Cherry, S.R., and Baltimore, D. 1999. Chromatin remodeling directly activates V(D)J recombination. *Proc. Natl. Acad. Sci. U.S.A.* 96:10788-10793.

100. Janeway, C.A., Travers, P., Walport, M., and Shlomchik, M. 2001. Immunobiology: the immune system in health and disease. Vol. 5. Garland Publishing, New York.

101. Lee, J., and Desiderio, S. 1999. Cyclin A/CDK2 regulates V(D)J recombination by coordinating RAG-2 accumulation and DNA repair. *Immunity* 11:771-781.

102. Lin, W.C., and Desiderio, S. 1993. Regulation of V(D)J recombination activator protein RAG-2 by phosphorylation. *Science* 260:953-959.

103. Lin, W.C., and Desiderio, S. 1994. Cell cycle regulation of V(D)J recombination-activating protein RAG-2. *Proc. Natl. Acad. Sci. U.S.A.* 91:2733-2737.

104. Mizuta, R., Mizuta, M., Araki, S., and Kitamura, D. 2002. RAG2 is down-regulated by cytoplasmic sequestration and ubiquitin-dependent degradation. *J. Biol. Chem.* 277:41423-41427.

105. Ross, A.E., Vuica, M., and Desiderio, S. 2003. Overlapping signals for protein degradation and nuclear localization define a role for intrinsic RAG-2 nuclear uptake in dividing cells. *Mol. Cell. Biol.* 23:5308-5319.

106. Schlissel, M.S., Constantinescu, A., Morrow, T., Baxter, M., and Peng, A. 1993. Double-strand signal sequence breaks in V(D)J recombination are blunt, 5' phosphorylated, RAG-dependent and cell cycle regulated. *Genes Dev.* 7:2520-2532.

107. Fugmann, S.D., Lee, A.I., Shockett, P.E., Villey, I.J., and Schatz, D.G. 2000. The RAG proteins and V(D)J recombination: complexes, ends, and transposition. *Annu. Rev. Immunol.* 18:495-527.

108. Bassing, C.H., Swat, W., and Alt, F.W. 2002. The mechanism and regulation of chromosomal V(D)J recombination. *Cell* 109:S45-S55.

109. Bogue, M.A., Wang, C., Zhu, C., and Roth, D.B. 1997. V(D)J recombination in Ku86-deficient mice: distinct effects on coding, signal, and hybrid joint formation. *Immunity* 7:37-47.

110. Pergola, F., Zdzienicka, M.Z., and Lieber, M.R. 1993. V(D)J recombination in mammalian cell mutants defective in DNA double-strand break repair. *Mol. Cell. Biol.* 13:3464-3471.

111. Kurimasa, A., Ouyang, H., Dong, L.J., Wang, S., Li, X., Cordon-Cardo, C., Chen, D.J., and Li, G.C. 1999. Catalytic subunit of DNA-dependent protein kinase: impact on lymphocyte development and tumorigenesis. *Proc. Natl. Acad. Sci. U.S.A.* 96:1403-1408.

112. Lieber, M.R., Hesse, J.E., Lewis, S., Bosma, G.C., Rosenberg, N., Mizuuchi, K., Bosma, M.J., and Gellert, M. 1988. The defect in murine severe combined deficiency: joining of signal sequences but not codig segments in V(D)J recombination. *Cell*

55:7-16.

113. Gao, Y., Chaudhuri, J., Zhu, C., Davidson, L., Weaver, D.T., and Alt, F.W. 1998. A targeted DNA-PKcs-null mutation reveals DNA-PK-independent functions for Ku in V(D)J recombination. *Immunity* 9:367-376.

114. Kulesza, P., and Lieber, M.R. 1998. DNA-PK is essential only for coding joint formation in V(D)J recombination. *Nucleic Acids Res.* 26:3944-3948.

115. Bailey, S.M., Meyne, J., Chen, D.J., Kurimasa, A., Li, G.C., Lehnert, B.E., and Goodwin, E.H. 1999. DNA double-strand break repair proteins are required to cap the ends of mammalian chromosomes. *Proc. Natl. Acad. Sci. U.S.A.* 96:14899-14904.

116. Boulton, S.J. 1996. Identification of a *Saccharomyces cerevisiae* Ku80 homologue: roles in DNA double strand break rejoining and in telomeric maintenance. *Nucleic Acids Res.* 24:4639-4648.

117. Melnikova, L., Biessmann, H., and Georgiev, P. 2005. The Ku protein complex is involved in length regulation of Drosophila telomeres. *Genetics* 170:221–235.

118. Stellwagen, A.E., Haimberger, Z.W., Veatch, J.R., and Gottschling, D.E.2003. Ku interacts with telomerase RNA to promote telomere addition at native and broken chromosome ends. *Genes Dev.* 17:2384-2395.

119. Boulton, S.J., and Jackson, S.P. 1998. Components of the Ku-dependent non-homologous end-joining pathway are involved in telomeric length maintenance and telomeric silencing. *EMBO J.* 17:1819-1828.

120. Baumann, P., and Cech, T.R. 2000. Protection of telomeres by the Ku protein in fission yeast. *Mol. Biol. Cell.* 11:3265–3275.

121. Mishra, K., and Shore, D. 1999. Yeast Ku protein plays a direct role in telomeric silencing and counteracts inhibition by rif proteins. *Curr. Biol.* 9:1123-1126.

122. Laroche, T., Martin, S.G., Gotta, M., Gorham, H.C., Pryde, F.E., Louis, E.J., and Gasser, S.M. 1998. Mutation of yeast Ku genes disrupts the subnuclear organization of telomeres. *Curr. Biol.* 8:653-656.

123. Myung, K., Ghosh, G., Fattah, F.J., Li, G., Kim, H., Dutia, A., Pak, E., Smith, S., and Hendrickson, E.A. 2004. Regulation of telomere length and suppression of genomic instability in human somatic cells by Ku86. *Mol. Cell. Biol.* 24:5050-5059.

124. Bianchi, A., and de Lange, T. 1999. Ku binds to telomeric DNA *in vitro*. *J. Biol. Chem.* 274:21223-21227.

125. Hsu, H.-L., Gilley, D., Blackburn, E.H., and Chen, D.J. 1999. Ku is associated with the telomere in mammals. *Proc. Natl. Acad. Sci. U.S.A.* 96:12454-12458.

126. van Steensel, B., and de Lange, T. 1997. Control of telomere length by the human telomeric protein TRF1. *Nature* 385:740-743.

127. Bianchi, A., Smith, S., Chong, L., Elias, P., and de Lange, T. 1997. TRF1 is a dimer and bends telomeric DNA. *EMBO J.* 16:1785-1794.

128. Hsu, H.-L., Gilley, D., Galande, S.A., Hande, M.P., Allen, B., Kim, S-H, Li, G.C., Campisi, J., Kohwi-Shigematsu, T., and Chen, D.J. 2000. Ku acts in a unique way at the mammalian telomere to prevent end joining. *Genes Dev.* 14:2807-2812.

129. Fisher, T.S., Taggart, A.K., and Zakian, V.A. 2004. Cell cycle-dependent regulation of yeast telomerase by Ku. *Nat. Struct. Mol. Biol.* 11:1198-1205.

130. d'Adda di Fagagna, F., Hande, M.P., Tong, W.M., Roth, D., Lansdorp, P., Wang, Z., and Jackson, S. 2001. Effects of DNA nonhomologous end-joining factors on telomere length and chromosomal stability in mammalian cells. *Curr. Biol.* 11:1192-1196.

131. Canudas, S., Houghtaling, B.R., Kim, J.Y., Dynek, J.N., Chang, W.G., and Smith, S. 2007. Protein requirements for sister telomere association in human cells. *EMBO J.* 26:4867-4878.

132. Ame, J.C., Spenlehauer, C., and de Murcia, G. 2004. The PARP Superfamily. *BioEssays* 26:882-893.

133. Hilz, H., and Stone, P. 1976. Poly(ADP-ribose) and ADP-ribosylation of proteins. *Rev. Physiol. Biochem. Pharmacol.* 76:1-55.

134. Ogata, N., Ueda, K., Kagamiyama, H., and Hayaishi, O. 1980. ADP-ribosylation of histone H1. Identification of glutamic acid residues 2, 14, and the COOH-terminal lysine residue as modification sites. *J. Biol. Chem.* 255:7616–7620.

135. Ogata, N., Ueda, K., and Hayaishi, O. 1980. ADP-ribosylation of histone H2B. Identification of glutamic acid residue 2 as the modification site. *J. Biol. Chem.* 255:7610–7615.

136. Kim, M.Y., Zhang, T., and Kraus, W.L. 2005. Poly(ADP-ribosyl)ation by PARP-1: 'PAR-laying' NAD+ into a nuclear signal. *Genes Dev.* 19:1951-1967.

137. d'Adda di Fagagna, F., Hande, M.P., Tong, W.-M., Lansdorp, P.M., Wang, Z.-Q., and Jackson, S.P. 1999. Functions of poly(ADP-ribose) polymerase in controlling telomere length and chromosomal stability. *Nat. Genet.* 23:76-80.

138. Schreiber, V., Dantzer, F., Ame, J.-C., and de Murcia, G. 2006. Poly(ADP-ribose): novel functions for an old molecule. *Nat. Rev.* 7:517-528.

139. Bonicalzi, M.-E., Haince, J.-F., Droit, A., and Poirier, G.G. 2005. Regulation of poly(ADP-ribose) metabolism by poly(ADP-ribose) glycohydrolase: where and when? *Cell. Mol. Life Sci.* 62:739–750.

140. Davidovic, L., Vodenicharov, M., Affar, E.B., and Poirier, G.G. 2001. Importance of poly(ADP-ribose) glycohydrolase in the control of poly(ADP-ribose) metabolism. *Exp. Cell Res.* 268:7-13.

141. Diefenbach, J., and Burkle, A. 2005. Introduction to poly(ADP-ribose) metabolism. *Cell. Mol. Life Sci.* 62:721-730.

142. Oka, J., Ueda, K., Hayaishi, O., Komura, H., and Nakanishi, K. 1984. ADP-ribosyl protein lyase. Purification, properties and identification of the product. *J. Biol. Chem.* 259:986-995.

143. Malanga, M., and Althaus, F.R. 2005. The role of poly(ADP-ribose) in the DNA damage signaling network. *Biochem. Cell Biol.* 83:354-364.

144. Burkle, A. 2001. Physiology and pathophysiology of poly(ADP-ribosyl)ation. *BioEssays* 23:95-806.

145. Prasad, R., Lavrik, O.I., Kim, S.J., Kedar, P., Yang, X.P., van de Berg, B.J., and Wilson, S.H. 2001. DNA polymerase beta-mediated long patch base excision repair. Poly(ADP-ribose) polymerase-1 stimulates strand displacement DNA synthesis. *J. Biol. Chem.* 276:32411-32414.

146. Brown, M.L., Franco, D., Burkle, A., and Chang, Y. 2002. Role of poly(ADP-ribosyl)ation in DNA-PKcs-independent V(D)J recombination. *Proc. Natl. Acad. Sci. U.S.A.* 99:4532-4537.

147. Masson, M., Niedergang, C., Schrieber, V., Muller, S., Menissier-de Murcia, J., and de Murcia, G. 1998. XRCC1 is specifically associated with poly(ADP-ribose) polymerase and negatively regulates its activity following DNA damage. *Mol. Cell. Biol.* 18:3563-3571.

148. Ferro, A.M., Higgins, N.P., and Olivera, B.M. 1983. Poly(ADP-ribosylation) of a DNA topoisomerase. *J. Biol. Chem.* 258:6000-6003.

149. Ferro, A.M., and Olivera, B.M. 1984. Poly(ADP-ribosylation) of DNA topoisomerase I from calf thymus. *J. Biol. Chem.* 259:547-554.

150. Leppard, J.B., Dong, Z., Mackey, Z.B, and Tomkinson, A.E. 2003. Physical and functional interaction between DNA ligase IIIα and poly(ADP-ribose) polymerase 1 in DNA single-strand break repair. *Mol. Cell. Biol.* 23:5919-5927.

151. Simbulan-Rosenthal, C.M., Rosenthal, D.S., Luo, R., Samara, R., Espinoza, L.A., Hassa, P.O., Hottiger, M.O., and Smulson, M.E. 2003. PARP-1 binds E2F-1 independently of its DNA binding and catalytic domains, and acts as a novel coactivator of E2F-1-mediated transcription during re-entry of quiescent cells into S phase. *Oncogene* 22:8460-8471.

152. Hayashi, K., Tanaka, M., Shimada, T., Miwa, M., and Sugimura, T. 1983. Size and shape of poly(ADP-ribose): examination by gel filtration, gel electrophoresis and electron microscopy. *Biochem. Biophys. Res. Commun.* 112:517-528.

153. Alvarez-Gonzalez, R., and Jacobson, M.K. 1987. Characterization of polymers of adenosine diphosphate ribose generated *in vitro* and *in vivo*. *Biochem.* 26:3218-3224.

154. Desnoyers, S., Shah, G.M., Brochu, G., Hoflack, J.C., Verreault, A., and Poirier, G.G. 1995. Biochemical properties and function of poly(ADP-ribose) glycohydrolase. *Biochimie* 77:433-438.

155. Rouleau, M., Aubin, R.A., and Poirier, G.G. 2004. Poly(ADP-ribosyl)ated chromatin domains: access granted. *J. Cell Sci.* 117:815-825.

156. D'Amours, D., Desnoyers, S., D'Silva, I., and Poirier, G.G. 1999. Poly(ADP-ribosyl)ation reactions in the regulation of nuclear functions. *Biochem. J.* 342:249-268.

157. de Murcia, J.M., Niedergang, C., Trucco, C., Ricoul, M., Dutrillaux, B., Mark, M., Oliver, F.J., Masson, M., Dierich, A., LeMeur, M., Walztinger, C., Chambon, P., and de Murcia, G. 1997. Requirement of poly(ADP-ribose) polymerase in recovery from DNA damage in mice and in cells. *Proc. Natl. Acad. Sci. U.S.A.* 94:7303-7307.

158. Hassa, P.O., Haenni, S.S., Elser, M., and Hottiger, M.O. 2006. Nuclear ADP-ribosylation reactions in mammalian cells: Where are we today and where are we going? *Microbiol. Mol. Biol. Rev.* 70:789-829.

159. Althaus, F.R., Kleczkowska, H.E., Malanga, M., Müntener, C.R., Pleschke, J.M., Ebner, M., and Auer, B. 1999. Poly(ADP-ribosyl)ation: a DNA break signal mechanism. *Mol. Cell. Biochem.* 193:5-11.

160. Aguilar-Quesada, R., Muñoz-Gámez, J.A., Martín-Oliva, D., Peralta, A., Valenzuela, M.T., Matínez-Romero, R., Quiles-Pérez, R., Menissier-de Murcia, J., de Murcia, G., Ruiz de Almodóvar, M., and Oliver, F.J. 2007. Interaction between ATM and PARP-1 in response to DNA damage and sensitization of ATM deficient cells through PARP inhibition. *BMC Mol. Biol.* 8:29.

161. Fernet, M., Ponette, V., Deniaud-Alexandre, E., Ménissier-de Murcia, J., de Murcia, G., Giocanti, N., Megnin-Chanet, F., and Favaudon, V. 2000. Poly(ADP-ribose) polymerase, a major determinant of early cell response to ionizing radiation. *Int. J. Radiat. Biol.* 76:1621-1629.

162. Tong, W.M., Yang, Y.G., Cao, W.H., Galendo, D., Frappart, L., Shen, Y., and Wang, Z.Q. 2007. Poly(ADP-ribose) polymerase-1 plays a role in suppressing mammary tumourigenesis in mice. *Oncogene* 26:3857-3867.

163. Domínguez-Bendala, J., Masutani, M., and McWhir, J. 2006. Down-regulation of PARP-1, but not of Ku80 or DNA-PKcs', results in higher gene targeting efficiency. *Cell Biol. Int.* 30:389-393.

164. Saberi, A., Hochegger, H., Szuts, D., Lan, L., Yasui, A., Sale, J.E., Taniguchi, Y., Murakawa, Y., Zeng, W., Yokomori, K., Helleday, T., Teraoka, H., Arakawa, H., Buerstedde, J.-M., and Takeda, S. 2007. RAD18 and Poly(ADP-ribose) polymerase independently suppress the access of nonhomologous end joining to double-strand breaks and facilitate homologous recombination-mediated repair. *Mol. Cell. Biol.* 27:2562-2571.

165. de Murcia, J.M., Niedergang, C., Trucco, C., Ricoul, M., Dutrillaux, B., Mark, M., Oliver, F.J., Masson, M., Dierich, A., LeMeur, M., Walztinger, C., Chambon, P., and de Murcia, G. 1997. Requirement of poly (ADP-ribose) polymerase in recovery from DNA damage in mice and in cells. *Proc. Natl. Acad. Sci. U.S.A.* 94:7303-7307.

166. Schultz, N., Lopez, E., Saleh-Gohari, N., and Helleday, T. 2003. Poly(ADP-ribose) polymerase (PARP-1) has a controlling role in homologous recombination. *Nucleic Acids Res.* 31:4959-4964.

167. McCabe, N., Turner, N.C., Lord, C.J., Kluzek, K., Bialkowska, A., Swift, S., Giavara, S., O'Connor, M.J., Tutt, A.N., Zdzinicka, M.Z., Smith, G.C.M., and Ashworth, A. 2006. Deficiency in the repair of DNA damage by homologous recombination and sensitivity to poly(ADP-ribose) polymerase inhibition. Cancer *Res.* 66:8109-8115.

168. Lindahl, T., Satoh, M.S., Poirier, G.G., and Klungland, A. 1995. Post-translational modification of poly(ADP-ribose) polymerase induced by DNA strand breaks. *Trends Biochem. Sci.* 20:405-411.

169. Henrie, M.S., Kurimasa, A., Burma, S., Menissier-de Murcia, J., de Murcia, G., Li, G.C., and Chen, D.J. 2003. Lethality in PARP-1/Ku80 double mutant mice reveals physiological synergy during embyrogenesis. *DNA repair* 2:151-158.

170. Tong, W.-M., Cortes, U., Hande, M.P., Ohgaki, H., Cavalli, L.R., Lansdorp, P.M., Haddad, B.R., and Wang, Z.-Q. 2002. Synergistic role of Ku80 and Poly(ADP-ribose) polymerase in suppressing chromosomal aberrations and liver cancer formation. *Cancer Res.* 62:6990-6996.

171. Galande, S., and Kohwi-Shigematsu, T. 1999. Poly(ADP-ribose) polymerase and Ku autoantigen form a complex and synergistically bind to matrix attachment sequences. *J. Biol. Chem.* 274:20521-20528.

172. Galande, S., and Kohwi-Shigematsu, T. 2000. Caught in the act: binding of Ku and PARP to MARs reveals novel aspects of their functional interaction. *Crit. Rev. Eukaryot. Gene Expr.* 10:63-72.

173. Ruscetti, T., Lehnert, B.E., Halbrook, J., Le Trong, H., Hoekstra, M.F., Chen, D.J., and Peterson, S.R. 1998. Stimulation of the DNA-dependent protein kinase by poly(ADP-ribose) polymerase. *J. Biol. Chem.* 273:14461-14467.

174. Li, B., Navarro, S., Kasahara, B., and Comai, L. 2004. Identification and biochemical characterization of a Werner syndrome protein complex with Ku70/80 and PARP-1. *J. Biol. Chem.* 279:13659-13667.

175. Ariumi, Y., Masutani, M., Copeland, T.D., Mimori, T., Takashi, S., Shimotohno, K., Ueda, K., Hatanaka, M., and Noda, M. 1999. Suppression of the poly(ADP-ribose) polymerase activity by DNA-dependent protein kinase *in vitro*. *Oncogene* 18:4616-4625.

176. Schild-Poulter, C., Hache, R.J.G., and Soubeyrand, S. 2004. Ku antigen: A versatile DNA binding protein with multiple cellular functions. *Dynamical Genetics*. 1-28.

177. Rodda, D.J., Giffin, W., and Haché, R.J.G. 1995. Multi-strand binding of nuclear factors to a repressor of mouse mammary tumor virus transcription can be distinguished kinetically. *Biochem. Biophys. Res. Comm.* 209:379-384.

178. Mari, P.-O., Florea, B.I., Persengiev, S.P., Verkaik, N.S., Bruggenwirth, H.T., Modesti, M., Giglia-Mari, G., Bezstarosti, K., Demmers, J.A.A., Luider, T.M., Houtsmuller, A.B., and van Gent, D.C. 2006. Dynamic assembly of end-joining complexes requires interaction between Ku70/80 and XRCC4. *Proc. Natl. Acad. Sci. U.S.A.* 103:18597-18602.

179. Hesse, J.E., Lieber, M.R., Mizuuchi, K., and Gellert, M. 1987. Extrachromosomal DNA substrates in pre-B cells undergo inversion or deletion at immunoglobulin V-(D)-J joining signals. *Cell* 49:775-783.

180. Lieber, M.R., Hesse, J.E., Mizuuchi, K., and Gellert, M. 1987. Developmental stage specificity of the lymphoid V(D)J recombination activity. *Genes Dev.* 1:751-761.

181. Bertinato, J., Schild-Poulter, C., and Haché, R.J.G. 2001. Nuclear localization of Ku antigen is promoted independently by basic motifs in the Ku70 and Ku80 subunits. *J. Cell Sci.* 114:89-99.

182. Maniatis, T., Fritsch, E.F., and Sambrook, J. 1982. Molecular cloning: A laboratory manual. Cold Spring Harbor Laboratory, Cold Spring Harbor.

183. Hanakahi, L.A. 2007. 2-step purification of the Ku DNA repair protein expressed in *Escherichia coli*. *Protein Expr. Purif.* 52:139–145.

184. Sawada, M., Sun, W., Hayes, P., Leskov, K., Boothman, D.A., and Matsuyama, S. 2003. Ku70 suppresses the apoptotic translocation of Bax to mitochondria. *Nat. Cell Biol.* 5:320-329.

185. Kanai, M., Hanashiro, K., Kim, S.H., Hanai, S., Boulares, A.H., Miwa, M., and Fukasawa, K. 2007. Inhibition of Crm1-p53 interaction and nuclear export of p53 by poly(ADP-ribosyl)ation. *Nat. Cell Biol.* 9:1175-1183.

186. Mosmann, T. 1983. Rapid colorimetric assay for cellular growth and survival: application to proliferation and cytotoxicity assays. *J. Immunol. Methods* 65:55-63.

187. Cortes, P., Weis-Garcia, F., Misulovin, Z., Nussenzweig, A., Lai, J.-S., Li, G., Nussenzweig, M.C., and Baltimore, D. 1996. *In vitro* V(D)J recombination signal joint formation. *Proc. Natl. Acad. Sci. U.S.A.* 93:14008-14013.

188. Wang, M., Wu, W., Wu, W., Rosidi, B., Zhang, L., Wang, H., and Iliakis, G. 2006. PARP-1 and Ku compete for repair of DNA double strand breaks by distinct NHEJ pathways. *Nucleic Acids Res.* 34:6170-6182.

189. Chiba-Falek, O., Kowalak, J.A., Smulson, M.E., and Nussbaum, R.L. 2005. Regulation of alpha-synuclein expression by poly (ADP ribose) polymerase-1 (PARP-1) binding to the NACP-Rep1 polymorphic site upstream of the SNCA gene. *Am. J. Hum. Genet.* 76:478-492.

190. Gottlieb, T.M., and Jackson, S.P. 1993. The DNA-dependent protein kinase: requirement for DNA ends and association with Ku antigen. *Cell* 72:131-142.

191. Calsou, P., Frit, P., Humbert, O., Muller, C., Chen, D.J., and Salles, B. 1999. *J. Biol. Chem.* 274:7848-7856.

192. Chem, J., and Stubbe, J. 2005. Bleomycins: towards better therapeutics. *Nat. Rev. Cancer* 5:102-112.

193. Adachi, N., So, S., and Koyama, H. 2004. Loss of nonhomologous end joining confers camptothecin resistance in DT40 cells. Implications for the repair of topoisomerase I-mediated DNA damage. *J. Biol. Chem.* 279:37343-37348.

194. Ninomiya, Y., Suzuki, K., Ishii, C., and Inoue, H. 2004. Highly efficient gene replacements in *Neurospora* strains deficient for nonhomologous end-joining. *Proc. Natl. Acad. Sci. U.S.A.* 101:12248–12253.

195. Povirk, L.F., Wübter, W., Köhnlein, W., and Hutchinson, F. 1977. DNA double-strand breaks and alkali-labile bonds produced by bleomycin. *Nucleic Acids Res.* 4:3573-3580.

196. Burger, R.M. 1998. Cleavage of nucleic acids by bleomycin. *Chem. Rev.* 98:1153-1170.

197. Radtke, K., Lornitzo, F.A., Byrnes, R.W., Antholine, W.E., and Petering, D.H. 1994. Iron requirement for cellular DNA damage and growth inhibition by hydrogen peroxide and bleomycin. *Biochem. J.* 302:655-664.

198. Claussen, C.A., and Long, E.C. 1999. Nucleic acid recognition by metal complexes of bleomycin. *Chem. Rev.* 99:2797-2816.

199. Dizadaroglu, M., Nackerdien, Z., Chao, B.C., Gajewski, E., and Rao, G. 1991. Chemical nature of *in vivo* DNA base damage in hyrdogen peroxide-treated mammalian cells. *Arch. Biochem. Biophys.* 285:388-390.

200. Cadet, J., Delatour, T., Douki, T., Gasparutto, D., Pouget, J.P., Ravanat, J.L., and Sauvaigo, S. 1999. Hydroxyl radicals and DNA base damage. *Mutat. Res.* 424: 9-21.

201. Pommier, Y. 1996. Eukaryotic DNA topoisomerase I: genome gate keeper and its intruders, camptothecins. *Semin. Oncol.* 23:1-10.

202. Adachi, N., So, S., and Koyama, H. 2004. Loss of nonhomologous end joining confers camptothecin resistance in DT40 cells. Implications for the repair of topoisomerase I-mediated DNA damage. *J. Biol. Chem.* 279:37343-37348.

203. Rogakou, E.P., Pilch, D.R., Orr, A.H., Ivanova, V.S., and Bonner, W.M. 1998. DNA double-stranded breaks induce histone H2AX phosphorylation on serine 139.

J. Biol. Chem. 273:5858-5868.

204. Koike, M., and Koike, A. 2008. Accumulation of Ku80 proteins at DNA double-strand breaks in living cells. *Exp. Cell Res.* 314:1061-1070.

205. Uematsu, N., Weterings, E., Yano, K., Morotomi-Yano, K., Jakob, B., Taucher-Scholz, G., Mari, P.-O., van Gent, D.C., Chen, B.P.C., and Chen, D.J. 2007. Autophosphorylation of DNA-PKcs regulates its dynamics at DNA double-strand breaks. *J. Cell Biol.* 177:219-229.

206. Mahajan, K.N., Gangi-Peterson, L., Sorscher, D.H., Wang, J., Gathy, K.N., Mahajan, N.P., Reeves, W.H., and Mitchell, B.S. 1999. Association of terminal deoxynucleotidyl transferase with Ku. *Proc. Natl. Acad. Sci. U.S.A.* 96:13926-13931.

207. Kim, J.-S., Krasieva, T.B., LaMorte, V.J., Taylor, A.M.R., and Yokomori, K. 2002. Specific recruitment of human cohesin to laser-induced DNA damage. *J. Biol. Chem.* 277:45149-45153.

208. Kysela, B., Doherty, A.J., Chovanec, M., Stiff, T., Ameer-Beg, S.M., Vojnovic, B., Girard, P.M., and Jeggo, P.A. 2003. Ku stimulation of DNA ligase IV-dependent ligation requires inward movement along the DNA molecule. *J. Biol. Chem.* 278:22466-22474.

209. Weinstock, D.M., and Jasin, M. 2006. Alternative pathways for the repair of RAG-induced DNA breaks. *Mol. Cell Biol.* 26:131-139.

210. Celli, G.B., Denchi, E.L., and de Lange, T. 2006. Ku70 stimulates fusion of dysfunctional telomeres yet protects chromosome ends from homologous recombination. *Nat. Cell Biol.* 8:885-890.

211. Tuteja, N., Tuteja, R., Ochem, A., Taneja, P., Huang, N.W., Simoncsits, A., Susic, S., Rahman, K., Marusic, L., Chen, J., Zhang, J., Wang, S., Pongor, S., and Falaschi, A. 1994. Human DNA helicase II: a novel DNA unwinding enzyme identified as the Ku autoantigen. *EMBO J.* 13:4991-5001.

212. West, R.B., Yaneva, M., and Lieber, M.R. 1998. Productive and nonproductive complexes of Ku and DNA-dependent protein kinase at DNA termini. *Mol. Cell Biol.* 18:5908-5920.

213. Jakob, B., Splinter, J., Schweinfurth, Y., Becker, G., Chen, D., and Taucher-Scholz, G. 2007. Fast recruitment of DNA-PKcs at DNA double-strand breaks. *Rad. Biophys.* 4:336.

214. Uliel, L., Weisman-Shomer, P., Oren-Jazan, H., Newcomb, T., Loeb, L.A., and Fry, M. 2000. Human Ku antigen tightly binds and stabilizes a tetrahelical form of the fragile X

syndrome d(CGG)n exoabded sequence. *J. Biol. Chem.* 275:33134-33141.

215. Bryant, H.E., and Helleday, T. 2006. Inhibition of poly (ADP-ribose) polymerase activates ATM which is required for subsequent homologous recombination repair. *Nucleic Acids Res.* 34:1685-1691.

216. Masutani, M., Nozaki, T., Nishiyama, E., Shimokawa, T., Tachi, Y., Suzuki, H., Nakagama, H., Wakabayashi, K., and Sugimura, T. 1999. Function of poly(ADP-ribose) polymerase in response to DNA damage: gene-disruption study in mice. *Mol. Cell. Biochem.* 193:149-152.

217. Fattah, K.R., Ruis, B.L., and Hendrickson, E.A. 2008. Mutations to Ku reveal differences in human somatic cell lines. *DNA Repair* 7:762-774.

218. Domínguez-Bendala, J., Masutani, M., and McWhir, J. 2006. Down-regulation of PARP-1, but not of Ku80 or DNA-PKcs', results in higher gene targeting efficiency. *Cell Biol. Int.* 30:389-393.

219. d'Arpa, P., and Liu, L.F. 1989. Topoisomerase-targeting antitumour drugs. *Biochem. Biophys. Acta.* 989:163–177.

220. Morrison, C., Smith, G.C., Stingl, L., Jackson, S.P., Wagner, E.F., and Wang, Z.Q. 1997. Genetic interaction between PARP and DNA-PK in V(D)J recombination and tumorigenesis. *Nat. Genet.* 17:479-482.

221. Moshous, D., Callebaut, I., de Chasseval, R., Corneo, B., Cavazzana-Calvo, M., Le Deist, F., Tezcan, I., Sanal, O., Bertrand, Y., Philippe, N., Fischer, A., and de Villartay, J.P. 2001. Artemis, a novel DNA double-strand break repair/V(D)J recombination protein, is mutated in human severe combined immune deficiency. *Cell* 105:177-186.

222. Mansilla-Soto, J., and Cortes, P. 2003. VDJ recombination: Artemis and its *in vivo* role in hairpin opening. *J. Exp. Med.* 197:543-547.

223. Postow, L., Ghenoiu, C., Woo, E.M., Krutchinsky, A.N., Chait, B.T., and Funabiki, H. 2008. Ku80 removal from DNA through double strand break–induced ubiquitylation. *J. Cell Biol.* 182:467-479.

224. Dar, M.E., Winters, T.A., and Jorgensen, T.J. 1997. Identification of defective illegitimate recombinational repair of oxidatively-induced DNA double-strand breaks in ataxia-telangiectasia cells. *Mutat. Res.* 384:169-179.

225. van Heemst, D., Brugmansa, L., Verkaika, N.S., and van Gent, D.C. 2004. End-joining of blunt DNA double-strand breaks in mammalian fibroblasts is precise and requires DNA-PK and XRCC4. *DNA repair* 3:43-50.

Appendices

Appendix I. Primers and oligonucleotides used in this study and primer-specific PCR conditions.

Oligonucleotides for EMSAs

Primer Name	Sequence
NS-23-For.	5′-CCCTCGAGGTCGACGGTATCGAT-3′
NS-23-Rev.	5′- ATCGATACCGTCGACCTCGAGGG-3′

Ku70 PCR mutagenesis primers:

Primer Name	Sequence	Tm (°C)
ΔPAR For	5′-CGGCAACAGGTCTTCTAGCTTGC-3′	59.0
ΔPAR Rev	5′-GCCGATATAGTGATCTCTGTGGGC-3′	59.0
ΔHelix 5 For	5′-CGGGTCATTGCCATGGGGGTTG-3′	60.0
ΔHelix 5 Rev	5′-GCCGGCATCTTCCTTGACTTGATG-3′	61.3
ΔSAP For	5′- CGGCGTACCCTTGCTGATGTGG-3′	60.2
SAP Mut1 F	5′-CCATGCTGAAAGCGGCCTGCCGGGCTTACG-3′	70.0
SAP Mut1 R	5′-CGTAAGCCCGGCAGGCCGCTTTCAGCATGG-3′	70.0
SAP Mut2 F	5′-GAAGAAGCAGGCGCTGCTGGCAGCCCTCACC-3′	73.3
SAP Mut2 R	5′-GGTGAGGGCTGCCAGCAGCGCCTGCTTCTTCAGC-3′	73.3

Covalently closed circle PCR primers:

Primer Name	Sequence	Tm (°C)
Control For.	5′-AAGTTCATCTGCACCACCGGCAAGC-3′	63.9
Control Rev.	5′-CAGCACGGGGCCGTCGCCGATGGG-3′	68.6
Ligation For.	5′-GCTGTGGAATGTGTGTCAGTTAGGG-3′	63.5
Ligation Rev.	5′-AGATCATCCTGATCGACAAGACCGG-3′	64.5

V(D)J recombination analysis PCR primers:

Primer Name	Sequence	Tm (°C)
R3-200	5′-TGTTCCAGTCTGTAGCACTG-3′	58.2
R14-200	5′-TCCAGCTGAACGGTCTGGT-3′	60.3
R3-290	5′-CAGCTGGCACGACAGGTTTCC-3′	67.5
R14-290	5′-TCCGGATGAGCATTCATCAGGC-3′	68.8
R7	5′-TTACGGGACTCTCGGCAGAAGCTA-3′	67.2
R8	5′-ATCCCGCCATGGTATCAACG-3′	60.5

Appendix II. Amino acid sequence of human Ku70 subunit

001 MSGWESYYKT EGDEEAEEEQ EENLEASGDY KYSGRDSLIF LVDASKAMFE SQSEDELTPF
061 DMSIQCIQSV YISKIISSDR DLLAVVFYGT EKDKNSVNFK NIYVLQELDN PGAKRILELD
121 QFKGQQGQKR FQDMMGHGSD YSLSEVLWVC ANLFSDVQFK MSHKRIMLFT NEDNPHGND**S**
181 **AKASRARTKA GDLRDT**GIFL DLMHLKKPGG FDISLFYRDI ISIAEDEDLR VHFEESSKLE
241 DLL**RKVRAKE TRKRALSRLK LKLNK**DIVIS VGIYNLVQKA LKPPPIKLYR ETNEPVKTKT
301 RTFNTSTGGL LLPSDTKRSQ IYGSRQIILE KEETEELKRF DDPGLMLMGF KPLVLLKKHH
361 YLRPSLFVYP EESLVIGSST LFSALLIKCL EKEVAALCRY TPRRNIPPYF VALVPQEEEL
421 DDQKIQVTPP GFQLVFLPFA DDKRKMPFTE KIMATPEQVG KMKAIVEKLR FTYRSDSFEN
481 PVLQQHFRNL EALALDLMEP EQAVDLTLPK VEAMNKRLGS LVDEFKELVY PPDYNPEGKV
541 TKRKHDNEGS GSKRPKVEYS EEELKTHISK GT**LGKFTVPM LKEACRAYGL KSGLKKQELL**
601 **EALTKHFQ**

Domain	Nucleotides	Amino Acids
α-Helix 5	540 to 598	180 to 196
PAR BINDING MOTIF	730 to 795	244 to 265
SAP DOMAIN	1717 to 1821	572 to 606

* The GeneBank accession number for the amino acid sequence of human Ku70 subunit is P12956.

** Underlined amino acids correspond to identified glutamate residues targeted by PARP1

Appendix III. Amino acid sequence of human Ku80 subunit

```
1    MVRSGNKAAVVLCMDVGFTMSNSIPGIESPFEQAKKVITMFVQRQVFAEN
51   KDEIALVLFGTDGTDNPLSGGDQYQNITVHRHLMLPDFDLLEDIESKIQP
101  GSQQADFLDALIVSMDVIQHETIGKKFEKRHIEIFTDLSSRFSKSQLDII
151  IHSLKKCDISLQFFLPFSLGKEDGSGDRGDGPFRLGGHGPSFPLKGITEQ
201  QKEGLEIVKMVMISLEGEDGLDEIYSFSESLRKLCVFKKIERHSIHWPCR
251  LTIGSNLSIRIAAYKSILQERVKKTWTVVDAKTLKKEDIQKETVYCLNDD
301  DETEVLKEDIIQGFRYGSDIVPFSKVDEEQMKYKSEGKCFSVLGFCKSSQ
351  UQRRFFMGNQVLKVFAARDDEAAAVALSSLIHALDDLDMVAIVRYAYDKR
401  ANPQVGVAFPHIKHNYECLVYVQLPFMEDLRQYMFSSLKNSKKYAPTEAQ
451  LNAVDALIDSMSLAKKDEKTDTLEDLFPTTKIPNPRFQRLFQCLLHRALH
501  PREPLPPIQQHIWNMLNPPAEVTTKSQIPLSKIKTLFPLIEAKKKDQVTA
551  QEIFQDNHEDGPTAKKLKTEQGGAHFSVSSLAEGSVTSVGSVNPAENFRV
601  LVKQKKASFEEASNQLINHIEQFLDTNETPYFMKSIDCIRAFREEAIKFS
651  EEQRFNNFLKALQEKVEIKQLNHFWEIVVQDGITLITKEEASGSSVTAEE
701  AKKFLAPKDKPSGDTAAVFEEGGDVDDLLDMI
```

* The GeneBank accession number for the amino acid sequence of human Ku80 subunit is NP_066964.

Appendix IV. Amino acid alignment of human and yeast Ku70 sequences.

```
Score = 56.2 bits (134),  Expect = 1e-05

Identities = 112/513 (21%), Positives = 201/513 (39%), Gaps = 57/513 (11%)

HKU70          1 MSGWESYYKTEGDEEAEEEQEENLEASGDYKYSGRDSLIFLVDASKAMFE     50
                 |....:.:...|      |..:.::.:|..|:...:.::|.::.|:.||:
YKU70          1 MRSVTNAFGNSG------ELNDQVDETGYRKFDIHEGILFCIELSETMFK     44

HKU70         51 SQSEDEL-TPFDMSIQCIQSVYISKIISSDRDLLAVVFYGTEKDKNSVNF     99
                 ..|:.|. :|....::.:..:....:|:.....:...||...::......
YKU70         45 ESSDLEYKSPLLEILESLDELMSQLVITRPGTAIGCYFYYCNREDAKEGI     94

HKU70        100 KNIYVLQELDNPGAKRILEL------------DQF----KGQQGQKRFQD    133
                 ..::.|::::....|::.:|            |.|    .|.:.|.|...
YKU70         95 YELFPLRDINATFMKKLNDLLEDLSSGRISLYDYFMFQQTGSEKQVRLSV    144

HKU70        134 MMGHGSDYSLSEVLWVCANLFSDVQFKMSHKRIMLFTNEDNP-HGNDSAK    182
                 :.....|..|.|:          ..|.::|:||:.|||:.|.| ...|..:
YKU70        145 LFTFMLDTFLEEI---------PGQKQLSNKRVFLFTDIDKPQEAQDIDE    185

HKU70        183 ASRARTKAGDLRDTGI-----FLDLMHLKKPGGFDISLFYRDIISIA---    224
                 .:|.|....||.|..:     |:.  :..||  || :.||.||:.:.
YKU70        186 RARLRRLTIDLFDNKVNFATFFIG--YADKP--FD-NEFYSDILQLGSHT    230

HKU70        225 -EDEDLRVHFE-ESSKLEDL----LRKVRAKETRKRALSRLKLKLNKDIV    268
                  |:..|...|: .|:|..|.    .|.:|.||. ||.:.:..|.|::...
YKU70        231 NENTGLDSEFDGPSTKPIDAKYIKSRILRKKEV-KRIMFQCPLILDEKTN    279

HKU70        269 ISVGI--------------YNLVQKALKPPPIKLYRETNEPVKTKTRTFN    304
                 ..||:               |.||.:         :.:..:...:|.:..|
YKU70        280 FIVGVKGYTMYTHEKAGVRYKLVYE---------HEDIRQEAYSKRKFLN    320

HKU70        305 TSTGGLLLPSDTKRSQIYGSRQIILEKEETE---ELKRFDDPGLMLMGFK    351
                 ..||. .:...|.:...||...|.|...:.:   |.....|..|.::||:
YKU70        321 PITGE-DVTGKTVKVYPYGDLDINLSDSQDQIVMEAYTQKDAFLKIIGFR    369

HKU70        352 PLVLLKKHHY---LRPSLFVYPEESLVIGSSTLFSALLIKCLEKEVAALC    398
                 .  ..|..||   :..|.|:.|:|:...||....::||....:|:..|:.
YKU70        370 S--SSKSIHYFNNIDKSSFIVPDEAKYEGSIRTLASLLKILRKKDKIAIL    417

HKU70        399 RYTPRRNIPPYFVALVPQEEELDDQKIQVTPPGFQLVFLPFADDKRKMPF    448
                 ....:.|..|....|.|       ..::....||.|..:||.|:.||.|
YKU70        418 WGKLKSNSHPSLYTLSP-------SSVKDYNEGFYLYRVPFLDEIRKFP-    459

HKU70        449 TEKIMATPE------QVGKMKAIVE------KLRFTYRSDSFENPVLQQH    486
                   .:::..:      ....||.:.:      .||..|....|:||:||:|
YKU70        460 --SLLSYDDGSEHKLDYDNMKKVTQSIMGYFNLRDGYNPSDFKNPLLQKH    507

HKU70        487 FRNLEALALDLMEPEQAVDLTLPKVEAMNKRLGSLV---DEFKELVY---    530
                 ::.|....|.       ::.|..:.|..|.:...::   |..::|.|
YKU70        508 YKVLHDYLLQ-------IETTFDENETPNTKKDRMMREDDSLRKLYYIRN    550

HKU70        531 ---------PPDYNPEGKVTK------RKHDNEGSGSKRPKVEYSEEELK    565
                          .|......|..|      :|.:::....|..|..:.::.
YKU70        551 KILESEKSEDPIIQRLNKYVKIWNMFYKKFNDDNISIKEEKKPFDKKP--    598

HKU70        566 THISKGTLGKFTVPMLKEACRAYGLKSGLKKQELLEALTKHFQ    608
                           ||.:
YKU70        599 ---------KFNI                                    602
```

Curriculum Vitae

Clayton Crawley

Education

Doctor of Philosophy Candidate, Department of Biochemistry
(Specialization in Human and Molecular Genetics)
University of Ottawa, Ottawa, ON., Canada
Successfully Defended, April 2009.

Masters of Science, Department of Biology
(Specialization in Molecular Biology)
University of Western Ontario, London, ON., Canada
Successfully Defended, August 2004.

Bachelor of Science, Honours Genetics.
University of Western Ontario, London, ON., Canada
Graduated with Distinction, June 2002.

Research Experience

Doctorate Research 09/2004 – 04/2009
University of Ottawa
Characterization of ADP-ribosylation of Ku70 by PARP-1 and its effect on the DNA binding of the Ku heterodimer. Dr. Robert Haché, Department of Biochemistry, Molecular Biology and Immunology.

Masters Research 09/2002 – 08/2004
University of Western Ontario
Isolated and expressed six prephenate dehydratase-like enzymes from *Arabidopsis* and examine expression patterns through RT-PCR. Dr. Susanne Kohalmi and Dr. Mark Bernards, Department of Biology.

Undergraduate Research 09/2001 – 05/2002
University of Western Ontario
Examined the difference in TGF-β mRNA levels in injured rat spinal cords with and without treatment. Dr. Lynn Weaver, Department of Neurosciences, Robarts Research Institute.

Publications:

Presented at Conference:

2008 Ottawa Health Research Institute Research Symposia
Ottawa, ON
"The effect of ribosylation by PARP-1 on the activity of Ku".
Crawley, C.D., Soubeyrand, S. and Haché, R.J.G.
* Winner of Poster Session Award

2008 Jacques Monod Conference – "Biological Responses to DNA Damage"
Roscoff, France
"The effect of ribosylation by PARP-1 on the activity of Ku".
Crawley, C.D., Soubeyrand, S. and Haché, R.J.G.

2006 Ottawa Health Research Institute Research Symposia
Ottawa, ON
"The regulation of Ku binding by PARP-1 *in vitro*".
Crawley, C.D., Soubeyrand, S. and Haché, R.J.G.

2005 Annual Meeting of the Canadian Society of Plant Physiologists
Edmonton, AB, Canada
"Expression analysis of select *PREPHENATE DEHYDRATASE-LIKE* (*PDL*) genes in *Arabidopsis thaliana*."
Hood, R.L., Crawley, C.D., Bernards, M.A., Kohalmi, S.E.
* Chosen for Selected Student Speaker Series

2004 The Genetics Society of Canada Conference
Toronto, ON, Canada
"Expression pattern analysis of six prephenate dehydratases-like genes in *Arabidopsis*".
Crawley, C.D., Bernards, M.A., and Kohalmi, S.E.

2004 Annual Meeting of the Canadian Society of Plant Physiologists
Guelph, ON, Canada
"Characterization of six prephenate dehydratases-like genes from *Arabidopsis thaliana* using RT-PCR analysis".
Crawley, C.D., Bernards, M.A., and Kohalmi, S.E.

2003 Eastern Regional Meeting of the Canadian Society of Plant Physiologists
Montreal, PQ, Canada
"*In silico* analysis of *Arabidopsis* prephenate dehydratases".
Crawley, C.D., Bernards, M.A., and Kohalmi, S.E.

Manuscripts in Preparation:

Crawley, C.D., Soubeyrand, S. and Haché, R.J.G. "Characterization of ADP-ribosylation of Ku70 by PARP-1 and its effect on the DNA binding of the Ku heterodimer."

Technical Experience:

Molecular genetics: Genomic DNA isolation; cloning and subcloning; generation and isotopic labelling of DNA probes from oligonucleotides and plasmids; Electromobility Shift Assays; Northern, Southern, and slot blot hybridization; restriction mapping.

Immunology: Immunofluorescent labelling of cellular proteins; immunoprecipitation; Western blot hybridization; *in vivo* V(D)J recombination assays.

Biochemistry: Spectrophotometric enzyme assays; protein quantitation; HPLC, ion exchange, and affinity chromatography; 1- and 2-D polyacrylamide gel electrophoresis isoelectric focusing.

Tissue Culture: Mammalian adherent cell culture; transfection, infection, and stable cell line selection.

Academic Honours, Awards and Distinctions

Special University Scholarship, *University of Western Ontario*, 2002-2004.

Teaching Assistant Award of Excellence Nominee, *University of Western Ontario*, May 2003.